UNIVERSITA' VITA-SALUTE SAN RAFFAELE

CORSO DI DOTTORATO DI RICERCA
INTERNAZIONALE IN MEDICINA MOLECOLARE

Curriculum in Gene and Cell Therapy

Dissecting innate immune barriers to efficient hematopoietic stem cell gene engineering

DoS: Dr. Anna Kajaste-Rudnitski

Second Supervisor: Dr. Leonie Unterholzner

Tesi di DOTTORATO di RICERCA di Erika Valeri

Matr. 015485

Ciclo di dottorato XXXV

SSD: BIO/11

Anno Accademico 2019/2020

CONSULTAZIONE TESI DI DOTTORATO DI RICERCA

la sottoscritta/**I** ERIKA VALERI
Matricola/**registration number** 015485
nata a/**born at** VAPRIO D'ADDA, MILANO
il/**on** 25/09/1993
autore della tesi di Dottorato di ricerca dal titolo / **author of the PhD Thesis titled** Dissecting innate immune barriers to efficient hematopoietic stem cell gene engineering

☐ AUTORIZZA la Consultazione della tesi / AUTHORIZES **the public release of the thesis**
☒ NON AUTORIZZA la Consultazione della tesi per 12 mesi /DOES NOT AUTHORIZE **the public release of the thesis for 12 months**

a partire dalla data di conseguimento del titolo e precisamente / **from the PhD thesis date, specifically**

Dal / **from** 19/12/2022 Al / **to** 19/12/2023

Poiché /**because**:

☒ l'intera ricerca o parti di essa sono potenzialmente soggette a brevettabilità/ **The whole project or part of it might be subject to patentability;**

☒ ci sono parti di tesi che sono già state sottoposte a un editore o sono in attesa di pubblicazione/ **Parts of the thesis have been or are being submitted to a publisher or are in press;**

☐ la tesi è finanziata da enti esterni che vantano dei diritti su di esse e sulla loro pubblicazione/ **the thesis project is financed by external bodies that have rights over it and on its publication.**

Data /Date 25/11/2022 Firma /Signature 

DECLARATION

This thesis has been:

- composed by myself and has not been used in any previous application for degree. Throughout the text I use both 'I' and 'We' interchangeably.
- has been written according to the editing guidelines approved by the University.

Permission to use images and other material covered by copyright has been sought and obtained. For the following image/s (specify), it was not possible to obtain permission and is/are therefore included in thesis under the "fair use" exception (Italian legislative Decree no. 68/2003).

All the results presented here were obtained by myself, except for:

1) *Transduction and gene expressions (Results, Figure 8A-C) were performed by my colleague Francesco Piras and already published (Piras et al, 2017).*
2) *Total amount of dsDNA and VSV-G copies measurements (Results, Figure 11D) were performed by Monica Soldi, Gene Transfer Technology and New Gene Therapy Strategies Unit, TIGET, San Raffaele Scientific Institute, Milan, Italy.*
3) *Design of the Knock-In strategy (Results, Figure 15A) was done in collaboration with Dr. Angelo Lombardo, Epigenetic Regulation and Targeted Genome Editing Unit, TIGET, San Raffaele Scientific Institute, Milan, Italy.*
4) *CRISPR/Cas9 KO library analysis (Results, Figure 15I) was done by Sara Valsoni, Bioinformatics Core, TIGET, San Raffaele Scientific Institute, Milan, Italy.*
5) *dNTPs measurement assays (Results, Figure 16I-J and Figure 19C) were performed in collaboration with Dr. Kim Baek, Emory University, Atlanta, GA, USA*
6) *Data mining (Results, Figure 20A) was performed by Monah Abou Alezz, Bioinformatics Core, TIGET, San Raffaele Scientific Institute, Milan, Italy.*
7) *Part of the materials and methods described in this thesis were already published by former members of the lab* (Petrillo *et al*, 2019; Piras *et al*, 2017)

All sources of information are acknowledged by means of reference.

ABSTRACT

Innate immune sensing and intrinsic expression of antiviral restriction factors may contribute to the poor permissivity of hematopoietic stem and progenitor cells (HSPC) to genetic engineering.

The first aim of my PhD thesis focuses on viral vectors sensing and stems from our observation that human HSPC respond differently to distinct viral vectors. While HIV-1-derived lentiviral vectors (LV) escape innate immune sensing, MLV-based γ-retroviral vectors (γRV) activate robust type I interferon (IFN) responses. Here we exploited human primary macrophages and PMA-U937 cells that recapitulate the same responses, as a model to better dissect mechanisms of RV recognition. We observed that γRV-mediated signaling is independent of reverse-transcribed DNA and occurred also with empty viral particles devoid of genomic RNA. In agreement, PMA-U937 cells knock-out for the canonical nucleic acid sensors cGAS, STING, RIG-I, or MAVS still up-regulated type I IFN responses upon γRV transduction, suggesting that IFN-induction is mainly driven by recognition of viral structural components. Interestingly, the γRV-mediated response was abrogated by inhibition of the TBK1 kinase, suggesting its involvement in the activation of the downstream antiviral responses. Remarkably, chimeric LV carrying the structural components of the γRV-induced type I IFN responses in macrophages, highlighting a direct role of the γRV structural components in vector recognition. To identify host factors involved in the sensing of the retroviral core we performed a CRISPR/Cas9 screening targeting interferon-stimulated genes. Current work is aimed at assessing the role of the most relevant candidate factors in the response to γRV transduction.

The second aim of my work tackles the role of antiviral host factors in poor permissivity of human HSPC to viral transduction. Specifically, we focused on the HIV-1 restriction factor SAMHD1 that hydrolyses intracellular dNTPs that are required for viral reverse transcription, dampening infection in non-diving and resting cells. The role of SMAHD1 has been poorly investigated in HSPC. To this aim, we used LV that incorporate the SIV accessory protein Vpx, which degrades SAMHD1. While Vpx-incorporation did not improve transduction efficiency in HSPC pre-stimulated with growth-promoting cytokines, a modest but significant advantage was observed in quiescent HSPC. Moreover, addition of exogenous deoxynucleosides (dNs) improved transduction in quiescent HSPC with a striking and synergistic benefit when combined with CsH, a compound we have shown to overcome an innate block to vector entry in HSPC that acts prior to SAMHD1. Of

note, the combination of dNs and CsH significantly improved transduction also in other quiescent cell sources, such as resting T cells. Importantly, we showed that with the combination of dNs and CsH we could achieve efficient transduction and higher engraftment in unstimulated HSPC as compared to stimulated cells, highlighting how shorter *ex vivo* culture preserves HSC biological properties. Together, our results indicate that gene transfer in unstimulated HSPC is hampered by different immune barriers, and strategies to overcome these barriers allow for improved genetic engineering in quiescent HSPC.

Overall, my PhD work, through in-depth investigation of vector-host interactions, sheds light on novel HSPC immune defense mechanisms and informs the development of improved gene therapy protocols.

1. TABLE OF CONTENTS

2. ACRONYMS AND ABBREVIATIONS

A: Adenosine
AAV: Adeno-Associated Virus
ABE: Adenosine Base Editors
ADA: Adenosine deaminase
AhR: Aryl hydrocarbon Receptor
AIM2: Absent In Melanoma 2
ALD: Adrenoleukodystrophy
AP-1: Activator Protein 1
ATM: Ataxia-Telangiectasia Mutated
AZT: azidothymidine
B: B-box domains
BaEV: Baboon Endogenous Virus
BE: Base Editors
BFU-E: Burst Forming Units-Erythroid
BIV: Bovine Immunodeficiency Virus
BM: Bone Marrow
C: Cytosine
CA: Capsid
CARD: Caspase Activation and Recruitment Domains
CB: Cord Blood
CBE: Cytosine Base Editors
CC: Coiled-Coiled domain
CFU: Colony Forming Unit
cGAMP: cyclic GMP-AMP synthase
CGD: Chronic Granulomatous Disease
CLP: Common Lymphoid Progenitors
CMP: Common Myeloid Progenitors
cPPT: central polypurine tract
CRISPR: Clustered Regularly Interspaced Short Palindromic Repeats
CsH: Cyclosporine H
CTD: C-Terminal Domain
CypA: Cyclophilin A

CPS: Carbamoyl-P Synthetase
DAMP: Damage-Associated Molecular Patterns
dA: deoxyadenosine
dATP: deoxyadenosine triphosphate
dC: deoxycytidine
dCTP: deoxycytidine triphosphate
DDR: DNA Damage Response
dG: deoxyguanosine
dGTP: deoxyguanosine triphosphate
DHODH: Dihydroorotate Dehydrogenase
DMSO: dimethyl sulfoxide
dNs: deoxynucleosides
dNTPs: deoxynucleotides triphosphate
DSB: Double Strand Break
ds: double stranded
dT: deoxythymidine
dTTP: deoxythymidine triphosphate
EIAV: Equine Infectious Anemia Virus
EMA: European Medicines Agency
EMCV: Encephalomyocarditis Virus
ER: Endoplasmic Reticulum
FACS: Fluorescence Activated Cell Sorting
FBS: Fetal Bovine Serum
FIV: Feline Immunodeficiency Virus
FLT3L: FMS-Like Tyrosine kinase 3 Ligand
G: Guanosine
GBE: Glycosylase Base Editors
G-CSF: Granulocyte-Colony Stimulating Factor
GMP: Granulocyte-Macrophage Progenitor
gRNA: guide RNA
GT: Gene Therapy
h: human
HD: Histidine Aspartate domain
HDR: Homology-Directed Repair

HIV: Human Immunodeficiency Virus
HLA: Human Leukocyte Antigen
HSC: Hematopoietic Stem Cells
HSCT: HSC Transplantation
HSPC: Human Hematopoietic Stem and Progenitor cells
HSV-1: Herpes Simplex Virus-1
hTRIM5a: human TRIM5α
IAV: Influenza A Virus
IDLV: Integrase-Deficient Lentiviral Vector
IF: Immunofluorescent Staining
IFI16: Interferon-gamma Inducible Protein 16
IFITMs: Interferon-Induced Transmembrane Proteins
IFN: Interferon
IFNAR: IFNα Receptor
IKKε: I-kappa-B Kinase-epsilon
IL: Interleukin
IMP: Inosine Monophosphate
IN: Integrase
ISG: Interferon Stimulated Genes
ITR: Inverted Terminal Repeats
KI: Knock-In
KO: Knock-Out
LCR: Locus Control Region
LGP2: Laboratory of Genetics and Physiology 2
Lin-: lineage negative
LPS: Lipopolysaccharide
LRRs: Leucine-Rich Repeats
LT-HSC: Long Term-HSC
LTR: Long Terminal Repeats
LV: Lentiviral Vector
MA: Matrix
MAVS: Mitochondrial Antiviral Signaling protein
MCMV: Mouse Cytomegalovirus
MDA5: Melanoma Differentiation-Associated protein 5

MDDC: Monocyte-Derived Dendritic Cells
MDM: Monocyte-Derived Macrophages
MEP: Megakaryocyte-Erythroid Progenitors
MLD: Metachromatic Leukodystrophy
MLV: Murine Leukemia Virus
MOI: Multiplicity of Infection
MoMLV: Moloney MLV
mPB: mobilized Peripheral Blood
MPP: Multipotent Progenitors
MPS-I: Mucopolysaccharidosis type I
NC: Nucleocapsid
nCas9: Cas9 nickase
NF-κB: Nuclear Factor kappa-light-chain-enhancer of activated B cells
NHEJ: Non-Homologous End Joining
NK: Natural Killer
NLS: Nuclear Localization Sequence
NSG: NOD Scid Gamma
OA: Orotic Acid
PAM: Protospacer Adjacent Motif
PAMP: Pathogen-Associated Molecular Patterns
PBS: Primer Binding Site
pDC: plasmacytoid Dendritic Cells
pegRNA: Prime-Editing Guide RNA
PGE2: Prostaglandin E2
PIC: Pre-Integration Complex
PID: Primary Immune Deficiencies
PPAT: Phosphoribosyl Pyrophosphate Amidotransferase
PR: Protease
PRR: Pattern Recognition Receptors
qLT-HSC: quiescent Long-Term repopulating HSC
R: RING domain
rh: rhesus monkeys
RIG-I: Retinoid acid-Inducible Gene-I
RLR: RIG-I-Like Receptors

RNP: Ribonucleoprotein complex
RRE: REV-Responsive Element
RSV: Rous Sarcoma Virus
RT: Reverse Transcriptase
RT: Reverse Transcription
RT: Room Temperature
RV: Retroviral Vectors
SAM: Sterile Alpha Motif
SAMHD1: SAM and HD containing protein 1
SCD: Sickle Cell Disease
SCF: Stem Cell Factor
SD: standard deviation
SDF-1α: Stromal cell-Derived Factor-1α
SEM: standard error of the mean
sgRNA: single guide RNA
SIN: Self-Inactivating
SIVmac: Simian Immunodeficiency Virus macaque
SR1: StemRegenin 1
ssODNs: single-stranded phosphorothioate-modified oligodeoxynucleotides
ss: single stranded
ST-HSC: Short-Term HSC
STING: stimulator of interferon genes
T: Thymine
TALENs: Transcription Activator-Like Effector Nucleases
TAR: Transactivation Response Element
TBK1: TANK-binding kinase 1
THPO: Thrombopoietin
TIR: Toll-Interleukin-1 Receptor
TLR: Toll-Like Receptors
TSCM: Stem Memory T Cells
UMP: uridine 5′-monophosphate
VA: Valproic Acid
VCN: Vector Copy Number
VLPs: Virus-Like Particles

VSV-G: Vesicular Stomatitis Virus Glycoprotein

WAS: Wiskott–Aldrich Syndrome

WNV: West Nile Virus

WPRE: Woodchuck Hepatitis Virus

WT: Wild Type

X-SCID: X-linked Severe Combined ImmunoDeficiency

ZFNs: Zinc Finger Nucleases

3. LIST OF FIGURES AND TABLES

4. INTRODUCTION

4.1. The hematopoietic system

The hematopoietic system is fundamental for sustaining physiological processes and in disease conditions, with specialized mature hematopoietic cell types that participate in oxygen supply, nutrient transport to tissues, immune response and wound healing processes (Loughran *et al*, 2020). Mature blood cells have a limited lifespan and their lifelong supply is provided through hematopoiesis, starting from a limited pool of multipotent hematopoietic stem cells (HSC) (Eaves, 2015; Orkin & Zon, 2008).

The cellular potential of HSC was discovered in the 50s by transplanting bone marrow (BM) cells into lethally preconditioned recipients, which lacked a functional hematopoietic system. Transplanted cells promoted mice survival, suggesting that donor BM contained HSC (Lorenz *et al*, 1952; Jacobson *et al*, 1951). Later, colony-forming unit (CFU) assays demonstrated the multilineage differentiation property of HSC as multilineage progenitors could arise from a single hematopoietic precursor (Till & McCulloch, 1961; BECKER *et al*, 1963).

With the identification of cell surface markers HSC started to be isolated from the BM and it became possible to better investigate their properties and functions (Kondo *et al*, 1997; Akashi *et al*, 2000). This led to the establishment of the classical hematopoietic hierarchy roadmap that illustrates the lineage relation between HSC and their progenies (Doulatov *et al*, 2012). According to this classical model, HSC differentiate gradually through a process in which they lose the potential of producing all the different hematopoietic cells, moving from multipotency to oligopotency to unipotency until cells can form only one type of mature blood cell (**Figure 1**).

Cells are classified in long-term (LT)-HSC or short-term (ST)-HSC, according to the expression of the CD34 surface marker (Morrison & Weissman, 1994). LT-HSC are a rare BM cell population that show long-term reconstitution ability. ST-HSC display only short-term reconstitution capacity. LT-HSC are almost quiescent thus minimizing possible DNA damage associated with cell cycle progression, and rely on ST-HSC and downstream progenitors to support steady-state hematopoiesis. ST-HSC give rise to multipotent progenitors (MPP) that display high differentiation ability while losing self-renewal ability (Yang *et al*, 2005). MPP can give rise to common myeloid progenitors (CMP) or common

lymphoid progenitors (CLP). CMP possess myeloid/erythroid/megakaryocyte potential and they further branch into megakaryocyte-erythrocyte progenitors (MEP) and granulocytes-macrophages progenitors (GMP). CLP display instead a lymphoid-restricted potential and differentiate in T cells, B cells, natural killer (NK) cells, and dendritic cells. This classic model of the hematopoietic hierarchy presents a series of punctuated lineage decisions taken by functionally homogeneous cells that are defined according to their cell surface markers expression (**Figure 1**).

Despite clearly explaining the HSC differentiation process, the classic model represents an oversimplification. More recent advances in single-cell technologies, cell tracking, and genetics have highlighted the great heterogeneity and complexity of HSC, allowing to expand the knowledge of hematopoiesis (Liggett & Sankaran, 2020). This led to a revised model of hematopoiesis, termed the continuum model (Velten *et al*, 2017; Laurenti & Göttgens, 2018). According to this model, the acquisition of lineage-specific fates is no more viewed as a stepwise process with transitions through the multi- bi- and unipotent stages. Instead, it emerges from low-primed non differentiated HSC and progenitors through a continuous process, suggesting the absence of specific boundaries between stem cells and progenitors (Laurenti & Göttgens, 2018) (**Figure 1**).

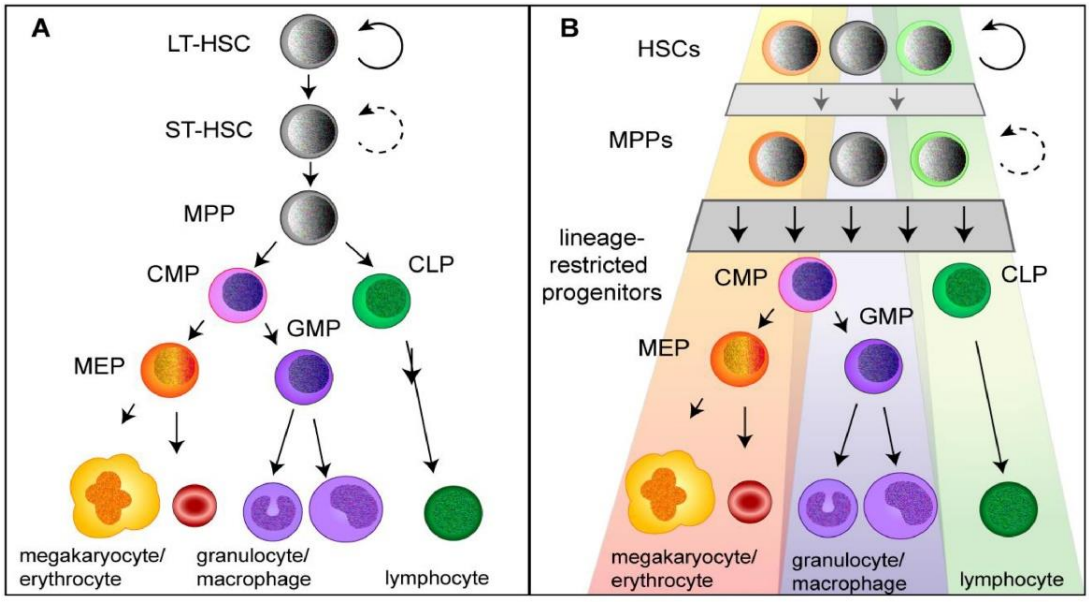

Figure 1. Hierarchical models of hematopoiesis *A) According to the classical view of hematopoiesis HSC differentiate into multipotent, bipotent and unipotent progenitors until they generate all mature hematopoietic cells. B) According to the continuum model of hematopoiesis low-primed undifferentiated HSPC differentiate into lineage-restricted cells (McRae et al, 2019).*

4.2. Hematopoietic stem cells gene therapy

In the last 60 years, allogeneic HSC transplantation (HSCT) has been the standard treatment for a growing number of human genetic diseases (Chabannon *et al*, 2018). HSCT demonstrated its efficacy in curing diseases such as X-linked Severe Combined Immunodeficiency (X-SCID) (Gatti *et al*, 1968) paving the way for the treatment of an increasing number of human diseases. However, the possibility to find donors with human leukocyte antigen (HLA) genotype matching still represents a limitation in this application (Styczyński *et al*, 2020) and the use of non-immunocompatible donors may lead to graft-versus-host disease (Ferrara *et al*, 2009).

To overcome the limitations and hurdles of allogeneic HSCT, innovative techniques aimed at genetically modifying autologous HSC have been explored. Indeed, several diseases were considered good candidates for HSC gene therapy (GT) such as primary immunodeficiencies that affect the lymphoid system, monogenic disorders that affect the erythroid lineages, storage and metabolic disorders as well as bone marrow failure syndromes (Naldini, 2019).

Hematopoietic stem and progenitor cells (HSPC) gene therapy approaches so far were based on *ex vivo* procedures. HSPC are collected from the mobilized peripheral blood (mPB) or bone marrow of a patient and are cultured *ex vivo* in a medium containing cytokines that promote the maintenance and expansion of long-term HSC. During the *ex vivo* culture, the cells are genetically modified, either through gene transfer or gene editing, then they are reinfused back into the patient, who receives a conditioning treatment to deplete HSPC from the BM and favor the engraftment of the newly engineered cells. Upon engraftment, HSC can self-renew and generate gene-corrected daughter cells along all the hematopoietic lineages driving the reversion of pre-existing pathologies (Naldini, 2019; Ferrari *et al*, 2021a) (**Figure 2**).

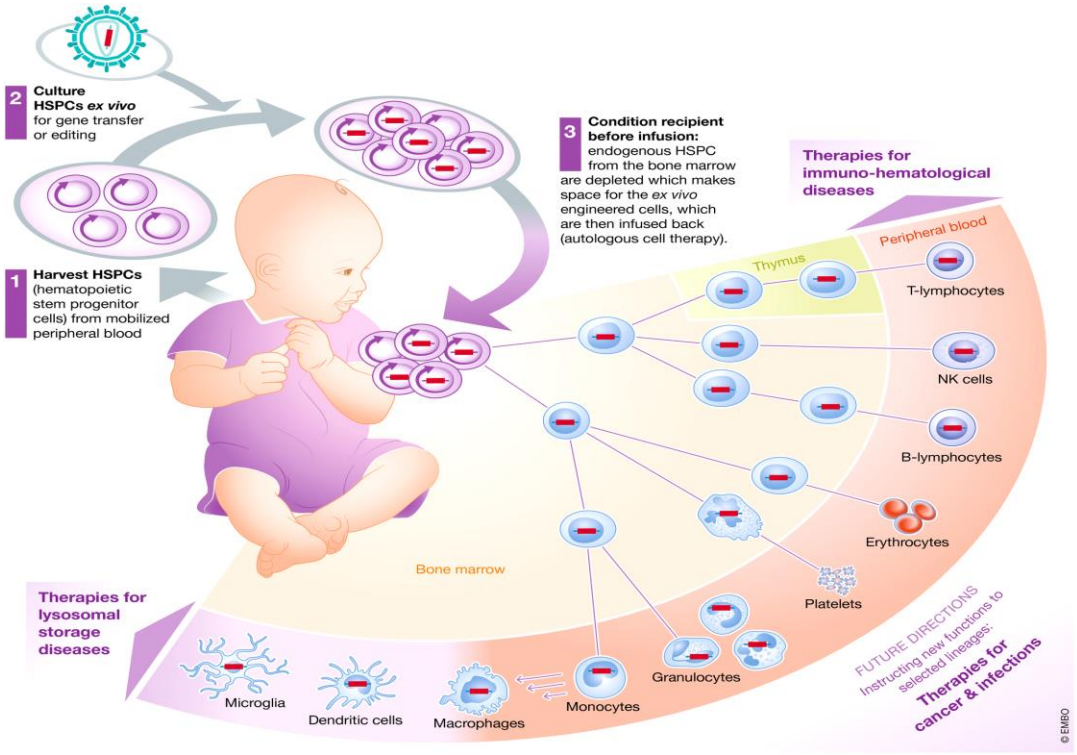

Figure 2. ***Schematic of a standard hematopoietic stem cell gene therapy protocol.*** *In a common gene therapy procedure HSPC are harvested from the BM or mPB of a patient (1) and are cultured ex vivo with cytokines that promote their growth and maintenance, while being subjected to gene transfer or gene editing approaches (2). The corrected cells are delivered to the patient who receives a conditioning regimen to make space in the BM for the corrected cells (3). Upon engraftment, gene-modified cells can self-renew and differentiate into mature blood cells, restoring pre-existing pathologies (Naldini, 2019).*

4.2.1. HSC collection and *ex vivo* culture

HSPC are harvested directly from the BM of the patient, through aspiration, or by leukapheresis upon administration of mobilizing agents. Although both sources have provided clinical benefits in clinical trials for immunodeficiencies (Ferrua *et al*, 2019), mobilized peripheral blood is currently the source of choice as it provides a higher number of HSPC, supporting a faster reconstitution, with a minimally invasive procedure (Gertz, 2010). Granulocyte colony-stimulating factor (G-CSF) and plerixafor are the two drugs currently used in gene therapy for mobilization (Ferrari *et al*, 2021a). G-CSF suppresses niche-supportive cytokines release in the BM, while plerixafor acts directly on HSC by antagonizing the CXCR4 chemokine receptors and impeding the binding with

the stromal cell-derived factor-1-alpha (SDF-1α) that promotes retention of HSC within the BM niche (Winkler *et al*, 2012).

Once isolated, the purified HSPC are cultured *ex vivo* for 2-5 days while they are stimulated with a mix of early-active cytokines. Stem cell factor (SCF), FMS-like tyrosine kinase 3 ligand (FLT3L), thrombopoietin (THPO), and Interleukin 3 (IL3) or 6 (IL6) are required to promote cell-cycle progression, essential for achieving good levels of lentiviral vector (LV) transduction of HSPC (Ailles *et al*, 2002). Moreover, multiple rounds of transduction at high vector doses with a high infectivity vector are required to reach clinically relevant gene targeting levels (Kajaste-Rudnitski & Naldini, 2015). The use of cytokines is further more important when performing gene editing procedures that rely on homology-directed repair (HDR) since the exit from the quiescence status is fundamental for engaging the DNA repair mechanisms (Genovese *et al*, 2014; Ferrari *et al*, 2020). However, despite being required for efficient transduction, the *ex vivo* culture adversely affects HSC engraftment and their repopulation capacity. This occurs due to cell cycle progression, which drives HSC differentiation and lineage commitment, and lack of expression of adhesion molecules that impairs their homing capacity within the BM (Glimm *et al*, 2000; Kallinikou *et al*, 2012; Larochelle *et al*, 2012; Mazurier *et al*, 2004; Zonari *et al*, 2017). Moreover, HSC vector manipulation can trigger harmful signaling events which may negatively impact primitive or more committed HSC progenitors affecting their clonogenic capacity and reducing the fraction of corrected LT-HSC (Piras *et al*, 2017; Schiroli *et al*, 2019; Ferrari *et al*, 2022). Indeed, among the drawbacks observed in some gene therapy trials is a delay in the engraftment of platelets and myeloid cells, which can be remedied by administering high numbers of HSPC to favor a faster hematopoietic reconstitution upon patient conditioning (Marktel *et al*, 2019).

To this aim, numerous studies are focusing on the identification of new pathways and novel compounds to devise HSC *ex vivo* expansion protocols (Zimran *et al*, 2021). The goal is to increase the number of gene-corrected HSC, without compromising their engraftment potential. StemRegenin 1 (SR1) emerged from a screening showing its ability to promote cord blood-derived HSPC *ex vivo* expansion by 50-fold and to increase the number of LT engrafting HSC in immunodeficient mice (Boitano *et al*, 2010). SR1 is a purine derivative and acts by antagonizing the aryl hydrocarbon receptor (AhR), which is crucial for self-renewal (Gasiewicz *et al*, 2014). A clinical trial using SR1 demonstrated early platelet and neutrophil recovery and better engraftments as compared to recipients

that received an equal number of non-expanded HSPC (Wagner *et al*, 2016). A different screening led to the identification of a pyrimidoindole derivative named UM171 able to expand the pool of primitive HSC more efficiently than StemRegenin 1 (Fares *et al*, 2014; Zonari *et al*, 2017). UM171 acts in an AhR-independent manner but its physiological target is still unclear (Fares *et al*, 2014). Other compounds such as nicotinamide (Horwitz *et al*, 2014) or valproic acid (VA) (Moussy *et al*, 2019) have been used to promote HSC expansion and engraftment. However, there is still a lack of a defined and robust protocol for expanding *ex vivo* LT-HSC from BM or mPB (Naldini, 2019).

Thus, the purpose of the current protocols is to reduce the culture period and HSC manipulation to the minimum required to reach sufficient transduction levels, despite several factors may influence the transduction efficiency (Naldini, 2019). Indeed, it has been shown that HSC have high intrinsic expression of antiviral interferon-stimulated genes (ISG) that can underpin their resistance to vector-mediated gene therapy approaches (Wu *et al*, 2018; Petrillo *et al*, 2018). Moreover, there could be variability among individuals in the expression of specific antiviral factors known to impair viral transduction (Petrillo *et al*, 2018) or in the quiescence state of the isolated HSC, which can overall influence the outcome of the vector manipulation.

The introduction of transduction enhancers may allow overcoming some of these limitations, reaching high gene transfer/editing levels while removing the need for multiple hits of transduction (Ferrari *et al*, 2021a). Different compounds have been identified as transduction enhancers such as poloxamers (Höfig *et al*, 2012; Schott *et al*, 2019), Rapamycin (Wang *et al*, 2014; Petrillo *et al*, 2015), Cyclosporine A (CsA) and H (CsH) (Petrillo *et al*, 2015, 2018) and Prostaglandin E2 (PGE2) (Heffner *et al*, 2018; Zonari *et al*, 2017). The mechanism of action varies from promoting viral attachment to increasing viral entry or post-entry steps such as viral integration. However, for some of the enhancers, such as PGE2, the mechanisms behind improved transduction are poorly understood and concerns for long-term safety remains. PGE2 and the poloxamer LentiBOOST™ are already in the clinics (Gentner *et al*, 2019; Kanter *et al*, 2019). Still, intensive investigation of the mechanism of action and long-term follow-up are required to demonstrate their efficient and safe profile.

4.2.2. Hematopoietic stem cell gene engineering

While HSPC are cultured *ex vivo,* they undergo gene transfer or gene editing procedures to insert a therapeutic gene within the host DNA or correct a specific DNA sequence. The corrected and functional copy of a gene can thus be maintained through the lifespan of the individual and can be transmitted to the progeny.

4.2.2.1. Retroviral vectors origin

Gamma (γ)-retroviral vectors (RV) and lentiviral vectors have been the most widely used transfer tools in gene therapy to date (Naldini, 2019). Viral vectors are generated from parental viruses, which are engineered to become replication-defective particles while maintaining the potential to integrate their genetic material within the host (Kay *et al*, 2001; Naldini, 2011).

γRV derive from murine leukemia viruses (MLV), while LV derive from human immunodeficiency virus 1 (HIV-1), both belonging to the Retroviridae family. Retroviruses are spherical or conical enveloped RNA viruses carrying two single-strand (ss) RNA genome molecules of 7 to 12 kb in length (Vogt, 1997).

Retroviruses can be defined as simple or complex viruses, according to their genome structure. γ-retroviruses, such as MLV, are simple retroviruses; HIV-1 instead is a complex retrovirus. Commonly, there are three domains within retroviral genome with Gag, Pol, and Env genes surrounded by two long terminal repeats (LTR) (Coffin *et al*, 1997). From the Gag domain the structural proteins capsid (CA), nucleocapsid (NC), and matrix (MA) are synthetized starting from a single polyprotein that requires proteolytic cleavage by the HIV-1 protease. The CA protein forms the viral core, which accommodates the viral genome that associates with the NC protein. The MA protein forms a layer that surrounds the viral core. Pol encodes for the viral enzymes reverse transcriptase (RT), integrase (IN), and protease (PR) that derive from the Gag-Pol precursor protein. The RT allows the synthesis of viral DNA from the RNA genome, the integrase mediates viral genome integration in the host, while the protease processes the precursors polyproteins, allowing viral cores maturation (Coffin *et al*, 1997). All three enzymes are located within the viral core. The transmembrane and envelope glycoproteins, essential in determining viral tropism, are generated from the Env domain. The LTR, essential for gene expression regulation, are composed of the U3, R,

and U5 sequences located at the ends of the viral genome. The packaging sequence (ψ) located outside the LTR is essential to encapsidate the genetic material in nascent virions (Beasley & Hu, 2002; Watanabe & Temin, 1982; Coffin *et al*, 1997; D'Souza & Summers, 2005). The viral particle is surrounded by a lipid envelope that originates from the outer layer of the cell and accommodate the viral envelope glycoproteins that bind cell surface receptors to mediate vector entry into the host.

In addition to these common elements, complex retroviruses carry other regulatory genes and accessory proteins. HIV-1 carry two regulatory genes called Tat and Rev. Tat promotes HIV transcription by binding to the transactivation response element (TAR) located at the beginning of the nascent RNA (Bieniasz *et al*, 1999). Rev promotes the nuclear export of spliced and unspliced transcripts by binding to the REV-responsive element (RRE) located in the Env region (Neville *et al*, 1997). Vif, Vpr, Vpu, and Nef are additional auxiliary factors, critical for HIV pathogenesis *in vivo* (Basmaciogullari & Pizzato, 2014; Seissler *et al*, 2017).

The retroviral life cycle starts with the binding between the viral envelope and the target cell membrane receptor (**Figure 3**). Successful binding mediates virion internalization, with release of the viral particle inside the cell (McClure *et al*, 1988; Sinangil *et al*, 1988). Once entered the cells, the RNA starts to be reverse transcribed into double-stranded (ds)DNA within the viral core where the proviral DNA associates with the integrase to form the pre-integration complex that coordinates integration concomitantly within the host chromatin leading to permanent infection of the host. There is no clear consensus on when and where uncoating occurs. It was thought to happen in the cytosol, concomitantly to RT (Aboud *et al*, 1979; Hulme *et al*, 2011; Cosnefroy *et al*, 2016) (**Figure 3**). However, recent evidence has suggested that it may take place during the nuclear import process before entering the nucleus (Francis & Melikyan, 2018; Fernandez *et al*, 2019) or even within the nucleus, near integration sites (Burdick *et al*, 2020). Upon integration, the viral genome is transcribed with generation of spliced and unspliced transcripts. Once in the cytoplasm, RNA is translated to synthesize the viral proteins. The precursor structural proteins and the replication enzymes associate with the full-length RNA genome in new viral particles. During the budding from the cell membrane, the immature core acquires the viral envelope glycoprotein and undergoes further processing promoting the maturation of new infectious viruses (Coffin *et al*, 1997) (**Figure 3**).

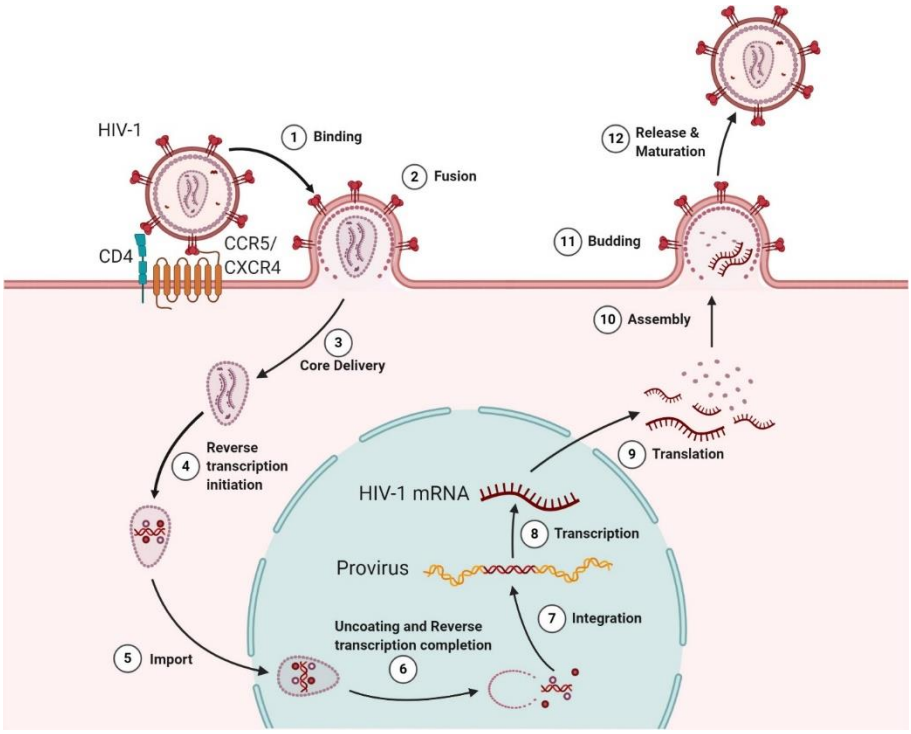

Figure 3. Retroviral life cycle. *The retroviral life cycle starts with the interaction between the viral surface envelope glycoprotein and the host cell surface receptors. This mediates fusion with cell membrane driving entry into the cell. Once inside the cell, the reverse-transcription starts and the viral core reaches the nucleus and disassembles upon completion of the reverse transcription. Reverse-transcribed DNA integrates into the host chromatin and upon transcription viral RNAs are transported to the cytoplasm to form viral proteins. RNA genome and viral proteins assemble at the cell surface forming new immature virions. Upon budding, immature cores are processed by the produced protease enzyme to allow maturation of new viruses (Ramdas et al, 2020).*

4.2.2.2. Retroviral vectors design and production

Both γRV and LV can accommodate an expression cassette of up to 8-12 Kb of exogenous DNA (Sheridan, 2011).

Different retroviruses have been engineered to generate RV, with Moloney (Mo) MLV being the most exploited for gene therapy purposes (Naldini, 2019; Ferrari *et al*, 2021a). The production of replication-defective RV was obtained by the split-packaging design through separation of the Gag-Pol genes and the Env gene into distinct plasmids provided in *trans.* The viral genome components instead were replaced by the gene of interest, maintaining the LTR regions and the ψ sequence (Maetzig *et al*, 2011). In the first RV generation, the expression of the therapeutic gene was dependent on enhancer-promoter sequences located on the viral LTR. The deletion of these viral sequences in

the U3 portion, and the inclusion of an internal promoter guided the generation of self-inactivating (SIN) viral vectors that displayed reduced risk of mobilization, recombination, and transactivation of proto-oncogenes near the integration sites (Dull *et al*, 1998; Yu *et al*, 1986). Still, RV show some limitation as delivery vehicles for *ex vivo* gene therapy application as lacking an active transport system across the nuclear membrane they can integrate only in cycling cells during mitosis, thus being used only for dividing cells (Bukrinsky *et al*, 1992). Moreover, despite the introduction of the SIN vector design, the integration profile of RV remains of concern as they preferentially integrate near cancer genes and can drive oncogenesis by insertional mutagenesis (Montini *et al*, 2009).

LV have demonstrated superior safety and efficacy compared to RV, due to more efficient gene transfer capacity and their safer integration profile (Naldini, 2019). Moreover, LV give the possibility of transducing both cycling and resting cells, thus representing a more versatile tool. Moreover, LV preferentially integrate within the bodies of transcription units, reducing genotoxic risk (Montini *et al*, 2006; Modlich *et al*, 2009; Biffi *et al*, 2011; Cesana *et al*, 2012). The design of LV has evolved through the years to minimize the risks associated with the use of a viral platform (**Figure 4**). As for RV, the three-plasmid design was initially used for the first generation of LV. The packaging plasmid encoded for Gag-Pol and all regulatory and accessory sequences. A second construct was used to carry the Env gene, while a third plasmid was used to carry the transgene and retained only the LTR, ψ, and RRE (from Env) essential sequences (Follenzi & Naldini, 2002). To improve the expression of the transgene, other sequences were included in the transfer plasmid (Vigna & Naldini, 2000). A regulatory region from the woodchuck hepatitis virus (WPRE) was introduced at the 3' end of the transgene to increase its expression (Donello *et al*, 1998). The addition in *cis* of the central polypurine tract (cPPT) showed to improve proviral DNA nuclear import (Follenzi *et al*, 2000). Advanced vector design with the deletion of all the accessory genes from the packaging plasmid led to the development of the second generation of LV (Kim *et al*, 1998; Zufferey *et al*, 1997). Further biosafety improvements in the third generation of LV included the deletion of Tat and Rev (**Figure 4**). Tat absence was compensated by the introduction of a strong promoter within the transfer vector while Rev was provided in *trans* by a fourth plasmid (Dull *et al*, 1998). As shown with retroviral vectors, the development of SIN-LV improved the safety of the platform. The Env gene of HIV was substituted by the glycoprotein of the vesicular stomatitis virus (VSV-G) to broaden the

tropism (Burns *et al*, 1993; Cronin *et al*, 2005) (**Figure 4**). In addition to VSV-G, other envelopes can be used to pseudotyped LV to successfully transduce the desired cell or tissue type (Sandrin *et al*, 2002; Girard-Gagnepain *et al*, 2014; Lévy *et al*, 2017).

For the production of γRV and LV, HEK293 or HEK293T producer cell lines are co-transfected with the above-described plasmids. Alternatively, stable producer cells with inducible expression of viral genes can be exploited to produce high-titer vectors in a scalable manner (Klages *et al*, 2000).

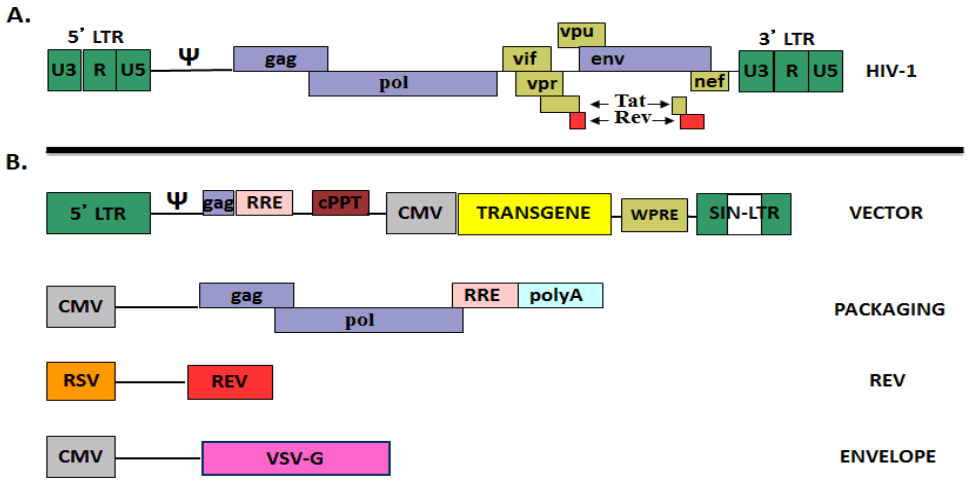

Figure 4. Lentiviral vectors design. A) *Schematic of HIV-1 genome with gag, pol, env, and accessory proteins coding genes flanked by the LTR.* ***B)*** *Third generation LV are produced by co-transfecting four plasmids. The self-inactivating LV transfer plasmid expresses the transgene under the control of exogenous promoter. The packaging sequence, RRE, cPPT, and the WPRE regulatory sequence are included in the transfer plasmid to improve LV performance. The packaging plasmid carries gag and pol. A third plasmid provides Rev in trans and the envelope plasmid codes for the envelope glycoproteins used to pseudotype LV to broaden its tropism (Shaw & Cornetta, 2014).*

4.2.2.3. Retroviral vectors in HSC gene therapy

The first gene therapy applications exploited MoMLV-derived γRV as transfer tool (Fischer *et al*, 2015; Ferrua & Aiuti, 2017). Despite proving the therapeutic potential of the technology, some patients enrolled in clinical trials developed leukemia due to semi-random integration of the vector near an oncogene (Hacein-Bey-Abina *et al*, 2008; Howe *et al*, 2008; Braun *et al*, 2014). Due to the risk of genotoxicity associated with the first generation of γRV, ameliorations of the vector platform were introduced such as the

previously mentioned design of SIN vectors (Miyoshi *et al*, 1998; Dull *et al*, 1998) and the use of LV (Naldini *et al*, 1996). Implementation of SIN γRV demonstrated an improved safety profile in the treatment of X-SCID (Cavazzana *et al*, 2016). However, the real safety improvement occurred with the development of HIV-derived LV.

LV are currently the most used vector in HSPC GT. LV-based HSC GT has allowed the treatments of hundreds of patients affected by multiple diseases, including Adrenoleukodystrophy (ALD), Metachromatic leukodystrophy (MLD), Wiskott–Aldrich syndrome (WAS), Chronic Granulomatous Disease (CGD), Primary Immune Deficiencies (PID), Mucopolysaccharidosis type I (MPS I), thalassemia, sickle cell disease (SCD), Fanconi anemia and HIV infection (Eichler *et al*, 2017; Sessa *et al*, 2016; Biasco *et al*, 2016; De Ravin *et al*, 2016; Cavazzana-Calvo *et al*, 2010; Ribeil *et al*, 2017; Thompson *et al*, 2018; Marktel *et al*, 2019; Río *et al*, 2019; DiGiusto *et al*, 2010). In most of the patients receiving the treatment, a remarkable disease correction was observed, with long-term hematopoietic reconstitution and a lack of detectable genotoxic events highlighting the efficacy and safety profile of LV (Ferrari *et al*, 2021a).

The European Medicines Agency (EMA) have approved three products so far: Strimvelis, for treatment of adenosine deaminase (ADA)-deficient specific form of SCID, Zynteglo for treating transfusion-dependent β-thalassaemic patients and more recently Libmeldy for the treatment of MLD (Aiuti *et al*, 2017; Schuessler-Lenz *et al*, 2020).

4.2.3. Gene editing

Gene editing procedures can allow the modification of specific genomic sequences thus correcting gene mutations, disrupting genes or inserting a healthy copy of a gene within 'safe harbors' (Pavani & Amendola, 2021). In addition, targeted gene addition can allow a physiological regulation of the curative gene (Genovese *et al*, 2014). A gene editing approach is based on the introduction of a double-strand break (DSB) by a nuclease, which is resolved either by non-homologous end joining (NHEJ), which is an error-prone repair mechanism, or by HDR when a donor cassette is provided (Wyman & Kanaar, 2006). While NHEJ can be exploited to inactivate genes, HDR can be exploited to correct gene mutation in disease conditions or to integrate a gene in a desired locus (Prakash *et al*, 2016).

4.2.3.1. Programmable nucleases

The real advances in gene editing occurred with the development of nucleases that recognized and cleaved a desired DNA sequence with high specificity. Among the traditional gene editing tools, there are Zinc Finger Nucleases (ZFNs), Transcription Activator-Like Effector Nucleases (TALENs), and Clustered Regularly Interspaced Short Palindromic Repeats (CRISPR) Cas-associated nucleases (Li *et al*, 2020).

In ZFNs and TALENs a small protein that recognizes trinucleotide or single nucleotide sequences, respectively, is fused to the FokI endonuclease domain. The DNA-binding region is engineered allowing the targeting of a precise DNA sequence that will be cleaved by the nuclease. Thanks to the use of multiple ZF or TALE motifs, longer DNA sequences can be recognized, providing the desired on-target specificity. FokI requires dimerization for the cleavage to occur, thus binding of two ZFNs or TALENs at different positions close to the cut site is required, naturally limiting the off-target effects and increasing the specificity and fidelity of these nucleases (Gupta & Musunuru, 2014). However, both platforms have limitations in the spectrum of DNA sequences that can target. In addition, their production is high cost and time-consuming, and their complex structure poses limitations to their delivery within the host. Thus, viral vectors such as adeno-associated virus (AAV) vectors or integrase-deficient LV (IDLV) may be exploited to facilitate their delivery (Gupta & Musunuru, 2014; Genovese *et al*, 2014).

These limitations, together with the recent finding about the bacterial CRISPR/Cas9 system, motivated the development of a new genome editing platform (Doudna & Charpentier, 2014; Shin & Oh, 2020) (**Figure 5**). The CRISPR/Cas9 system consists of a Cas9 nuclease and single guide RNA (sgRNA) of 20 nucleotide base pairs in length, which recognizes a desired DNA sequence specifically followed by a DNA motif called protospacer adjacent motif (PAM). The Cas9 and the sgRNA form a complex that targets the selected locus where the Cas9 induces a DSB near the PAM site (**Figure 5**). The most used Cas9, from Streptococcus pyogenes, cut upon recognition of the NGG PAM (Le Rhun *et al*, 2019). Thus, the PAM site distribution is a potential limitation of this technology. However, many efforts have allowed increasing the repertoire of usable Cas9, identifying other bacterial Cas9 (Ran *et al*, 2015; Müller *et al*, 2016) or developing unconventional PAM profiles by structure-guided engineering (Kleinstiver *et al*, 2015, 2016). This technology is easier to design and cost-effective. Still, safety may represent an issue as, despite the PAM requirement, mismatches can lead to unwanted breaks in

the genome that can cause off-target events or DNA rearrangements (Zhang *et al*, 2015). Therefore, the screening of undesired DSB in the genome is essential, especially for clinical translation.

Electroporation is currently the preferred strategy to deliver programmable nucleases *ex vivo* for HSPC GT purposes. A ribonucleoprotein complex (RNP) made of recombinant Cas9 protein pre-assembled with sgRNA is delivered to the cells allowing high and transient nuclease activity. The donor template, for HDR applications, is provided by electroporation of single-stranded phosphorothioate-modified oligodeoxynucleotides (ssODNs) (Pattabhi *et al*, 2019; Romero *et al*, 2019) or by transducing HSPC with IDLV or AAV6 vectors (Genovese *et al*, 2014; Schiroli *et al*, 2017; Rai *et al*, 2020).

In HSC, *ex vivo* gene editing can result in high NHEJ efficiency (Wu *et al*, 2019). However, there are constraints to the HDR due to the quiescence status of the cells, as this repairing machine is mostly express when cells are in S/G2 phase (Genovese *et al*, 2014). Thus, the gene correction levels that can be achieved in the LT-HSC are low (Schiroli *et al*, 2019).

Several strategies have been devised to maximize HDR efficiency in HSC. Culturing HSPC for 48-72h with inclusion of SR1, UM171, and PGE2 in the culture media allows increasing the HDR efficiency minimizing the effect of prolonged *ex vivo* culture on HSC repopulation capacity (Charlesworth *et al*, 2018; Ferrari *et al*, 2020). Initially, AAV6 showed superiority as template delivery vehicle as compared to IDLV (Schiroli *et al*, 2017; Pavel-Dinu *et al*, 2019). However, more recent data are highlighting a genotoxic burden associated with the use of AAV due to persistent inverted terminal repeats (ITR)-driven DNA damage response (DDR) activation. Optimization of the IDLV platform on the contrary allows to reach higher editing in LT-HSPC and shows a safer profile (Ferrari *et al*, 2022), supporting the use of IDLV for clinical translation. Finally, strategies aimed at forcing cell cycle progression have shown benefits in HDR-based editing efficiency in HSC (Ferrari *et al*, 2021b).

Two clinical trials are currently ongoing in HSC with ZFNs and CRISPR technologies to knockout the erythroid enhancer of BCL11A with the aim of increasing fetal hemoglobin levels in the context of β-thalassemia and SCD (Frangoul *et al*, 2021).

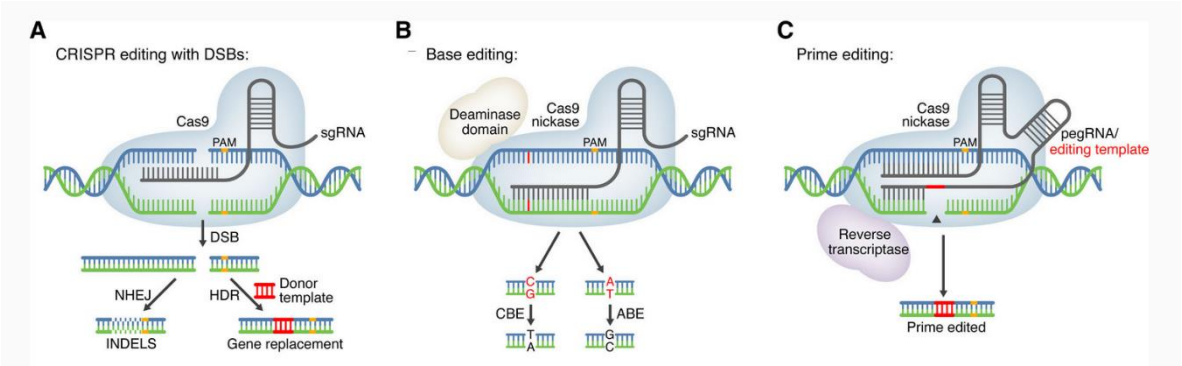

Figure 5. Gene editing platforms. A) *CRISPR/Cas9 nuclease induces a DSB in the genome, which can be repaired either by error-prone NHEJ or by HDR if a donor template is provided.* ***B)*** *Base editor converts adenosine into guanosine or cytosine into thymine without introducing dsDNA breaks in the genome.* ***C)*** *Prime editors can introduce specific DNA sequences in a desired locus (Rittiner et al, 2020).*

4.2.3.2. Base editors and prime editors

Base editors (BE) and prime editors (PE) are more recently developed gene editing platforms that allow high-precision gene modification without the need of introducing DSB in the genome and do not rely on the availability of a DNA template (**Figure 5**).

Different BE have been designed such as cytosine base editors (CBE), that deaminate a desired cytosine (C) into thymine (T) (Komor *et al*, 2016; Nishida *et al*, 2016), adenosine base editors (ABE), to deaminate adenosine (A) into guanosine (G) (Gaudelli *et al*, 2017), and glycosylase base editors (GBE), which allow interconversions between pyrimidines and purines (Kurt *et al*, 2021).

Base editors rely on a fusion protein composed of a Cas9 nickase (nCas9), a Cas9 able to generate a single-strand break, and a nucleobase deaminase enzyme, which is targeted to the desired locus by a sgRNA. Upon DNA binding, the DNA sequence is locally denatured, allowing the deaminase to bind the base of interest and catalyze the deamination reaction, which upon DNA replication will result in the desired base modification (Gaudelli *et al*, 2017) (**Figure 5**). BE can be exploited to mutate the start codon of a gene thus preventing its harmful expression, to restore gene expression by reverting a premature stop codon, or to silence a gene by inserting a stop codon within the coding sequence that will cause truncated mRNA degradation by the nonsense-mediated decay (Billon *et al*, 2017; Kuscu *et al*, 2017). Base editors have been exploited, as an alternative to NHEJ, to knockout BCL11A in gene therapy approaches for SCD and β-thalassemia (Zeng *et al*, 2020).

Prime editors can overcome the limited range of conversions that can be achieved by base editors, allowing the generation of all possible transitions and transversions, thus expanding the clinical applicability to a broad range of mutations (Kantor *et al*, 2020). In prime editors, nCas9 is fused to a reverse transcriptase enzyme. The complex is delivered to a desired sequence by a prime-editing guide (peg)RNA (Urnov, 2020), which provides the template for the reverse transcription. Upon DNA binding, nCas9 induces a break on the target strand and promotes hybridization with a primer-binding site (PBS) located at the 3' of the pegRNA. A new DNA fragment is synthetized by the reverse transcriptase and it will contain the mutation of interest specified by the PBS. After DNA repair, this sequence will be introduced in the target site (Anzalone *et al*, 2019; Yang *et al*, 2019) (**Figure 5**). *In vitro,* prime editors have demonstrated the potential to correct SCD-causing mutations (Anzalone *et al*, 2019).

Both BE and PE represent a promising therapeutic alternative for efficient and safe genome engineering as they avoid the introduction of DNA breaks and rely on a repair mechanism that, differently from the HDR, is active in both dividing and quiescent cells (Yeh *et al*, 2018), rendering them an attractive tool for HSC gene therapy. Nevertheless, base editors can promote non-specific RNA modification or introduce bystander mutations (Grünewald *et al*, 2019), with byproducts indels observed also with prime editors (Anzalone *et al*, 2019). Thus, continuous efforts are in place to improve the specificity and safety of these new emerging platforms (Doman *et al*, 2020).

4.2.4. Gene therapy hurdles: a focus on gene transfer

Despite the latest achievements in HSPC GT, which proved to be a safe approach for relieving clinical manifestations or even curing a broad range of hematological disorders, there are still some limitations that need to be addressed to broaden its applicability (Naldini, 2019; Ferrari *et al*, 2021a). A major limitation is the extent of gene transfer that can be achieved in repopulating HSC. Indeed, high variability in the outcome of clinical trials has been observed both among different trials and among patients enrolled in the same trial (Piras & Kajaste-Rudnitski, 2021). For instance, limited transduction turned out to be a major hurdle to achieve transfusion independency that represents the desired therapeutic benefit in β-thalassemia and SCD (Thompson *et al*, 2018; Marktel *et al*, 2019).

As previously mentioned, to achieve clinically relevant gene marking levels, HSC are subjected to prolonged *ex vivo* culture in presence of growth-promoting cytokines and are transduced twice at high vector doses. This implies costly large-scale vector production while impairing HSPC biological properties (Kallinikou *et al*, 2012; Larochelle *et al*, 2012; Glimm *et al*, 2000; Zonari *et al*, 2017). Different factors may affect the gene transfer into HSC, such as the vector design, the transduction protocol, and the nature of isolated HSC, according to the age and the disease condition of the patient (Naldini, 2019). Despite these variabilities, HSC *per se* are poorly permissive to viral transduction if compared to other cell types (Sutton *et al*, 1999). This is partly due to their quiescence status and their intrinsic high expression levels of ISG, which physiologically protect them against viral infection (Wu *et al*, 2018) while representing a barrier for vector-mediated gene transfer.

Indeed, one of the causes of the low permissiveness of HSPC to gene transfer may be ascribed to the viral origin of the vectors (Piras & Kajaste-Rudnitski, 2021). LV and γRV share with retroviruses the entry step and the process of integration of the viral genome in the nucleus (**Figure 3**). Each of these steps may be susceptible to host antiviral factors termed restriction factors, limiting the number of viral particles able to reach the nucleus (Piras & Kajaste-Rudnitski, 2021). The discovery of restriction proteins has guided the development of drugs or compounds to overcome them promoting better transduction (Wang *et al*, 2014; Petrillo *et al*, 2015; Zonari *et al*, 2017; Heffner *et al*, 2018; Petrillo *et al*, 2018).

Furthermore, recognition of viral vectors can activate signaling pathways that affect transduction efficiency and the biology of the cells, transiently or long-term (Piras *et al*, 2017; Schiroli *et al*, 2019; Ferrari *et al*, 2022). The responses to the vector depends on cellular sensors that are located within different cellular compartments and that can recognize as foreign different vector components or DNA breaks triggering activation of interferon responses or DDR (Piras & Kajaste-Rudnitski, 2021).

Devising strategies to counteract these cellular responses is important to ensure high gene transfer levels and sustain the fitness of the genetically engineered LT-HSC. Thus, a better understanding of vector-host crosstalk during HSC gene engineering will be fundamental to identify new approaches to overcome cellular restriction and sensing of viral vectors and guiding the progression toward more efficient gene therapy protocols (Piras & Kajaste-Rudnitski, 2021).

4.3. Vector-host crosstalk

4.3.1. Innate immune sensing

The innate immune system has a central role in host defense activating biological responses that are fundamental to mount efficacious adaptive immune responses to clear pathogens. Innate immune cells, such as monocytes, macrophages, neutrophils, dendritic cells, and epithelial cells express pattern recognition receptors (PRR) which are germline-encoded host proteins capable of recognizing general structures of pathogens, called pathogen-associated molecular patterns (PAMP) or molecules produced upon damage, named damage-associated molecular patterns (DAMP) (Amarante-Mendes *et al*, 2018). PAMP may include lipopolysaccharide (LPS), mannose, peptidoglycans, or bacterial and viral genetic material. Examples of DAMP are uric acid and extracellular ATP (Tang *et al*, 2012).

Commonly, the activation of PRR initiates signaling events that culminate in the recruitment of transcription factors, such as IRF3, IRF7, and NF-κB. This lead to the transcription of pro-inflammatory cytokines, such as TNFα, IL6, IL8, or type I interferons (IFN), which in turn up-regulate ISG, which exert the effector functions (Zhang & Liang, 2016).

There are different types of PRR, which differ in ligand specificity, can be cell-type specific, can localize in different cellular compartments, and can trigger activation of distinct signaling pathways. Among PRR mainly involved in the detection of viral nucleic acids, there are toll-like receptors (TLRs), retinoid acid-inducible gene-I (RIG-I)-like receptors (RLRs), and cytosolic DNA sensors (**Figure 6**).

Because retroviral vectors possess both RNA or DNA genome, according to the step of their life cycle, the presence of host nucleic acid sensors can lead to unwanted innate immune responses that can impair the transduction efficiency and affect the HSC properties. In addition, differently from their parental viruses that enter the cells by direct fusion, VSV-G pseudotyped vectors exploit the endocytic route, thus exposing their genome not only to cytosolic sensors but also potentially to endosomal TLR.

4.3.1.1. Toll-like receptors

There are 10 different TLR in humans (Bryant *et al*, 2015). TLR1, TLR2, TLR4, TLR5, TLR6, and TLR10 are located on the cell surface, where they mainly detect microbial structures. TLR3, TLR7, TLR8, and TLR9 localize on the endosomal membrane where they sense nucleic acids (Armant & Fenton, 2002). Among the nucleic acid sensors, TLR3 recognizes dsRNA molecules, TLR7 and TLR8 sense ssRNA and TLR9 detects unmethylated CpG-rich dsDNA (Armant & Fenton, 2002) (**Figure 6**).

TLR are transmembrane receptors consisting of three domains. An amino-terminal leucine-rich repeats (LRRs) region exposed to the lumen, a membrane-spanning domain, and a cytosolic toll-interleukin-1 receptor (TIR) portion. Upon ligand binding, TLR dimerize and the intracellular TIR domains associate promoting the recruitment of TIR-containing adaptor proteins, Myd88 and TRIF. TLR7, 8, and 9 recruits MyD88, IRAK, and TRAF6 with consequent activation of NFkB and recruitment of the IRF7 transcription factor. TLR3 instead recruits TRIF, TRAF3, and TRAF6, with subsequent phosphorylation of TANK-biding kinase (TBK1) and recruitment of IRF3 (El-Zayat *et al*, 2019).

Different TLR have been described to be involved in the response to different viruses. TLR3 activates immune responses against RNA viruses, such as West Nile virus (WNV) and encephalomyelitis virus (EMCV), but also DNA viruses like herpes simplex virus 1 (HSV-1), probably due to recognition of intermediate dsRNA molecules. TLR7 and TLR8 trigger immune responses against influenza A virus (IAV), HIV, and VSV. TLR9 sense DNA viruses, like MCMV, HSV-1/2 and adenoviruses (Xagorari & Chlichlia, 2008; Okude *et al*, 2021).

4.3.1.2. RNA sensors

The RLR family in mammals is composed of three members: RIG-I, melanoma differentiation-associated protein 5 (MDA5), and laboratory of genetics and physiology 2 (LGP2) (Hartmann, 2017; Goubau *et al*, 2013). They localize in the cytoplasm where they sense RNA genomes released by invading viruses triggering robust interferon responses, which induce their strong upregulation in various tissues (Xu *et al*, 2017) (**Figure 6**).

The RLR receptors share a common structural architecture with a C-terminal domain (CTD) that interacts with viral genome, a central DExD/H box catalytic helicase core that

hydrolyzes ATP, and two N-terminal caspase activation and recruitment domains (CARD) that are fundamental for the induction of the downstream signaling cascade (Liu & Gack, 2020; Rehwinkel & Gack, 2020). LGP2 lacks the CARD domains, making its role more controversial. Still, it has been suggested that LGP2 can help other family members in viral genome detection and signaling (Deddouche *et al*, 2014).

Specificity in RNA binding is determined by different RNA-binding loops within the CTD. RIG-I recognizes short RNA molecules. A 5'-triphosphate or diphosphate end as well as blunt-end base pair region at the 5' terminus are important for RIG-I activation (Hornung *et al*, 2006). MDA5 instead binds preferentially to dsRNA molecules longer than 1 kb (Kato *et al*, 2008). Binding between receptors and RNA mediates ATP-dependent exposure of the CARD domains that can bind CARD domains of mitochondrial antiviral signaling protein (MAVS) located on the surface of mitochondria. This initiates the recruitment of different signaling mediators including TRAF3 and I-kappa-B kinase-epsilon (IKKε)/TBK1 that activate IRF3 and IRF7 with subsequent production of interferon (Rehwinkel & Gack, 2020).

The RNA genome of viral vectors may represent a source of PAMP. Like their parental viruses, the genome of LV and γRV is capped at the 5' end, resembling host RNA and thus representing a poor activator for RIG-I (Chiu *et al*, 2002). However, it has been shown that RIG-I can recognize secondary structures within the HIV RNA genome, triggering the activation of immune responses (Solis *et al*, 2011; Berg *et al*, 2012). More recently, DDX41, an RNA helicase usually involved in RNA splicing, was described to be able to recognize RNA:DNA hybrids, that are produced during the RT of MLV genome. Recognition of RNA:DNA hybrids by DDX41 triggers STING-dependent signaling in murine macrophages and dendritic cells, through mechanisms that still need to be determined (Stavrou *et al*, 2018).

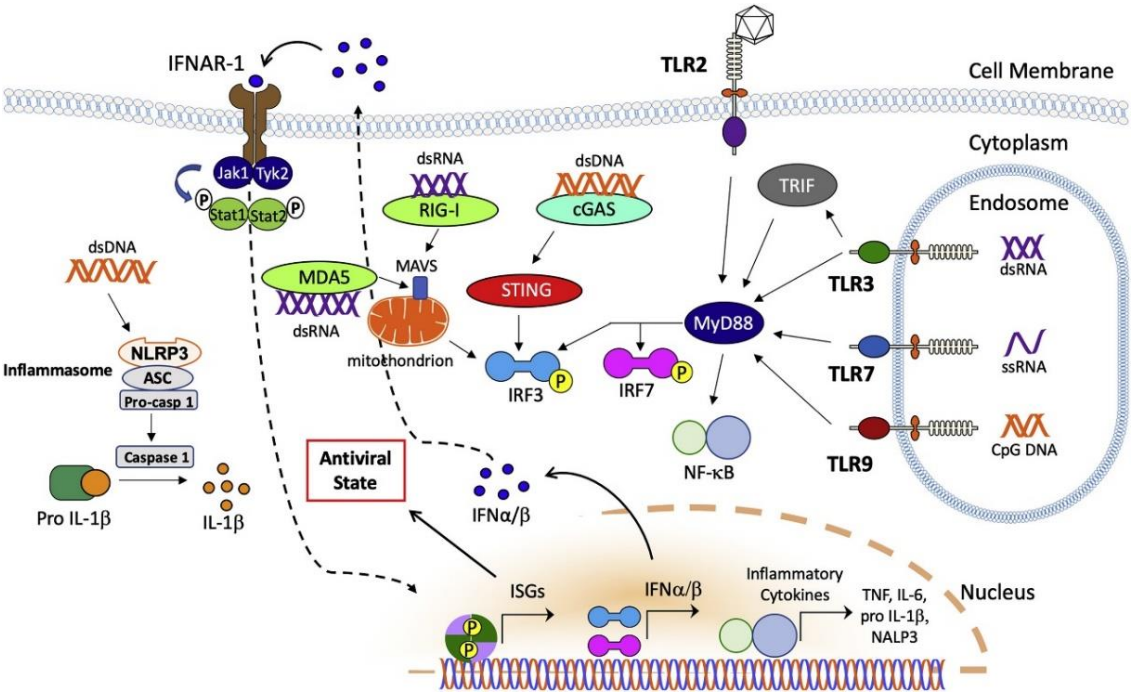

Figure 6. Innate immune sensing of exogenous nucleic acids. *The most common pathways involved in the recognition of exogenous nucleic acids are shown. Endosomal nucleic acids, either DNA, dsRNA, or ssRNA are sensed by endosomal TLRs, such as TL3, TLR7, and TL9. Cytosolic dsDNA is recognized by cGAS, which activates its downstream adaptor STING. RIG-I, MDA5, and their downstream adaptor MAVS are involved in the recognition of cytosolic dsRNA molecules. All these pathways culminate in the activation of transcription factors and production of interferons and pro-inflammatory cytokines. IFN released by the cells binds the IFNAR receptor on the neighboring cells causing up-regulation of ISG and induction of antiviral immunity (Shirley et al, 2020).*

4.3.1.3. DNA sensors

Self-DNA usually localizes in the nucleus or mitochondria, thus cytosolic viral DNA molecules alarm the cells and trigger the activation of cytosolic DNA sensors to ultimately induce antiviral responses (Schlee & Hartmann, 2016). Among the best-described cytosolic DNA sensors, we find absent in melanoma 2 (AIM2), IFN-gamma inducible protein 16 (IFI16), and cyclic GMP-AMP synthase (cGAMP).

Recognition of cytosolic DNA by AIM2 and IFI16 mediates the assembly of the inflammasome, a multiprotein complex that orchestrates a programmed inflammatory cell death named pyroptosis (Hayward *et al*, 2018).

The activation of type I IFN responses is mainly orchestrated by cGAS (**Figure 6**). cGAS binds to dsDNA molecules independently from the sequence with long dsDNA are

more potent in activating cGAS in respect to short molecules (Xiao & Fitzgerald, 2013). cGAS localizes mainly in the cytoplasm but can be present also in the nucleus (Volkman *et al*, 2019). Moreover, host DNA is accessible when the nuclear envelope disassembles during mitosis, thus mechanisms that prevent activation of cGAS against self-DNA are essential. Indeed, it has been shown that upon nuclear envelope breakdown, cGAS is phosphorylated by mitotic kinases, which results in its inactivation (Zhong *et al*, 2020). In addition, interaction with nucleosomes prevents cGAS activation, allowing its localization in the nucleus without triggering any aberrant activation (Kujirai *et al*, 2020).

Upon DNA binding, cGAS synthetizes the second messenger 2'3'-cGAMP that binds to the stimulator of IFN genes (STING) that localizes on the endoplasmic reticulum (ER) membrane. Once activated, STING moves to the Golgi while recruiting other signaling proteins. Palmitoylation is essential for its activation (Mukai *et al*, 2016) with subsequent interaction with TBK1 that phosphorylates IRF3 leading to IFN responses. STING can also induce nuclear translocation of NFkB with subsequent production of pro-inflammatory mediators (Chen *et al*, 2016) (**Figure 6**).

In addition to taking part in the inflammasome, IFI16 can mediate IFN responses upon intracellular DNA recognition, cooperating with the cGAS-STING pathway to promote defense mechanisms against viral DNA in specific cell types (Unterholzner *et al*, 2010; Almine *et al*, 2017).

The cytosolic DNA sensor cGAS has been described as critical sensor for retroviruses in primary monocyte-derived macrophages (MDM) and dendritic cells (DC) and cell lines. It recognizes the reverse-transcribed DNA when TREX1- or SAMHD1-dependent blocks to RT are removed (Gao *et al*, 2013; Stavrou *et al*, 2015). Additionally, capsid stability is fundamental to avoid innate sensing of viral genomes. Indeed, mutations in HIV-1 capsid that disrupt interaction with host cellular cofactors lead to earlier uncoating and mediate cytosolic cGAS-dependent recognition of DNA, with activation of IFN responses (Rasaiyaah *et al*, 2013). Similarly, a variant of MLV capsid that affects its stability induces stronger IFN production in MDM in respect to the original virus (Stavrou *et al*, 2013). In addition to cGAS, also IFI16 has been described as a sensor for lentiviral reverse-transcribed DNA. Upon binding to DNA, IFI16 activates STING-mediated signaling promoting the synthesis of antiviral mediators in myeloid cells (Jakobsen *et al*, 2013).

4.3.2. Viral vectors sensing in human hematopoietic stem cells

How all these factors play a role in sensing viral nucleic acids derived from gene therapy vectors in HSC is still under investigation (Piras & Kajaste-Rudnitski, 2021). HSC express a number of TLR (Nagai *et al*, 2006), suggesting that they are competent for pathogen immune detection and activation of effector functions. Moreover, it has been shown both *in vitro* and *in vivo* that TLR engagement affects HSC function (Sioud *et al*, 2006). TLR7/8 activation leads to myeloid progenitor skewing *in vitro*, while *in vivo* stimulation with the TLR4 ligand LPS, induces HSPC cycling and exhaustion with lymphoid versus myeloid bias (Esplin *et al*, 2011). In addition to TLR, HSC express cytosolic sensors like RLR and DNA sensors (Bowman & Trompouki, 2021). Despite their classical role in the host defense through exogenous nucleic acids detection, their activation is important to shape HSC formation during physiological processes such as development and regeneration (Lefkopoulos *et al*, 2020).

Based on these premises HSC are armed to potentially recognize and respond to different nucleic acids derived from viral vectors. In this regard, we have recently shown that distinct gene therapy vectors are differently recognized by HSPC (Piras *et al*, 2017). In particular, LV and AAV do not induce any immune response in HSC, thus escaping both endosomal and cytosolic nucleic acid recognition. Moreover, the removal of some of the critical host factors required for LV capsid stability is insufficient to activate type I IFN responses in human HSPC, suggesting that additional protective mechanisms are in place in these cells (Petrillo *et al*, 2015). However, despite avoiding immune recognition, both LV and AAV trigger induction of DNA damage response in HSPC with activation of apoptotic responses *in vitro* and reduced engraftment of ST-HSC *in vivo* (Piras *et al*, 2017; Schiroli *et al*, 2019). DDR occurs in a DSB-independent manner and is proportional to the amount of viral DNA that enters the nucleus (Piras *et al*, 2017). The steps leading to the induction of p53 are not fully understood. It could be that extra DNA in the nucleus alarms the cells that in turn activate the DDR. The yet-to-be-identified sensor of exogenous nuclear DNA could be a known DSB sensor or an innate immune sensor that links nucleic acid recognition with DDR in HSPC. In this regard, different reports are highlighting non-canonical roles for immune sensors in DDR (Dunphy *et al*, 2018; Unterholzner & Dunphy, 2019; Jiang *et al*, 2019). Whether IFI16 or nuclear cGAS may participate in viral vector recognition in HSPC still requires investigation. Differently from LV and AAV, γRV are unable to evade immune detection

and activate a robust IFN response in HSPC (Piras *et al*, 2017). We have shown that vector recognition is independent of the reverse transcription process, thus excluding canonical DNA sensors as the mediators of type I IFN in HSPC. Whether γRV share other common recognition mechanisms with the parental MLV remains to be addressed. Viral RNA genome may trigger activation of endosomal TLR or cytosolic RLR in HSPC, while structural components may represent an alternative detection platform for host immune factors. These different possibilities will be investigated in this thesis.

4.3.3. Host restriction factors

Different steps of the viral life cycle can be targeted by host antiviral factors, thus limiting viral replication and spread (Petrillo *et al*, 2015; Piras & Kajaste-Rudnitski, 2021). Most of the restriction factors are ISG highlighting their fundamental role in innate immune responses against viruses (Schoggins, 2019).

Viruses have the ability to continuously evolve and develop new strategies to overcome host restrictions, by expressing proteins able to directly target and inactivate specific antiviral factors or by masking viral domains that represent the main recognition site for host proteins. This ability of viruses to rapidly evolve has guided the adaptation of host immune responses, with mammalian cells expressing numerous, often redundant, host antiviral proteins (Duggal & Emerman, 2012).

Retroviral vectors used in gene therapy, like LV and γRV, can be targeted by restriction factors at multiple steps of their life cycle from entry to RNA reverse transcription into DNA, until viral DNA integration in the host genome. Moreover, differently from viruses, viral vectors are pseudotyped with different envelope glycoproteins and lack the expression of viral accessory proteins which overall may affect the place and the way in which they are recognized by host target cells.

4.3.3.1. IFITMs

IFN-induced transmembrane proteins (IFITMs) are antiviral host factors capable of restricting of a broad range of viruses including HIV, SARS, EBOLA, IAV, Dengue, WNV, and VSV (Brass *et al*, 2009; Huang *et al*, 2011; Weidner *et al*, 2010). IFITM2 and IFITM3 localize mainly in the early and late endosomes and lysosomes (Chesarino *et al*, 2014a,

2014b) while IFITM1, lacking the endo-lysosomal sorting motif, localizes in early endosomes and on the cell surface (Bailey *et al*, 2014).

Despite the knowledge about IFITMs' activity is continuously improving, the precise antiviral restriction mechanism of the different IFITMs is not fully elucidated and it varies according to their cellular localization, the type of invading virus, and on the target cells. IFITM3 exerts its antiviral function by blocking viral entry into target cells (Bailey *et al*, 2014; Smith *et al*, 2014). It has been proposed that IFITM3 can mediate alterations of the cell membrane like altering the lipid composition, increasing the curvature, or decreasing fluidity overall interfering with the viral fusion process (Amini-Bavil-Olyaee *et al*, 2013; Suddala *et al*, 2019; Tartour *et al*, 2017). Additional restriction by IFITM3 is dependent on its incorporation in nascent virions (Tartour *et al*, 2017; Zhao *et al*, 2019). The presence of IFITM3 and other IFITMs proteins on the viral membrane can lead to reduced infectivity, likely altering membrane fusion dynamics. Despite their prominent role in viral restriction, to date, no viral protein capable of specifically targeting IFITMs has been described.

We have demonstrated that IFITM3 is a major restriction factor against viral gene therapy vectors in both human and murine HSPC (Petrillo *et al*, 2018) restricting endocytic entry of VSV-G vectors. Indeed, when vectors are pseudotyped with the baboon envelop (BaEV) glycoprotein or with the amphotropic envelope glycoprotein, both of which mediate entry by fusion (Girard-Gagnepain *et al*, 2014; Ragheb *et al*, 1995), no restriction by IFITM3 is reported (Petrillo *et al*, 2018). Differently from LV and γRV, AAV6 remains insensitive to IFITM3, in line with the absence of a viral envelope (Petrillo *et al*, 2018).

4.3.3.2. SAMHD1

Sterile Alpha Motif (SAM) and Histidine Aspartate Domain (HD) containing protein 1 (SAMHD1) is a deoxynucleotide triphosphohydrolase that hydrolyses the deoxynucleotide triphosphates (dNTPs) into deoxynucleosides (dNs) and inorganic triphosphate, thus playing a central role in maintaining balanced dNTP intracellular concentrations (Goldstone *et al*, 2011) (**Figure 7**).

As dNTPs are largely consumed during replication, quiescent cells display intrinsic lower levels of intracellular dNTPs. In line, SAMHD1 has been described to potently restrict HIV-1 in non-dividing myeloid cells, as well as resting $CD4^+$ T cells, where it

limits viral RT by downregulating the intracellular dNTP pools (Lahouassa *et al*, 2012; Baldauf *et al*, 2012). SAMHD1 possesses also an RNase activity. However, how this contributes to SAMHD1-mediated restriction remains unclear (Antonucci *et al*, 2018; Ballana & Esté, 2015). SAMHD1 has been described as restriction factors for viruses like HIV-2, SIV, and MLV among others (White *et al*, 2013).

SAMHD1 comprises an N-terminal portion, with a nuclear localization sequence (NLS), a SAM domain involved in oligomerization, a functional HD domain through which binds nucleic acids, and a C-terminal variable domain (White *et al*, 2013). Despite the presence of a NLS, the catalytic activity and thus its antiviral function is independent of its localization, which can be nuclear or cytoplasmic (Hofmann *et al*, 2012). Deoxyguanosine triphosphate (dGTP)-dependent tetramerization is a key step for SAMHD1 activity (Yan *et al*, 2013). The dNTPase function correlates with cell cycle progression. During G0-G1 phases, SAMHD1 is dephosphorylated and can actively hydrolyze dNTPs. However, when cells enter the S phase and higher amounts of dNTPs are necessary for DNA synthesis, SAMHD1 is phosphorylated by cell cycle kinases such as cyclin A, CDK1/2 and 6 abolishing the antiviral function (Cribier *et al*, 2013; Pauls *et al*, 2014; Ruiz *et al*, 2015; Franzolin *et al*, 2013).

In line with the occurrence of RT, LV transduction is restricted in both human and murine myeloid cells (Wittmann *et al*, 2015; Bobadilla *et al*, 2013). HIV-2 and SIV encode an accessory protein, Vpx, that overcomes SAMHD1-mediated restriction (Goujon *et al*, 2008) (**Figure 7**). Upon interaction with SAMHD1, Vpx recruits the Cullin-4 E3 ubiquitin ligase complex that ubiquitinates SAMHD1 and promotes its proteasomal degradation (Laguette *et al*, 2011; Hrecka *et al*, 2011; Ahn *et al*, 2012). HIV-1 lacks Vpx and thus remains sensitive to SAMHD1 (Laguette *et al*, 2011). Virus-like particles (VLP) carrying Vpx or direct incorporation of Vpx into virions has demonstrated to be sufficient to counteract SAMHD1 in myeloid and resting $CD4^+$ T cells (Sunseri *et al*, 2011; Bobadilla *et al*, 2013) (**Figure 7**). Similarly, treatment of the culture media with dNs increases HIV-1 infection and LV transduction in macrophages and non-activated lymphocytes (Kootstra *et al*, 2000; O'Brien *et al*, 1994; Korin & Zack, 1999; Ravot *et al*, 2002; Ghassemi *et al*, 2022).

SAMHD1 may contribute to the low LV transduction efficiency also in HSPC. However, counteracting SAMHD1 through the accessory viral protein Vpx or with the delivery of exogenous dNs did not significantly improve LV transduction in stimulated HSPC (Li *et al*, 2015). As SAMHD1 restriction is limited to non-dividing cells, SAMHD1 role in LV

transduction may be more relevant in the context of unstimulated HSPC. Indeed, exogenous administration of dNTPs in murine unstimulated HSPC resulted in two folds increase in lentiviral transduction (Mikkola *et al*, 2000). Moreover, the presence of additional early restriction blocks to viral transduction in HSPC, like IFITM3, may potentially mask SAMHD1-mediated effect on LV transduction.

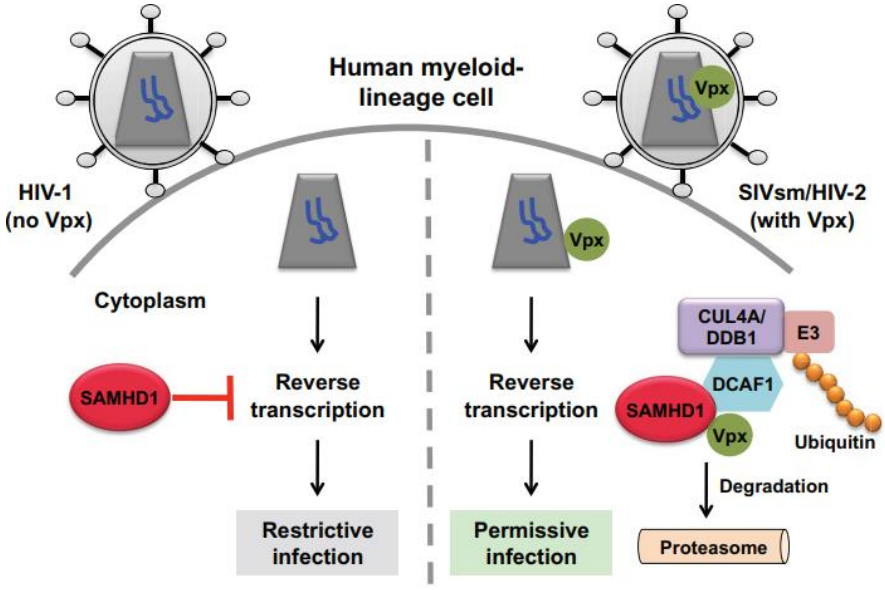

Figure 7. SAMHD1 restriction and Vpx counteraction of SAMHD1*. In human myeloid-lineage cells, HIV-1 infection is counteracted by SAMHD1, which acts at the level of viral RT by lowering the cellular dNTPs. HIV-1 does not encode accessory proteins to counteract this restriction. HIV-2 and SIVmac instead express Vpx that mediates SAMHD1 proteasomal degradation through recruitment of the host cell E3 ubiquitin ligase complex. This allows efficient viral reverse transcription and a permissive infection to occur (St Gelais & Wu, 2011).*

4.3.3.3. TRIM5

Tripartite motif (TRIM) proteins are a big family of E3 ligases (Han *et al*, 2011) implicated in many different cellular processes (Rajsbaum *et al*, 2014; Hatakeyama, 2017; Mandell *et al*, 2020).

TRIM members possess an N-terminal RING domain (R), one or two B-box domains (B), and a coiled-coil domain (CC), collectively termed RBCC structure. The RING portion possess an E3 ubiquitin ligase activity while the B-box and CC domains are important for protein oligomerization. The C-terminal region may differ among members, with a SPRY motif being the most common one. This domain is implicated in the interaction

with the viral capsid and specifies the spectrum of antiviral activity (Sawyer *et al*, 2005; Yap *et al*, 2005; Stremlau *et al*, 2005).

There are six main TRIM5 isoforms in human. TRIM5α has a SPRY domain and is the most expressed one (Battivelli *et al*, 2011). In some monkey species, the SPRY motif has been substituted by a cellular factor named cyclophilin A (CypA) leading to the evolution of the TRIM-CypA protein (Stoye & Yap, 2008). Both TRIM5α and TRIM-Cyp have species-specific antiretroviral activity (Stremlau *et al*, 2005). Rhesus monkey (rh)TRIM5α is unable to restrict SIVmac strains, while potently restricts HIV-1 and other SIV strains (Stremlau *et al*, 2004). On the other side, human (h)TRIM5α does not inhibit HIV-1 while N-tropic MLV and EIAV are strongly restricted (Yap *et al*, 2004; Keckesova *et al*, 2004).

It is currently suggested that the lack of human TRIM5α restriction of HIV-1 is not due to a lack of binding with the HIV-1 capsid. Usually, the cellular CypA protects HIV-1 capsid from recognition by hTRIM5α. When capsid-CypA interaction is disrupted, TRIM5α associates with viral cores and HIV-1 becomes susceptible to its restriction (Kim *et al*, 2019). Additionally, accelerated turnover of TRIM5α, mediated by the IFNα-dependent activation of the immunoproteasome, reprograms hTRIM5α for effective restriction of HIV-1 (Jimenez-Guardeño *et al*, 2019).

To exert its antiviral activity TRIM5α directly interacts with the incoming retroviral capsid through the SPRY domain, leading to its premature uncoating and impairing reverse transcription, thus arresting the progression of post-entry steps (Stremlau *et al*, 2006; Perron *et al*, 2007). TRIM5α monomers weakly associate with the viral core and the interactions through the CC and B domains are essential for higher-order assembly and to promote the formation of a hexagonal lattice on HIV-1 capsid (Ganser-Pornillos *et al*, 2011; Li *et al*, 2016). The subsequent recruitment of the proteasome machinery through the RING domain helps in degrading the viral RT complex (Kutluay *et al*, 2013; Wu *et al*, 2006).

TRIM5α acts also as a sensor of the viral core, mediating induction of innate immune responses. Assembly on the retroviral cores triggers N-terminal polyubiquitination of TRIM5α. N-terminally anchored ubiquitin chains promote TAK1 activity and induction of activator protein 1 (AP-1) and NFκB pathways (Pertel *et al*, 2011; Fletcher *et al*, 2018) and promote capsid proteasomal degradation (Fletcher *et al*, 2018).

Since hTRIM5α does not restrict HIV-1, LV transduction of HSC does not suffer from hTRIM5α restriction. Moreover, disruption of the interaction with CypA does not increase

susceptibility to TRIM5 in HSPC, as we have shown that transduction with a capsid mutant that is no more able to interact with CypA is not impaired (Petrillo *et al*, 2015), highlighting possible cell-type specific effects. Similarly, commonly used γRV in gene therapy are derived from the NB-tropic MoMLV which is insensitive to hTRIM5α (Perron *et al*, 2004; Ulm *et al*, 2007), thus not representing a major critical factor for HSPC transduction. Still, it has been suggested that hTRIM5α levels may correlate with transduction levels achieved in hHSPC (Evans *et al*, 2014). Whether this is directly dependent on TRIM5α or is an indirect effect remains to be elucidated.

4.3.4. Overcoming hurdles to gene engineering in HSPC

The innate immune sensors and restriction factors described above, as well as other critical factors potentially yet to be identified, can be targeted pharmacologically or can be counteracted by engineering gene therapy vectors to carry antagonizing accessory proteins, overall increasing the efficiency and safety of GT strategies.

Cyclosporine H (CsH) represents a prototypic example of a compound used to enhance HSC gene transfer that counteracts an antiviral restriction block. We have shown that CsH can be added during the *ex vivo* culture of HSPC to overcome IFITM3-mediated restriction (Petrillo *et al*, 2018). CsH acts by transiently degrading IFITM3 thus relieving an early restriction block to VSV-G vector entry into the cells. CsH strongly increases gene marking levels in the most primitive HSC compartment *in vivo*, without affecting cell viability or engraftment capacity. Since CsH leads to increased availability of IDLV, it potently improves also gene editing efficiency (Petrillo *et al*, 2018). We have reported that also Rapamycin significantly improves transduction in human and murine HSPC (Petrillo *et al*, 2015) and recently it has been proposed that this can be due to transient IFITM3-depletion (Shi *et al*, 2018). However, Rapamycin shows some degree of toxicity in respect to CsH, especially in the mPB-derived HSPC (Petrillo *et al*, 2019), and the fold enhancement achieved with Rapamycin is lower to CsH, with their combination being additive (Petrillo *et al*, 2018), suggesting possible differences in their mechanism of action. Recently, another compound, caraphenol A, has been shown to relieve LV restriction in HSPC by altering the amounts of IFITM2 and IFITM3 in late endosomes (Ozog *et al*, 2019). IFITM3 restriction can also be overcome by using fusion-dependent envelopes for pseudotyping LV (Petrillo *et al*, 2018). However, non-VSV-G

pseudotyped LV usually display a very low titer rendering it difficult to achieve clinically relevant gene marking levels.

Another strategy that can be exploited to counteract restriction factors is based on the natural activity of viral accessory proteins. Vpx incorporation, as described above (Bobadilla *et al*, 2013), can increase transduction efficiency in primary myeloid cells and has already been exploited in relevant preclinical settings (Escobar *et al*, 2014; Chiriaco *et al*, 2014), while only limited benefit has been observed in HSPC (Li *et al*, 2015). Whether Vpx effect can be more evident if coupled with early-acting transduction enhancers remains to be investigated.

As our knowledge about host-vector interactions increases, more tools to enhance transduction become available rendering mandatory the investigation of aspects related to dose-dependent vector signaling. For instance, the use of transduction enhancers may cause loss of gene marking (Masiuk *et al*, 2019), which may be ascribed to strong vector-dependent activation of DDR (Piras *et al*, 2017). We have shown that ataxia-telangiectasia mutated (ATM) protein inhibition can be exploited to prevent LV- or AAV-mediated p53 activation in HSPC, rescuing the delay in HSPC engraftment *in vivo* (Piras *et al*, 2017; Schiroli *et al*, 2019). Another approach to overcome p53 is by transiently overexpressing GSE56, a p53-derived peptide that exert an inhibitory function (Ossovskaya *et al*, 1996), which is currently exploited in gene editing procedures (Schiroli *et al*, 2019; Ferrari *et al*, 2020).

Overall, a better knowledge of basic immune mechanisms behind HSC-vector crosstalk may guide the amelioration of vectors and gene therapy platforms with the aim of maximizing the outcome of cell manipulation while preserving cell fitness.

5. AIM OF THE WORK

Hematopoietic stem cell gene therapy has demonstrated great potential in the treatment of blood monogenic disorders. Still, prolonged *ex vivo* culture and multiple rounds of transduction are necessary to reach the desired and sufficient gene marking levels. One of the reasons behind poor permissiveness to transduction is the viral origin of the vectors. On one side, HSPC express innate immune sensors that can recognize the vector as foreign and trigger activation of immune pathways, on the other side antiviral factors can hamper lentiviral transduction acting at different steps of the retroviral life cycle, with an overall impact on gene therapy output.

On these premises, my PhD project focuses on shed light on the complex network of vector-host interactions with two main aims focusing on the two aspects of this interaction:

1. Investigate the molecular mechanism behind viral vector-mediated signaling in HSPC, focusing on γRV-induced response.
2. Investigate the restriction mechanisms that contribute to HSPC resistance to viral vector transduction, focusing on SAMHD1 role in stimulated and unstimulated HSPC.

Investigation of immune players of cell-vector interaction would allow us to expand our knowledge of the innate immune defense pathways of human HSPC and support the development of improved gene therapy protocols.

6. RESULTS

6.1. Investigating innate immune responses to viral vectors in human hematopoietic stem cells

6.1.1. Lentiviral vectors escape innate immune sensing in HSPC while γ-retroviral vectors lead to robust activation of type I interferon responses

Previous results of the lab have shown that different viral gene therapy vectors elicit distinct responses in hematopoietic stem and progenitor cells (Piras *et al*, 2017). While LV and AAV6 vectors escape innate immune recognition, γRV induce strong type I interferon responses in HSPC, as measured by the upregulation of different interferon-stimulated genes (**Figure 8A**). Interestingly, this recognition occurs despite γRV is less efficient in transducing HSPC as compared to LV (**Figure 8B**). Moreover, it has been shown that the activation of type I IFN responses in HSPC seems not to be mediated by the reverse-transcribed DNA genome, as transduction in presence of azidothymidine (AZT), a reverse-transcription inhibitor, still triggered strong levels of ISG upregulation (**Figure 8C**) (Piras *et al*, 2017).

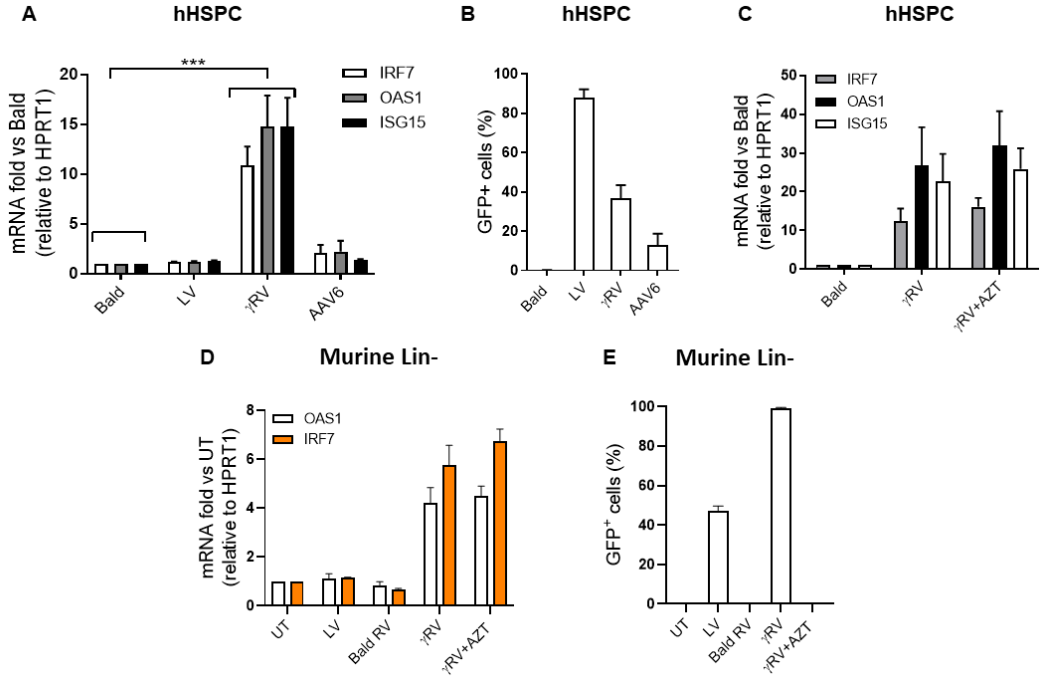

Figure 8. Lentiviral vectors escape innate immune sensing in HSPC while γ-retroviral vectors lead to robust activation of type I interferon responses. A) *Human cord blood (CB)-derived CD34⁺ were transduced with LV (MOI=100), p24 equivalent of bald control vector, γRV (MOI=100), or AAV (MOI=10000). IRF7, OAS1, ISG15 levels were measured 48h post-transduction. mRNA expression was normalized to HPRT1 and expressed in fold versus bald control vector (mean ± SEM, for IRF7 and OAS1 n = 18 for Bald and LV, n = 12 for γRV and n = 8 for AAV6, for ISG15 n = 10 for Bald, LV , n = 8 for γRV and n = 2 for AAV6, Dunn's adjusted Kruskal-Wallis test, ***p ≤ 0.001) (Piras et al, 2017).* ***B)*** *Human CB-CD34⁺ were transduced with vectors as in figure 8A. Percentages of transduced cells were assessed at 5 days post-transduction by FACS (mean ± SEM, n = 11 for Bald and LV, n = 12 for γRV and n = 8 for AAV6, for ISG15 n = 10 for Bald, n = 12 for LV , n = 9 for γRV and n = 13 for AAV6) (Piras et al, 2017).* ***C)*** *Human CB-CD34⁺ were transduced with γRV (MOI=100) in presence or not of the reverse-transcription inhibitor Azidothymidine (AZT). IRF7, OAS1, ISG15 levels were measured 48 h post-transduction. mRNA expression was normalized to HPRT1 and expressed in fold versus Bald control vector (mean ± SEM, n = 6 for γRV, γRV + AZT)* (Piras *et al*, 2017). ***D)*** *Murine lineage negative cells were transduced with the indicated vectors (MOI=100). OAS1 and IRF7 levels were measured 48h post-transduction. mRNA expression was normalized to HPRT1 and expressed in fold versus untransduced condition (UT) (mean ± SEM, n=2).* ***E)*** *Percentages of transduced cells from figure 8D were assessed at 5 days post-transduction by FACS (mean ± SEM, n=2).*

The response to γRV is conserved across species, as similar activation of IFN response was induced in murine HSPC, where we confirmed a reverse-transcription independent recognition of the vector (**Figure 8E**). Given the strong immunogenicity of viral nucleic acids (Habjan & Pichlmair, 2015; Hartmann, 2017) and given the lack of impact of RT inhibitors on γRV signaling, we hypothesized that the RNA genome could be the main source of ISG induction, prompting us to further elucidate the mechanisms behind γRV recognition.

6.1.2. γRV induce an early, reverse-transcription independent upregulation of interferon-stimulated genes in primary human macrophages

In the attempt to better dissect the mechanisms of γRV recognition, we searched for alternative cheaper and easier to handle experimental models as compared to human/murine hematopoietic stem cells that could recapitulate the responses to γRV. We found that human primary macrophages responded to transduction similarly to HSPC in terms of type I IFN responses, with LV escaping innate immune recognition and γRV triggering robust upregulation of ISG (**Figure 9A**). This recognition occurred despite low γRV transduction efficiencies in differentiated, non-proliferating cells (**Figure 9B**). In line with the HSPC phenotype, ISG induction was still significant upon transduction in presence of AZT (**Figure 9C-D**). The upregulation of ISG upon exposure to γRV was

observed as early as 6h post transduction with levels increasing over time reaching a peak around 24h. The response strongly decreased once the vector was washed away at 24h (**Figure 9E-F**). We next wondered whether ISG induction in MDM was dependent on IFN release, and thus on the type I IFN signaling. IFNα mRNA levels showed upregulation at 12-24h post transduction (**Figure 9G**). Moreover, the response to the vector was completely lost when we transduced the cells in presence of an anti IFNα receptor (IFNAR) antibody (**Figure 9H**), suggesting a link between ISG upregulation and type I IFN signaling. These results were confirmed in the murine setting as murine lineage negative (Lin-) HSPC from mice knock-out (KO) for the IFNα receptor (Müller *et al*, 1994) completely failed to elicit an immune response against the vector (**Figure 9I**), despite being as efficiently transduced as their wild type (WT) counterparts (**Figure 9J**).

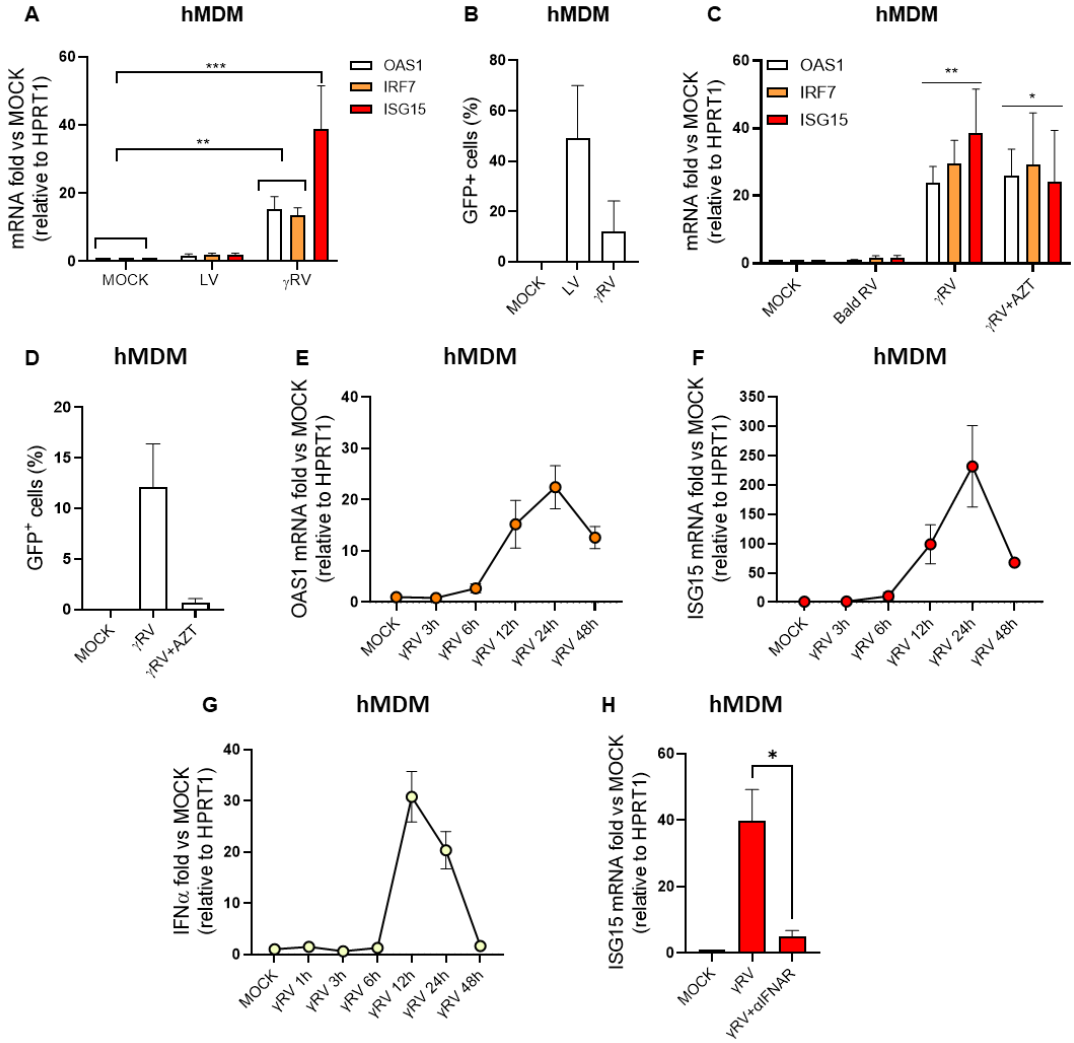

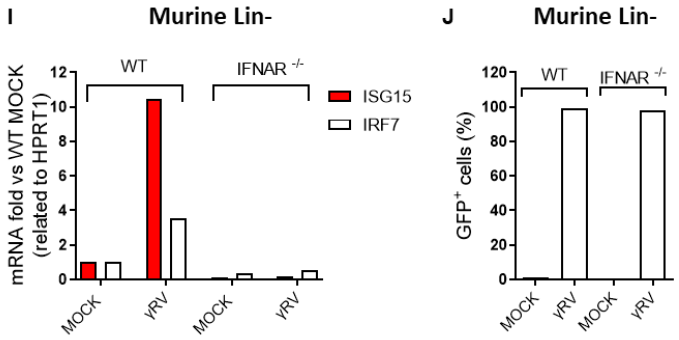

Figure 9. γRV induce an early, reverse-transcription independent upregulation of interferon-stimulated genes in primary human macrophages. A) *Human MDM were transduced with LV or γRV (MOI=10). ISG levels were measured 24h post-transduction. mRNA expression was normalized to HPRT1 and expressed in fold versus mock control (mean ± SEM, for OAS1 n=4 for LV, n=5 for γRV, for IRF7 n=3 for LV n=4 for γRV, for ISG15 n=7, Dunn's adjusted Kruskal-Wallis test, **p≤0.01; ***p≤0.001).* ***B)*** *Human MDM were transduced with LV or γRV (MOI=10). Percentages of transduced cells were assessed at 5 days post-transduction by FACS (mean ± SEM, n=8).* ***C)*** *Human MDM were transduced with γRV in presence or not of AZT or by volume equivalent of a bald RV vector. ISG levels were measured 24 h post-transduction. mRNA expression was normalized to HPRT1 and expressed in fold versus mock control (mean ± SEM, for OAS1 n=3 for bald γRV, n=6 for γRV, n=4 for γRV+AZT, for IRF7 n=2 for bald γRV, n=5 for γRV, n=3 for γRV+AZT, for ISG15 n=5 for bald γRV, n=7 for γRV, n=4 for γRV+AZT, Dunn's adjusted Kruskal-Wallis test, *p≤0.05; **p≤0.01).* ***D)*** *Human MDM were transduced as in C. Percentages of transduced cells were assessed at 5 days post-transduction by FACS (mean ± SEM, n=3 for Bald γRV, n=8 for γRV, n=5 for γRV+AZT).* ***E-F)*** *OAS1 (E) and ISG15 (F) levels were analyzed at the indicated time points in MDM after γRV exposure. mRNA expression was normalized to HPRT1 and expressed in fold versus mock control (mean ± SEM, n=2 for 3h, n=4 for 6-12, n=5 for 24h, n=1 for 48h).* ***G)*** *IFNα level was analyzed at the indicated time points in MDM after γRV exposure. mRNA expression was normalized to HPRT1 and expressed in fold versus mock control (mean ± SEM, n=1 for 3h, n=2 for 6-12, n=3 for 24h, n=1 for 48h).* ***H)*** *Human MDM were transduced with γRV in presence or not of the anti-INFAR. ISG15 level was measured 24h post-transduction. mRNA expression was normalized to HPRT1 and expressed in fold versus mock control (mean ± SEM, n=4, Mann Whitney test, *p≤0.05).* ***I)*** *Murine Lin- from WT or IFNAR KO mice were transduced with γRV (MOI=100). ISG15 level was measured 48h post-transduction. mRNA expression was normalized to HPRT1 and expressed in fold versus WT mock control (n=1).* ***J)*** *Percentages of transduced cells from figure I were assessed at 5 days post-transduction by FACS (n=1).*

6.1.3. γRV is recognized in the cytosol in a nucleic-acid independent manner

Our previous data excluded the reverse-transcribed DNA as the trigger of γRV recognition, leading us to hypothesize that the innate immune responses upon γRV exposure could be induced by the viral RNA genome. We first investigated the involvement of endosomal TLRs in γRV recognition, as these vectors are pseudotyped with the VSV glycoprotein, which mediates entry through endocytosis. ssRNA is a natural ligand of TLR7/TLR8 (Heil *et al*, 2004; Diebold *et al*, 2004). TLR7 has been implicated in

the sensing of different RNA viruses (Diebold *et al*, 2004; Lund *et al*, 2004). Moreover, it has been identified as a murine leukemia virus sensing receptor in mice (Kane *et al*, 2011). In addition, ssRNA genomes may internally base pair forming secondary structures, which can trigger activation of TLR3 (Tatematsu *et al*, 2013). For these reasons, we tested which impact blocking TLRs activation or signaling during transduction with γRV would have on ISG induction. While the TLR3/dsRNA complex inhibitor controlled the response induced by the synthetic dsRNA analogue poly (I:C) (**Figure 10A**), it had no impact on the response to γRV (**Figure 10B**), likely excluding TLR3 as a candidate sensor. In absence of a direct antagonist targeting TLR7/8, we exploited an inhibitor for their downstream adaptor MyD88. Again, while the MyD88 inhibitory peptide (Pepinh-MYD) antagonized the response induced by lipopolysaccharide (LPS) (**Figure 10C**), ISG induction upon γRV exposure was not affected (**Figure 10E**). Similarly, Lin- cells from MyD88$^{-/-}$ mice (Hou *et al*, 2008) maintained vector recognition ability (**Figure 10F-10G**). To more broadly target other TLRs, potentially involved in vector sensing, we tested the impact of inhibiting the adaptor protein TRIF. While the TRIF inhibitory peptide (pepinh-TRIF) strongly reduced poly (I:C)-dependent signaling (**Figure 10D**), no effect was observed when combined with γRV transduction (**Figure 10E**). We next investigated other potential TLR-mediated but nucleic-acid independent sources of immune activation. As VSV-G has been reported to trigger a specific antiviral TLR4-dependent interferon response in myeloid cells (Georgel *et al*, 2007), we decided to rule out the possibility that VSV-G sensing could participate in RV-mediated signaling. The TLR4 inhibitor CLI-095 efficiently blocked canonical LPS-driven stimulation of the receptor (**Figure 10H**) but did not impaired the activation of type I IFN response occurring upon γRV transduction (**Figure 10I**). Similar data were obtained in Lin- from TLR4$^{-/-}$ mice (Hoshino *et al*, 1999), in which γRV induced ISG upregulation similarly to WT Lin- cells (**Figure 10J**) at comparable level of transduction (**Figure 10K**).

Together, this data supports the notion that recognition of γRV is not mediated by TLRs and other RNA sensors could be involved. In agreement, when we pseudotyped the γRV with the baboon endogenous retroviral envelope (BaEV) or with the RD114 envelope that both mediate entry by direct plasma membrane fusion, we still observed a significant induction of type I IFN responses upon transduction (**Figure 10L**) suggesting that viral recognition likely occurs in the cytosol. At this point, to directly assess whether the vector RNA genome was required for RV-induced signaling we produced virus-like particles (VLP) devoid of the genomic RNA. Surprisingly these empty vectors that lack

viral RNA genome still triggered significant ISG expression (**Figure 10M**), suggesting that viral recognition is occurring in a nucleic-acid independent manner and highlighting a possible role for the structural components of the vector.

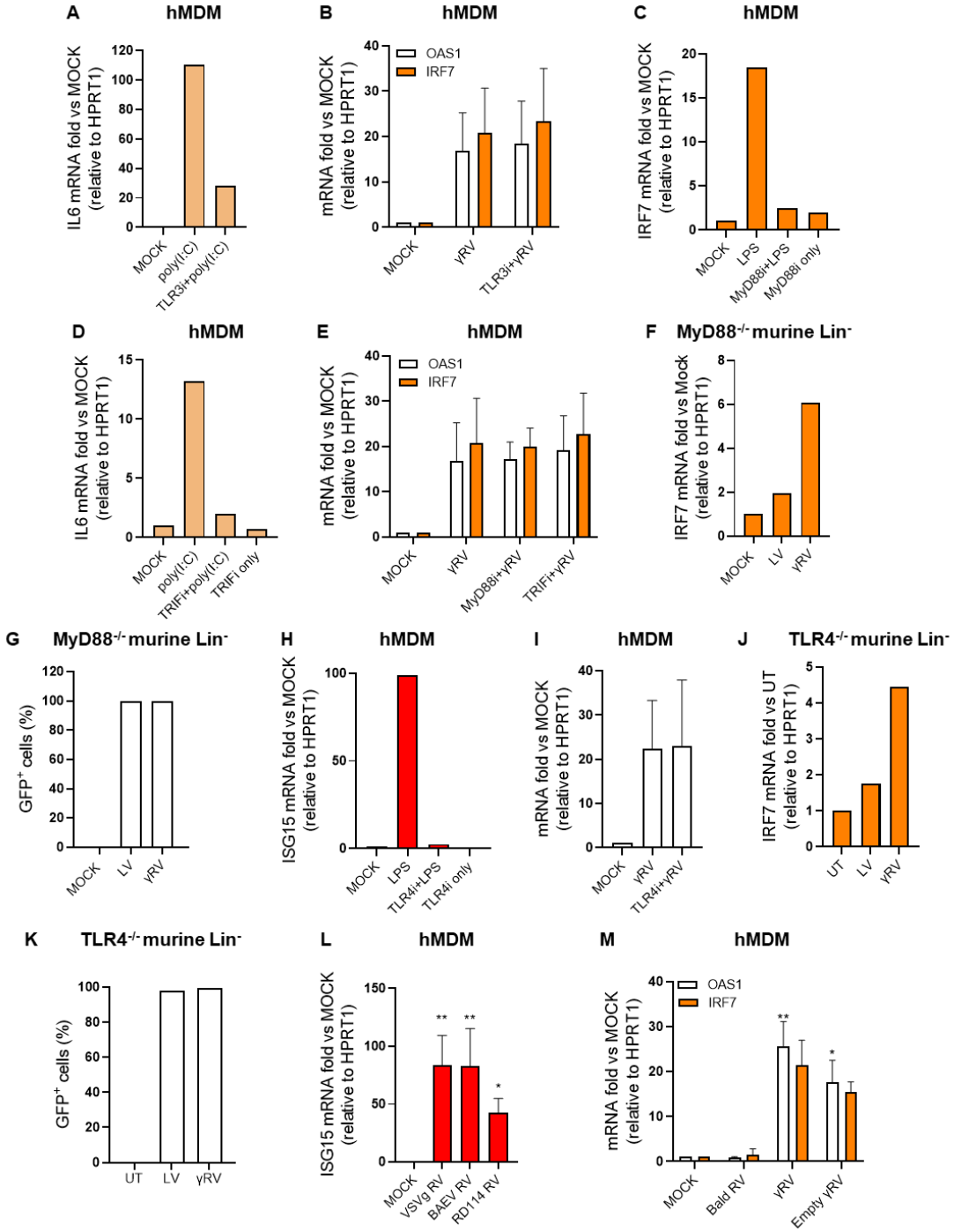

Figure 10. γRV is recognized in the cytosol in a nucleic-acid independent manner. A) *hMDM were stimulated with poly(I:C) in presence or not of the TLR3 inhibitor. IL6 level was measured 24h post-transduction. mRNA expression was normalized to HPRT1 and expressed in fold versus mock control (n=1).* ***B)*** *hMDM were transduced with γRV (MOI=10) in presence or not of TLR3/dsRNA complex inhibitor. ISG levels were measured 24h post-transduction. mRNA expression was normalized to HPRT1 and expressed in fold versus mock control (mean ± SEM, n=3).* ***C)*** *hMDM were stimulated with LPS in presence or not of the MyD88 inhibitory peptide. IRF7 level was measured 24h post-transduction. mRNA expression was normalized to HPRT1 and expressed in fold versus mock control (n=1).* ***D)*** *hMDM were stimulated with poly(I:C) in presence or not of the TRIF inhibitory peptide. IL6 level was measured 24h post-transduction. mRNA expression was normalized to HPRT1 and expressed in fold versus mock control (n=1).* ***E)*** *hMDM were transduced with γRV (MOI=10) in presence or not of the MyD88 or TRIF inhibitory peptides. ISG levels were measured 24h post-transduction. mRNA expression was normalized to HPRT1 and expressed in fold versus mock control (mean ± SEM, n=3).* ***F)*** *Murine Lin- cells from MyD88 KO mice were transduced with LV or γRV (MOI=100). IRF7 level was measured 48h post-transduction. mRNA expression was normalized to HPRT1 and expressed in fold versus mock control (n=1).* ***G)*** *Percentages of transduced cells from figure F were assessed at 5 days post-transduction by FACS (n=1).* ***H)*** *hMDM were stimulated with LPS, in presence or not of the TLR4 inhibitor. ISG15 level was measured 24h post-transduction. mRNA expression was normalized to HPRT1 and expressed in fold versus mock control (n=1).* ***I)*** *hMDM were transduced with γRV (MOI=10) in presence or not of TLR4 inhibitor. OAS1 level was measured 24h post-transduction. mRNA expression was normalized to HPRT1 and expressed in fold versus mock control (mean ± SEM, n=2).* ***J)*** *Murine Lin- cells from TRL4 KO mice were transduced with LV or γRV (MOI=100). IRF7 level was measured 48h post-transduction. mRNA expression was normalized to HPRT1 and expressed in fold versus mock control (n=1).* ***K)*** *Percentages of transduced cells from figure H were assessed at 5 days post-transduction by FACS (n=1).* ***L)*** *hMDM were transduced with VSV-G γRV, BAEV γRV or RD114 γRV (MOI=10). ISG15 level was measured 24h post-transduction. mRNA expression was normalized to HPRT1 and expressed in fold versus mock control (mean ± SEM, n=5 for VSV-G-γRV and BAEV-γRV, n=6 for RD114-γRV, Dunn's adjusted Kruskal-Wallis test vs. mock control, *p≤0.05; **p≤0.01).* ***M)*** *hMDM were transduced with γRV (MOI=10) or volume equivalent of empty γRV particles. ISG levels were measured 24h post-transduction. mRNA expression was normalized to HPRT1 and expressed in fold versus mock control (mean ± SEM, n=4 for OAS1, n=3 for IRF7, Dunn's adjusted Kruskal-Wallis test, *p≤0.05; **p≤0.01).*

6.1.4. Interferon-stimulated genes response is not induced by vector contaminants

It is known that laboratory grade vector productions lead to retained contaminants within the vector stock (Merten *et al*, 2016; Soldi *et al*, 2020). Since different triggers can activate macrophages, in line with their essential role in orchestrating immune responses, we tried to carefully rule out the contribution of possible non-specific responses mediated by our vector preparation to the induction of type I IFN responses by γRV. Plasmids from the producer cells can activate antiviral immune responses through TLR9 in plasmacytoid dendritic cells (pDC) (Pichlmair & Reis e Sousa, 2007). However, we did not observe any lowering of the ISG response when we transduced the cells in presence of a synthetic oligonucleotide that antagonizes TLR9 (**Figure 11A**).

Another possibility could be that plasmid DNA is packaged within the viral core from the producer cells and it is released only upon viral uncoating within the target cells. As the cGAS/STING pathway plays a central role in detection of cytosolic DNA, we directly assessed its involvement in γRV signaling. Importantly, pharmacological inhibition of STING did not affect the response to γRV (**Figure 11B**), despite efficiently dampening ISG induction upon stimulation with the direct STING agonist 2'3' cGAMP (**Figure 11C**). We next measured the total amount of dsDNA and checked for the presence of contaminating plasmid within γRV, empty γRV and LV stocks. Despite contaminants were detected in all of the preparations, total DNA levels were comparable between γRV and LV (**Figure 11D**). Moreover, DNase treatment of full and empty γRV stocks did not affect the response to these vectors (**Figure 11E**), despite efficiently reducing the amount of contaminants (**Figure 11D**).

Overall, our data suggest that the γRV vector preparations did not carry contaminants responsible for eliciting ISG induction in MDM, supporting the possibility that structural components of the vectors are the main trigger of RV sensing.

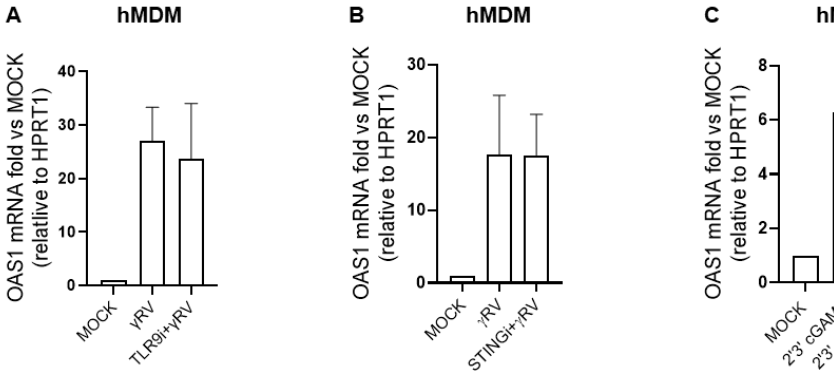

D vector stocks

	dsDNA		VSV-G Copies	
	STOCK	+ DNase I	STOCK	+ DNase I
γRV	18.2 ug/ml	7.6 ug/ml	1.35E+10 copies/ml	6.7E+07 copies/ml
eγRV	54.7 ug/ml	13.2 ug/ml	1.2E+10 copies/ml	8.7E+07 copies/ml
LV	15.5 ug/ml		1.2E+10 copies/ml	

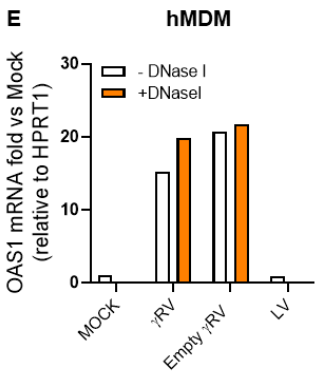

Figure 11. Interferon-stimulated genes response is not induced by vector contaminants. ***A)*** *hMDM were transduced with γRV (MOI=10) in presence or not of TLR9 anatgonist. OAS1 level was measured 24h post-transduction. mRNA expression was normalized to HPRT1 and expressed in fold versus mock control (mean ± SEM, n=2).* ***B)*** *hMDM were transduced with γRV (MOI=10) in presence or not of the synthetic indole derivative H151, a STING inhibitor. OAS1 level was measured 24h post-transduction. mRNA expression was normalized to HPRT1 and expressed in fold versus mock control (mean ± SEM, n=4).* ***C)*** *hMDM were stimulated with the 2'3' cGAMP, STING ligand, in presence or not of H151. OAS1 level was measured 24h post-transduction. mRNA expression was normalized to HPRT1 and expressed in fold versus mock control (n=1).* ***D)*** *Total amount of dsDNA and VSV-G copies were measured within a γRV, empty γRV and LV vector stocks before and after 2 hours treatment with DNaseI at 37°C (n=1 stock for each indicated vector).* ***E)*** *hMDM were transduced with γRV (MOI=10), volume equivalent of empty γRV or LV (MOI 10) treated or not with DNaseI for 2 hours at 37°C. OAS1 level was measured 24h post-transduction. mRNA expression was normalized to HPRT1 and expressed in fold versus mock control (n=1).*

6.1.5. Canonical nucleic acid sensors are dispensable for γRV recognition

To further exclude the role of nucleic acids in γRV-dependent induction of type I IFN, we decided to validate genetically our preliminary observations pointing towards a mechanism of structural rather than nucleic acid recognition of the vector. For this purpose, we exploited the pro-monocytic U937 cell line to generate KO for the canonical nucleic acid sensors. Interestingly we observed that U937 cells were unresponsive to viral vectors, despite being efficiently transduced by both LV and γRV (**Figure 12A-B**). However, upon differentiation in macrophage-like cells through PMA treatment they started to recapitulate the γRV sensing phenotype observed in primary MDM. Indeed, in PMA-differentiated U937 cells γRV triggered upregulation of ISG in a nucleic acid-independent manner (**Figure 12C**), despite being restricted due to the unproliferative status of the cells (**Figure 12D**). We thus exploited this cell line to address the contribution of different cytosolic nucleic acid sensors in γRV recognition. We generated KO cell lines for the cGAS and STING, involved in DNA sensing. After validation (**Figure 12E-F**), the cells were PMA differentiated and transduced with LV or γRV. Importantly we observed that both KO cell lines still upregulated ISG upon RV but not LV exposure (**Figure 12G**), confirming that the cGAS/STING pathway is not activated upon γRV recognition. We next focused on RNA sensing, generating KO cell lines for RIG-I and MAVS (**Figure 12H-I**). PMA-differentiated KO cells were still capable of responding to γRV (**Figure 12J**), confirming also that the RNA genome is not the main trigger of antiviral responses against γRV in MDM.

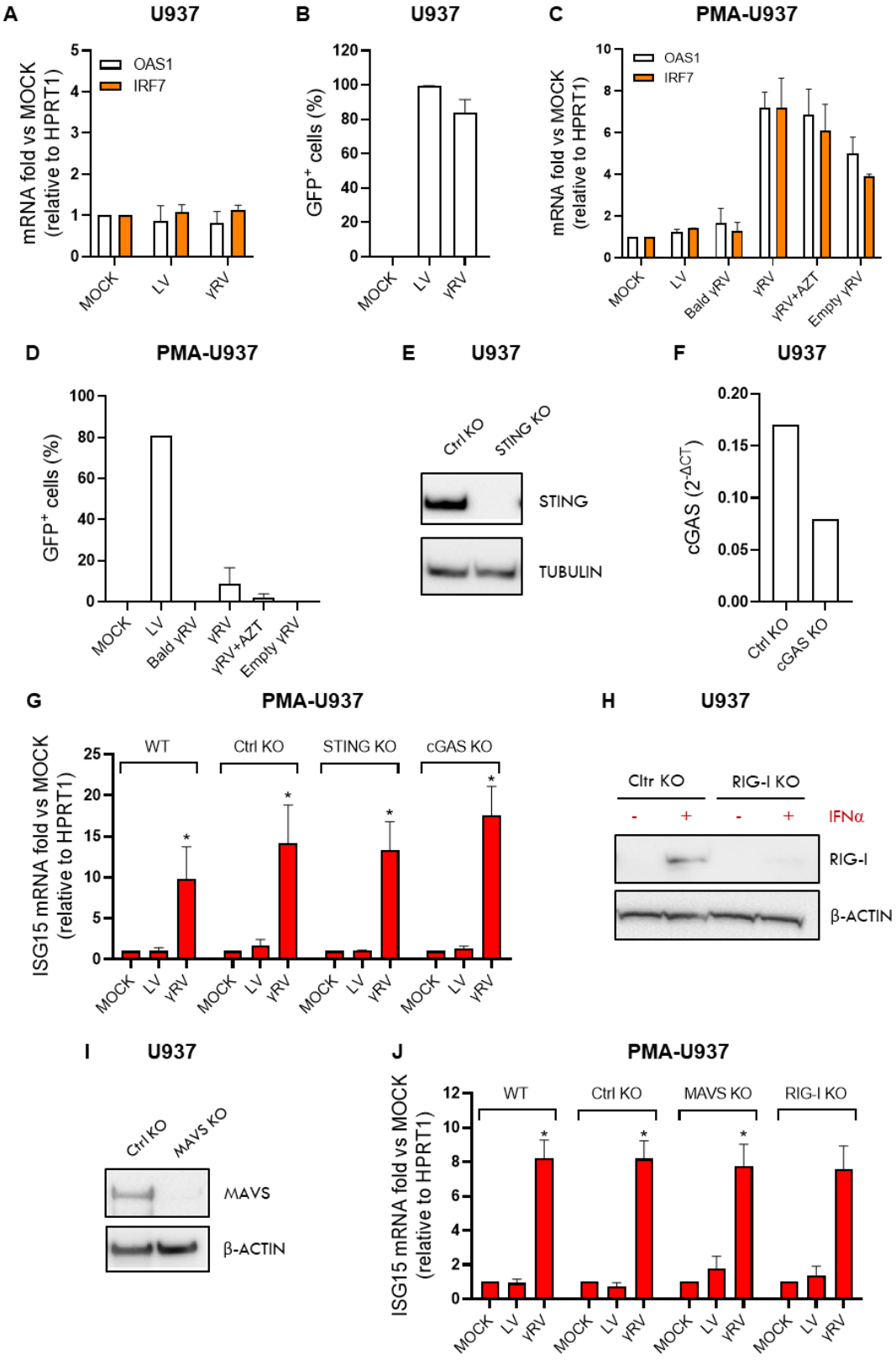
A
U937
mRNA fold vs MOCK (relative to HPRT1)
OAS1
IRF7
MOCK
LV
vRV
B
U937
GFP+ cells (%)
C
PMA-U937
Bald vRV
vRV+AZT
Empty vRV
D
PMA-U937
E
U937
Ctrl KO
STING KO
STING
TUBULIN
F
U937
cGAS (2-ΔCT)
cGAS KO
G
PMA-U937
ISG15 mRNA fold vs MOCK (relative to HPRT1)
WT
Ctrl KO
STING KO
cGAS KO
H
U937
Cltr KO
RIG-I KO
IFNα
RIG-I
β-ACTIN
I
U937
MAVS KO
MAVS
β-ACTIN
J
PMA-U937
MAVS KO
RIG-I KO

Figure 12. Canonical nucleic acid sensors are dispensable for γRV recognition. A) *U937 cells were transduced with γRV (MOI=50), volume equivalent of bald γRV and LV (MOI=50). ISG levels were measured 24h post-transduction. mRNA expression was normalized to HPRT1 and expressed in fold versus mock control (mean ± SEM, n=3).* ***B)*** *Percentages of transduced cells from figure 12A were assessed at 5 days post-transduction by FACS (mean ± SEM, n=3).* ***C)*** *PMA differentiated U937 cells were transduced with LV (MOI=50), γRV (MOI=50), volume equivalent of bald and empty γRV, or γRV in presence of AZT. ISG levels were measured 24h post-transduction. mRNA expression was normalized to HPRT1 and expressed in fold versus mock control (mean ± SEM, n=3).* ***D)*** *Percentages of transduced cells from figure 12C were assessed at 5 days post-transduction by FACS (mean ± SEM, n=2).* ***E)*** *U937 cells were transduced with LV expressing Cas9 and a gRNA targeting STING or Cas9 only as a control. STING protein levels were evaluated by western blot analysis in STING KO and control U937 cells and compared to TUBULIN protein levels.* ***F)*** *U937 cells were transduced with LV expressing Cas9 and a gRNA targeting cGAS or Cas9 only. Relative cGAS expression in cGAS KO and control KO U937 cells was evaluated by qPCR, normalized to HPRT1.* ***G)*** *PMA differentiated WT, cGAS KO, STING KO and control KO U937 cells were transduced with LV or γRV (MOI=50). ISG15 level was measured 24h post-transduction. mRNA expression was normalized to HPRT1 and expressed in fold versus each mock control (mean ± SEM, n=3/4, Dunn's adjusted Kruskal-Wallis test versus each mock, *p≤0.05).* ***H)*** *U937 cells were transduced with LV expressing Cas9 and a gRNA targeting RIG-I or Cas9 only. RIG-I protein levels were evaluated by western blot analysis in RIG-I KO and control KO cells after over/night treatment ± IFNα and compared to B-ACTIN protein levels.* ***I)*** *U937 cells were transduced with LV expressing Cas9 and a gRNA targeting MAVS or Cas9 only. MAVS protein levels were evaluated by western blot analysis in MAVS KO and control U937 cells and compared to B-ACTIN protein levels.* ***J)*** *PMA differentiated WT, RIG-I KO, MAVS KO and control KO U937 cells were transduced with LV or γRV (MOI=50). ISG15 level was measured 24h post-transduction. mRNA expression was normalized to HPRT1 and expressed in fold versus each mock control (mean ± SEM, n=3-6, Dunn's adjusted Kruskal-Wallis test versus each mock, *p≤0.05).*

6.1.6. γRV structural components are key mediators of type I IFN response

To validate our hypothesis of a structural-mediated recognition of the vector, we wondered whether the γRV structural components could be sufficient to transfer the innate triggering phenotype to the usually stealth LV. For this purpose, we built a chimeric vector in which the matrix and the capsid of the LV were replaced with the structural components MA, p12, and CA of γRV (**Figure 13A**). We first verified that the resulting chimeric Gag polyprotein could be correctly processed by the HIV protease (**Figure 13B**), performing a western blot (WB) against the p30 capsid protein of MLV. Mature p30 was detected within two different chimeric vector stocks, comigrating with the WT MLV counterpart (**Figure 13C**). Moreover, correct intermediate cleavage products of the Gag precursor were also produced (**Figure 13C**). Interestingly, MDM exposed to this chimeric vector triggered strong upregulation of ISG, similarly to the response induced by γRV (**Figure 13D**), highlighting the key role of the structural components of the γRV in eliciting these responses. To further dissect which structural component is the mediator of the recognition, we built other chimeric constructs

replacing only the capsid or only the matrix within the LV packaging plasmid (**Figure 13E**). Unfortunately, we failed to produce LV with capsid of γRV, likely highlighting the requirement of MLV matrix for correct assembly of the MLV viral core as previously reported for infectious viruses (Yamashita & Emerman, 2004). Albeit with less efficiency, we verified that the chimeric Gag from the LV carrying the γRV matrix protein was correctly processed, by performing a WB against the p24 capsid of HIV (**Figure 13F**). MDM transduced with this chimeric construct did not upregulate type I IFN responses (**Figure 13G**), indirectly supporting a prominent role of the capsid, rather than of the matrix, in mediating vector recognition in these cells.

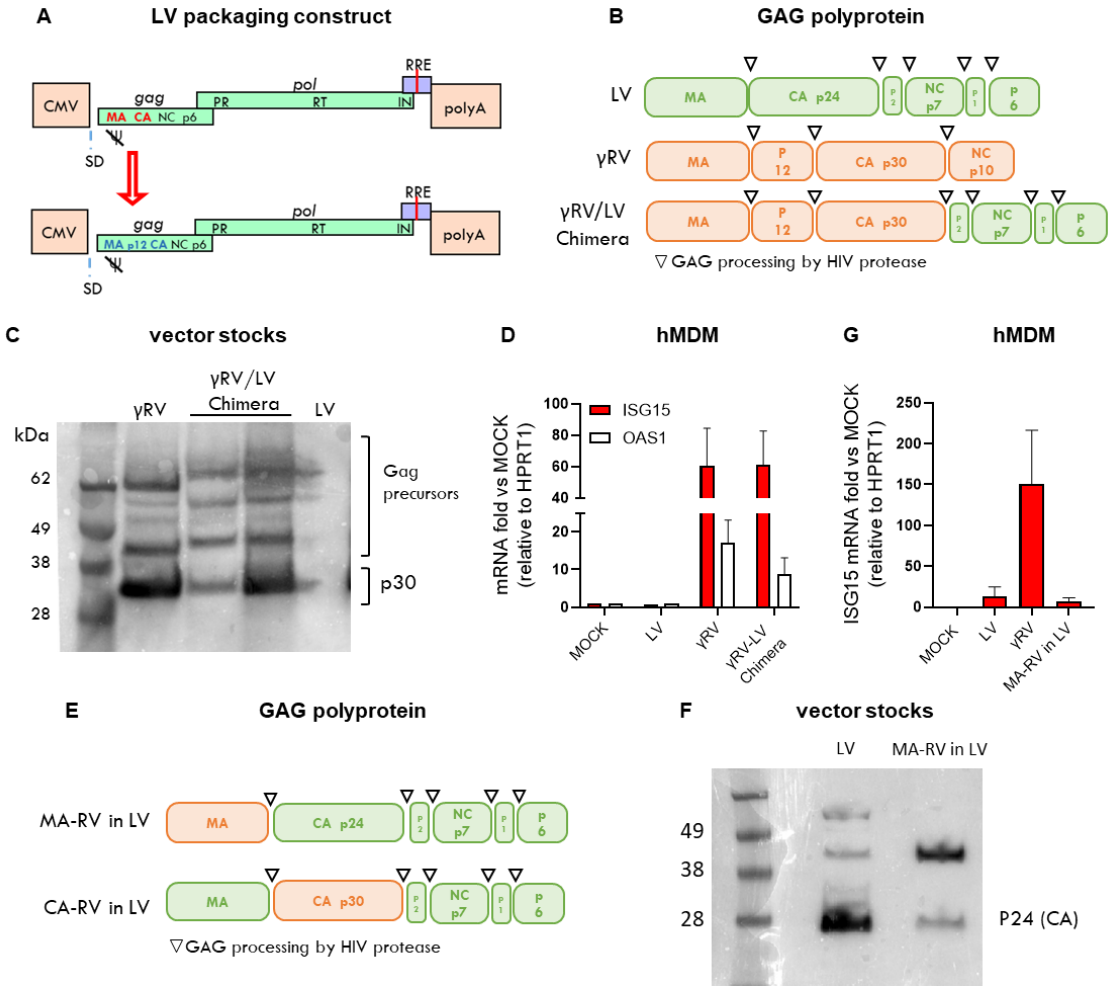

Figure 13. γRV structural components are key mediators of type I IFN response. A) *Scheme of the modified LV packaging construct where LV matrix and capsid are replaced with MA, P12 and CA of the γRV.* ***B)*** *Scheme of the cleavage sites within GAG polyprotein of LV, γRV and the chimeric LV/γRV.* ***C)*** *The presence of MLV capsid p30 protein and correct processing of chimeric Gag polyprotein was evaluated by WB within two different chimeric LV/γRV vector stocks and*

compared to γRV and LV vector stocks. ***D)*** *hMDM were transduced with LV, γRV or chimeric LV/γRV (MOI 5). ISG levels were measured 24h post-transduction. mRNA expression was normalized to HPRT1 and expressed in fold versus mock control (mean ± SEM, n=2/3).* ***E)*** *Scheme of the cleavage sites within the modified GAG polyprotein of RV matrix in LV chimeric construct and RV capsid in LV chimeric construct.* ***F)*** *Correct processing of the chimeric Gag polyprotein from RV matrix in LV chimeric construct was evaluated by WB using an antibody against the p24 capsid protein of HIV.* ***E)*** *hMDM were transduced with LV, γRV or chimeric RV matrix iin LV (MOI 5). ISG levels were measured 24h post-transduction. mRNA expression was normalized to HPRT1 and expressed in fold versus mock control (mean ± SEM, n=3).*

6.1.7. γRV-induced response is orchestrated by the TBK1 kinase

As viral structural components have been reported to mediate interactions with host factors that can restrict infection and elicit immune responses (Pertel *et al*, 2011; Fletcher *et al*, 2018), we decided to address the involvement of a known restriction factor capable of recognizing MLV. We investigated the role of TRIM5a in γRV sensing despite it has been shown to restrict N-tropic but not NB-tropic MLV from which the γRV derives. In agreement, TRIM5α KO cell lines (**Figure 14A**) maintained their antiviral immune phenotype, triggering ISG expression upon RV exposure (**Figure 14B**), excluding TRIM5α as our structural candidate sensor.

In the effort to narrow down on the sensors and pathways contributing to γRV mediated type I IFN activation, we evaluated the role of common mediators of interferon production that are located in the cytoplasm. TBK1, along with its analogue IKKε, is a central kinase that links innate immune activation by different PRRs to regulation of transcriptional programs leading to cytokines production and type I interferon responses. As many different substrates are emerging for TBK1 (Zhou *et al*, 2020), we wanted to investigate its possible role in γRV recognition. Surprisingly, pharmacological inhibition of TBK1 completely abrogated ISG induction in MDM exposed to γRV (**Figure 14C**). A similar reduction was observed upon cells exposure to the known TBK1-dependent stimulus poly(I:C), validating the specificity of the inhibitor (**Figure 14D**). To further dissect the role of TBK1, we evaluated TBK1 activation by immunofluorescent (IF) staining in MDM 6h after transduction. Interestingly, a significant number of phosphorylated-TBK1 (p-TBK1) foci per cell was detected in RV-exposed MDM as compared to MOCK untransduced cells (**Figure 14E-F**), supporting direct engagement of this kinase upon vector recognition. Genetic validation experiments in the U937 cell line are ongoing to confirm the involvement of TBK1 in γRV sensing.

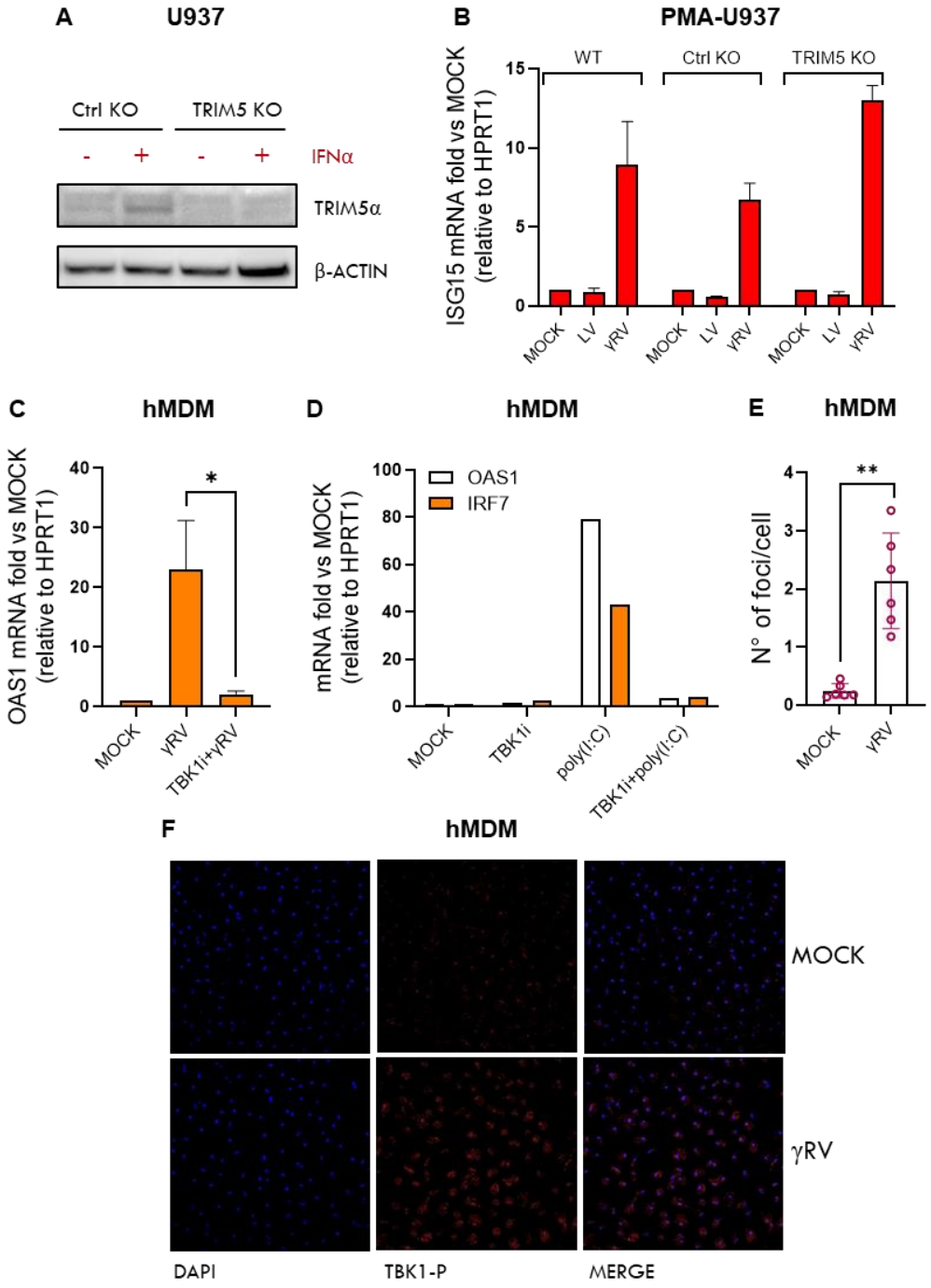

Figure 14. γRV-induced response is orchestrated by the TBK1 kinase. A) *U937 cells were transduced with LV expressing Cas9 and a gRNA targeting TRIM5α or Cas9 only as a control. TRIM5α protein levels were evaluated by WB in TRIM5α KO and control KO cells after over/night treatment ± IFNα and compared to B-ACTIN protein levels.* ***B)*** *PMA differentiated WT, TRIM5α and control KO U937 cells were transduced with LV or γRV (MOI=50). ISG15 level was measured 24h post-transduction. mRNA expression was normalized to HPRT1 and expressed in fold versus each mock control (mean ± SEM, n=4/6).* ***C)*** *hMDM were transduced with γRV (MOI=10) after 6h pre-*

*exposure or not to the TBK1 inhibitor. OAS1 level was measured 24h post-transduction. mRNA expression was normalized to HPRT1 and expressed in fold versus mock control (mean ± SEM, n=4, Mann Whitney test, *p≤0.05).* ***D)*** *hMDM were stimulated with poly(I:C) in presence or not of TBK1 inhibitor. ISG levels were measured 24h post-transduction. mRNA expression was normalized to HPRT1 and expressed in fold versus mock control (n=1).* ***E-F)*** *hMDM were transduced with γRV (MOI=10). TBK1 phosphorylation was evaluated by IF staining 6h post-transduction. The number of P-TBK1 foci per cell was quantified by ImageJ (E) (mean ± SEM, n=6, Mann Whitney test, **p≤0.01). Representative zoomed images are shown (F).*

6.1.8. CRISPR/Cas9 screening to identify host factors involved in RV recognition

Based on the notion that many innate immune sensors are also ISG (Schoggins & Rice, 2011), we set up a screening exploiting a published, commercially available CRISPR/Cas9 KO library targeting 1902 human ISG (OhAinle *et al*, 2018) with the aim of identifying host proteins participating in the structural recognition of the γRV. First, we needed to generate a tractable assay in which to easily visualize and screen for the γRV responder cells. For this aim, we generated a reporter system exploiting our U937 cell line model. We designed a Knock-In (KI) strategy for inserting the dTomato reporter sequence under the control of the ISG15 promoter (**Figure 15A**), one of the most upregulated genes upon γRV exposure in our context. We first designed and tested three different guides RNA, targeting the last exon of ISG15, before the stop codon. Once selected the best performing one (**Figure 15B**), we built a donor template cassette with homology arms for ISG15 based on the gRNA cut site. Within the homology arms, we inserted the last part of the ISG15 gene devoid of its stop codon, a 2A self-cleaving peptide and the dTomato reporter sequence (**Figure 15A**). Nucelofection of U937 cells with ribonucleoprotein complex followed by delivery of AAV6 vector carrying the donor template allowed the insertion of the reporter sequence at the end of our gene of interest. Through this strategy, the dTomato reporter would be transcribed and translated under the control of the ISG15 promoter while maintaining the expression and function of the ISG15 gene. Upon the editing procedure, we detected around 23% of edited cells by FACS based on their basal dTomato expression (**Figure 15C-D**). However, to avoid working with cells with a high basal dTomato, and thus ISG15, expression level, we searched for clones carrying the targeted insertion among the reporter negative population. For this purpose, we sorted at single cell level the dTomato negative cells and, upon expansion, stimulated each single clone with IFNα to identify the edited clones able to upregulate dTomato together with the IFN-induced ISG15 gene

in response to IFNα (**Figure 15E**). Interestingly, among the 72-screened clones 13 edited clones became 100% dTomato$^+$ upon IFNα stimulation (**Figure 15F**). We next evaluated the ability of these clones to recognize γRV upon differentiation into macrophage-like cells with PMA, looking at the percentages of cells becoming dTomato$^+$ upon γRV transduction. At the end, we selected the best candidate clone as the one showing the highest percentage of dTomato$^+$ cells after RV transduction and the lowest increase in basal dTomato expression due to PMA differentiation (**Figure 15G**) to perform the CRISPR screening. We thus transduced our reporter cell line with the pooled library at limited multiplicity of infection (MOI) to achieve a single copy of a unique gRNA per cell upon puromycin selection of the transduced cells. We then differentiated with PMA the pooled KO population that was next transduced with γRV (**Figure 15H**). Based on the idea that cells KO for factors potentially involved in γRV sensing lose their ability to respond to the vector, we sorted the reporter negative cells to search for gRNA enriched in that population. In parallel, dTomato$^+$ cells were also sorted to help exclude candidate factors. Sorted cells, together with the bulk population, were PCR amplified and sequenced. Bioinformatic analysis allowed us to identify factors for which an enrichment of guides in the negative population was observed in respect to the bulk population of represented guides (**Figure 15I**). As expected, ISG15 was among these candidate factors as cells KO for this gene could not transcribe and translate the reporter cassette. Additional confirmation of the validity of the screening was the presence of STAT1 and IFNAR among the enriched genes as STAT1 is a signaling mediator for type I IFN and IFN does not signal without its receptor. We are currently analyzing the results from a second independent screening experiment that will allow us to increase the significance of the results obtained and narrow down the list of candidate factors. Future work will focus on the validation of the role of candidate factors in the response to γRV.

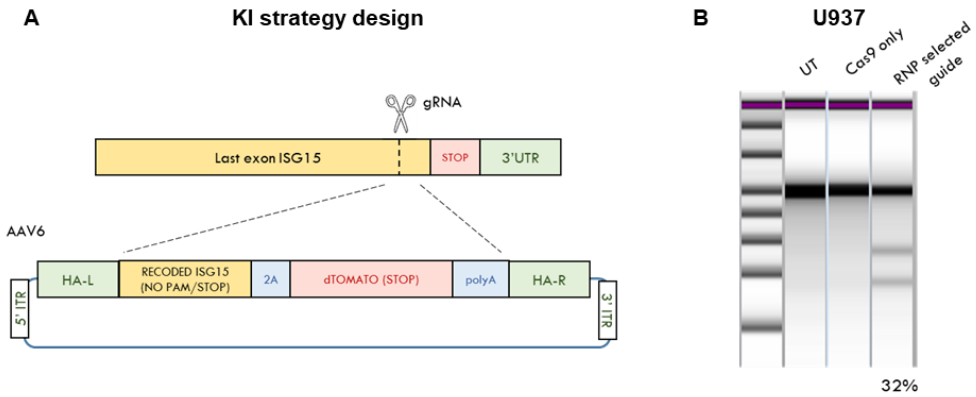

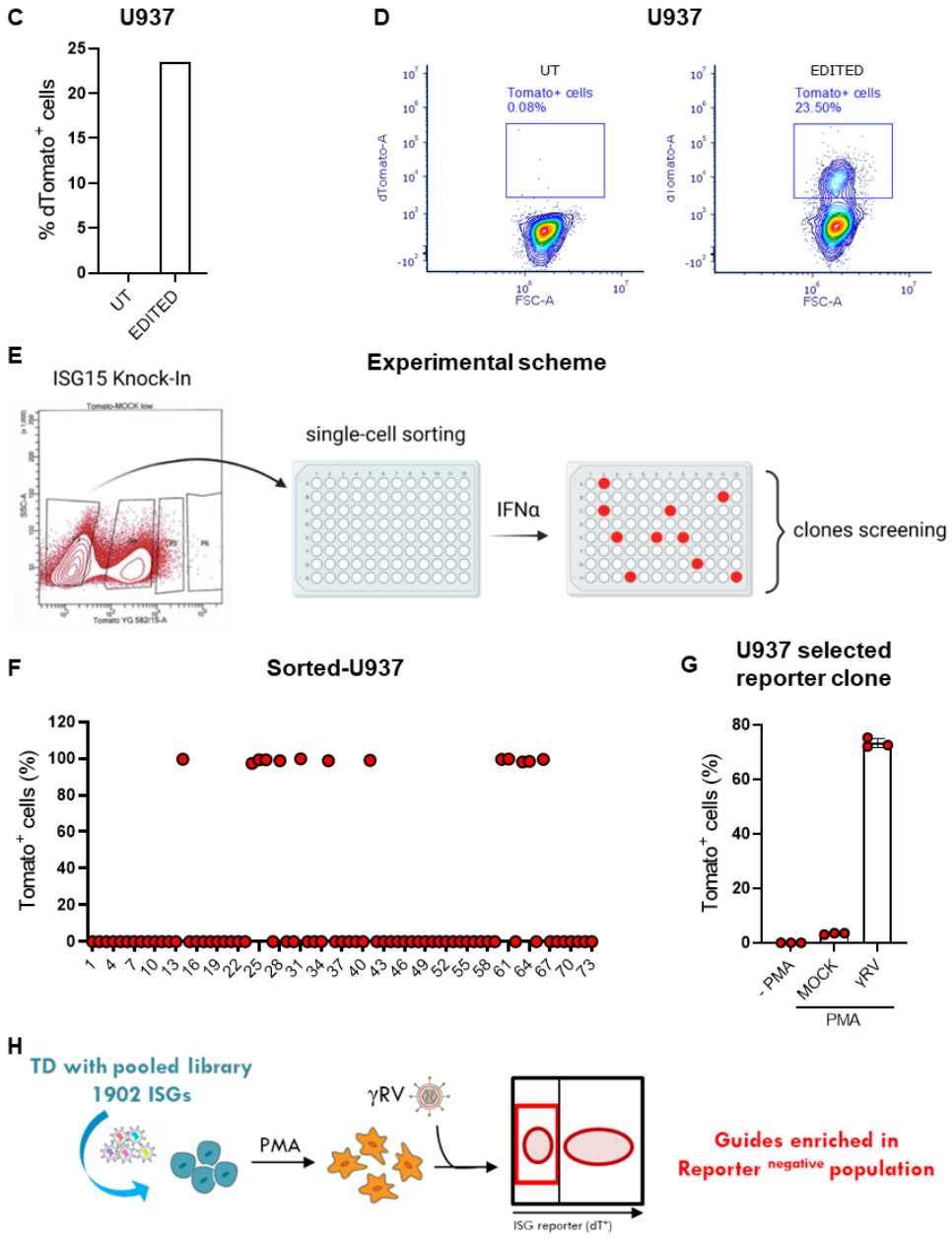

I

Gene	# of sgrnas	Score	P value	FDR	Rank	# of good sgrnas	LFC
STAT1	4	4.46E-06	1.22E-05	0.024752	1	4	11.228
IFNAR1	7	2.91E-05	0.00017297	0.120462	2	7	4.6291
ISG15	7	3.31E-05	0.00017785	0.120462	3	6	4.353
RALA	4	0.00026554	0.0012157	0.24703	4	2	-0.309
ZNF205	3	0.00031552	0.00053354	0.24703	5	2	10.588
CAMSAP2	7	0.00036034	0.0010354	0.24703	6	6	3.1288
KLHL31	4	0.00052414	0.0013911	0.256976	7	4	5.1866
ZNF613	5	0.00077313	0.0031403	0.455693	8	3	9.6198
ZBTB43	5	0.0008814	0.003345	0.455693	9	3	9.6117
CD276	3	0.00099555	0.0011865	0.24703	10	1	-2.926

Figure 15. CRISPR/Cas9 screening to identify host factors involved in RV recognition. ***A)*** *Schematic of the Knock-In strategy to generate an IFN-responsive reporter cell line in U937 cells.* ***B)*** *U937 cells were nucleofected with pre-assembled RNP complex made of Cas9 protein and gRNA targeting the last exon of ISG15 gene or Cas9 only as a control. Cut efficiency was evaluated 3 days post nucleofection by non homologous end joining (NHEJ) assay. Tape station results are shown.* ***C-D)*** *U937 cells were nucleofected with RNP complex made of Cas9 protein and gRNA targeting the last exon of ISG15 gene, followed by delivery of AAV6 vector carrying the donor template as shown in figure A. Editing efficiency was evaluated by FACS 3 days post nucleofection. Representative FACS plots are shown in figure D.* ***E)*** *Schematic of the experimental procedure to select KI clones from the reporter negative population after editing shown in C-D.* ***F)*** *Single cell sorted negative U937 cells were stimulated with IFNα over/night and knock-in events were identified by FACS analysis.* ***G)*** *U937 reporter clones from figure F were differentiated with PMA and transduced with γRV (MOI=50). Percentages of dTomato^{+} cells were evaluated by FACS 24h post-transduction and compared to PMA-differentiated mock untransduced cells and non PMA differentiated cells. Results from the selected clone are shown.* ***H)*** *Schematic of the CRISPR/Cas9 screening with the CRISPR/Cas9 ISG KO library.* ***I)*** *List of genes for which an enrichments in gRNA in the sorted negative population was found in respect to the gRNA present in the bulk population of cells transduced with the library. The top 10 genes are shown.*

6.2. Investigating antiviral restriction mechanisms in human hematopoietic stem cells

6.2.1. Combinatorial relief of SAMHD1 restriction of reverse transcription together with the earlier IFITM3-mediated block to lentiviral vector entry enhances transduction in quiescent HSPC

To address the role of SAMHD1 in human HSPC, we used lentiviral vectors that directly incorporate the SIVmac accessory protein Vpx into the LV particle (Bobadilla *et al*, 2013) (**Figure 16A**). We first validated the system in primary human MDM in which we confirmed significant increase in LV transduction upon Vpx-mediated degradation of SAMHD1 (**Figure 16B**).

Other groups have already explored the role of SAMHD1 in HSPC with minimal impact of Vpx observed on transduction efficiency of *ex vivo* cultured HSPC (Li *et al*, 2015). Since we have shown that the IFITM3 that acts prior to the SAMHD1-imposed block to reverse-transcription potently restricts VSV-G-mediated LV entry into HSPC (Petrillo *et al*, 2018), we wondered whether SAMHD1-mediated restriction could be revealed by CsH, a compound able to overcome IFITM3 restriction (Petrillo *et al*, 2018). To this aim, we evaluated the effect of Vpx incorporation in combination with CsH. In line with previous reports (Li *et al*, 2015), Vpx did not improve lentiviral transduction of stimulated HSPC, alone or in combination with CsH (**Figure 16C**). Thus, we wondered whether Vpx effect could be more relevant in the context of unstimulated, quiescent HSPC. To test this hypothesis we transduced freshly isolated, quiescent HSPC with Vpx-LV in presence or absence of CsH. After 16h, we washed the cells and we added cytokines to the culture media together with an inhibitor of RT, to evaluate only the transduction that occurred in the unstimulated cells (**Figure 16D**). Interestingly Vpx-incorporation improved transduction of quiescent HSPC in a slight but significant manner (**Figure 16E**). Of note, Vpx-mediated increase in transduction in unstimulated HSPC was independent of CsH, with the combination resulting in an additive increase in gene marking levels over control transduced HSPC (**Figure 16E**). Importantly, this advantage was strong in the most primitive $CD34^+CD133^+CD90^+$ subset of HSPC (**Figure 16F**). Vpx delivery did not alter overall subpopulation composition, suggesting that the HSPC phenotype was not affected (**Figure 16G**). Moreover, in support of the safety of Vpx delivery, we did not observed

any induction of DNA damage response or type I IFN responses upon transduction with Vpx-incorporating LV, as measured by p21 and ISG15 expression respectively (**Figure 16H**).

We next assesses the effect of Vpx delivery on the intracellular dNTP pools in both stimulated and unstimulated HSPC. While Vpx exposure only minimally influenced dNTPs levels in stimulated HSPC, a stronger effect was observed in quiescent cells, with a particular increase in the levels of dATP and dGTP (**Figure 16I-J**). In line with the transduction data, these results indicate that the nucleotide pool may restrict quiescent but not stimulated HSPC.

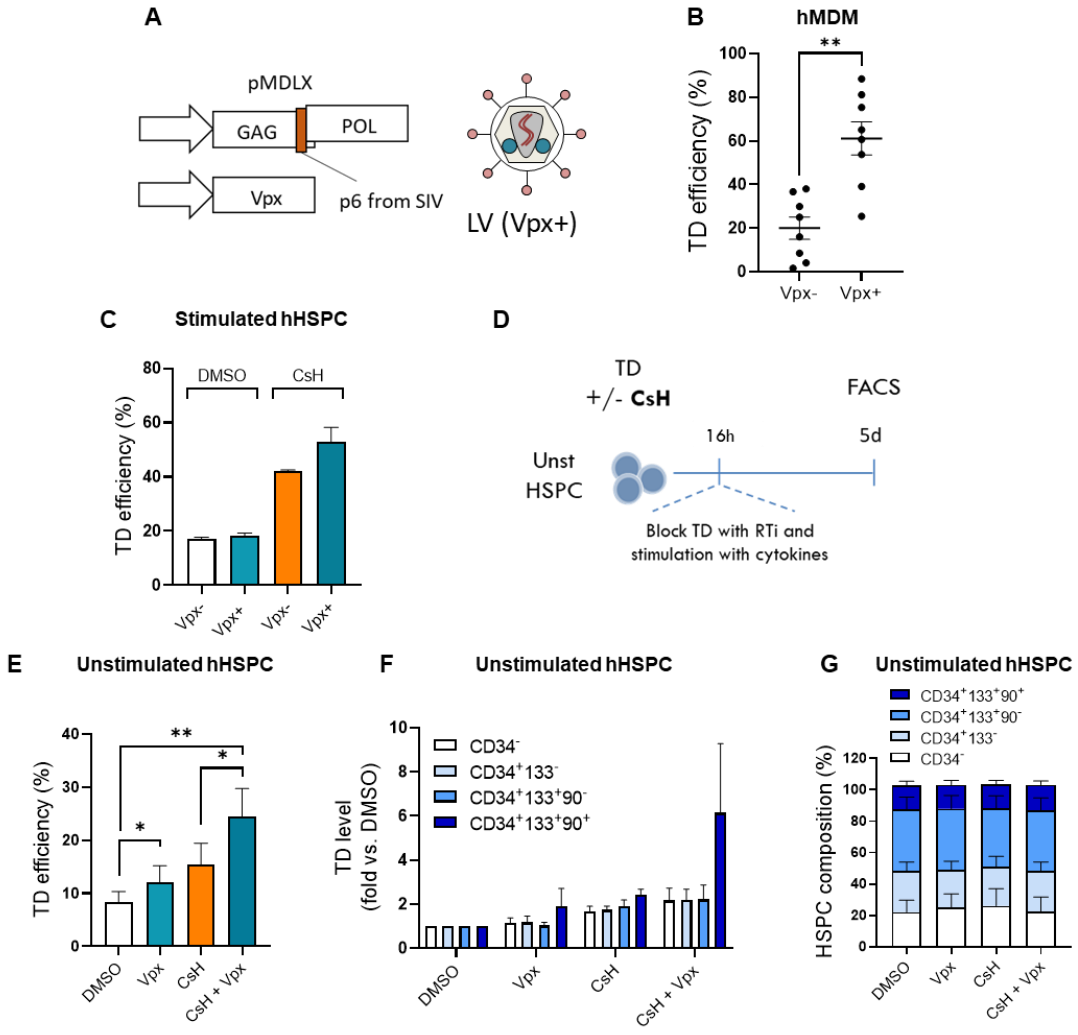

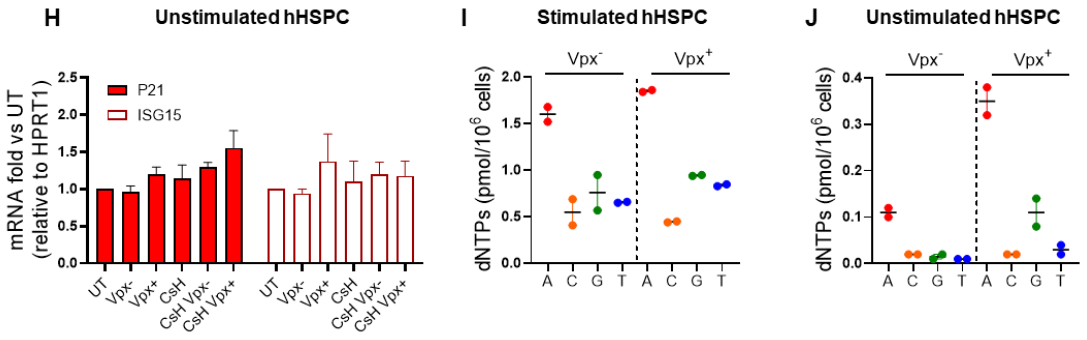

Figure 16. Combinatorial relief of SAMHD1 restriction of reverse transcription together with the earlier IFITM3-mediated block to lentiviral vector entry enhanced transduction in quiescent HSPC. A) *Schematic representation of the pMDLX packaging plasmid used for the production of Vpx incorporating lentiviral vector (LV). A mutation in the p6 from SIVmac allows packaging of Vpx that is provided in trans during the vector production (Bobadilla et al, 2013).* ***B)*** *hMDM were transduced with LV that either or not directly incorporate Vpx into the LV particle at MOI 1. Percentages of transduced cells were assessed at 5 days post-transduction by FACS (mean ± SEM; n=8; Wilcoxon signed rank test, **p=0.0078).* ***C)*** *Transduction efficiencies (MOI=1) in stimulated hHSPC ± Vpx± 8 µM CsH, measured by FACS at 5 days (mean ± SEM; n=2).* ***D)*** *Schematic representation of the transduction experiment in unstimulated HSPC.* ***E)*** *Transduction efficiencies (MOI=25) in unstimulated hHSPC ± Vpx ± 8 µM CsH (mean ± SEM; n=8; Wilcoxon signed rank test, *for p<0.05, **for p<0.01).* ***F)*** *Transduction efficiencies in the different subpopulations of unstimulated hHSPC from figure E.* ***G)*** *The composition of unstimulated hHSPC was evaluated by FACS 5 days post transduction.* ***H)*** *DNA damage or type I IFN responses upon LV-Vpx delivery in unstimulated hHSPC were measured 24h post transduction in terms of p21 and ISG15 expression respectively, by fold increase versus untransduced cells (mean ± SEM; n=3).* ***I-J)*** *Intracellular dNTP levels were measured in stimulated (I) and unstimulated (J) hHSPC 24h post transduction ± Vpx in presence of CsH (n=1).*

6.2.2. Exogenous deoxynucleosides synergize with CsH to significantly enhance lentiviral transduction in quiescent HSPC

As the increase in cellular dNTPs levels upon Vpx delivery might still be suboptimal for efficient viral reverse-transcription, we evaluated the effect of providing an excess of nucleotides on gene transfer efficacy, as an alternative strategy to overcome SAMHD1-mediated restriction (Baldauf *et al*, 2012; Lahouassa *et al*, 2012). However, we observed that dNTPs addition did not affect the transduction efficiency of unstimulated HSPC, even in combination with CsH (**Figure 17A**). Deoxynucleosides (dNs), precursors of dNTPs, during transduction have been reported to better penetrate within cells (Shepard *et al*, 2019). Remarkably, dNs alone rendered HSPC as permissive as CsH alone (**Figure 17B**), but the most prominent effect was obtained by combining CsH and dNs during transduction of quiescent HSPC, yielding up to 6-fold increase in transduction over CsH alone control condition (**Figure 17C**). This benefit was significant among all fractions of

HSPC with the strongest effect observed in the most primitive $CD34^+CD133^+CD90^+$ compartment, resulting in an average 18-fold increase in transduction over CsH alone (**Figure 17D**). Importantly dNs addition did not affect HSPC subpopulation composition, supporting preservation of the HSPC phenotype (**Figure 17E**). Of note, dNs retained their ability to enhance transduction in unstimulated HSPC over a dose range of 25-1000 μM, with higher or lower concentrations still improving transduction but with a lower effect as compared to the intermediate 100 and 500 μM doses (**Figure 17F**). As we observed that dNs addition increased transduction also of IDLV (**Figure 17G**), we tested the effect of dNs addition on the efficiency of IDLV-based gene editing (**Figure 17H**). As expected, despite overall low efficiency due to the quiescent status of these cells, combination of CsH and dNs enhanced targeted genome editing in unstimulated HSPC (**Figure 17I-J**), without affecting the composition of HSC subpopulations (**Figure 17K**). Of note, similarly to Vpx, adding dNs did not improve transduction in pre-stimulated HSPC, even in combination with CsH (**Figure 17L**), further suggesting that the intracellular dNTP pools of stimulated HSPC are not limiting for viral reverse transcription.

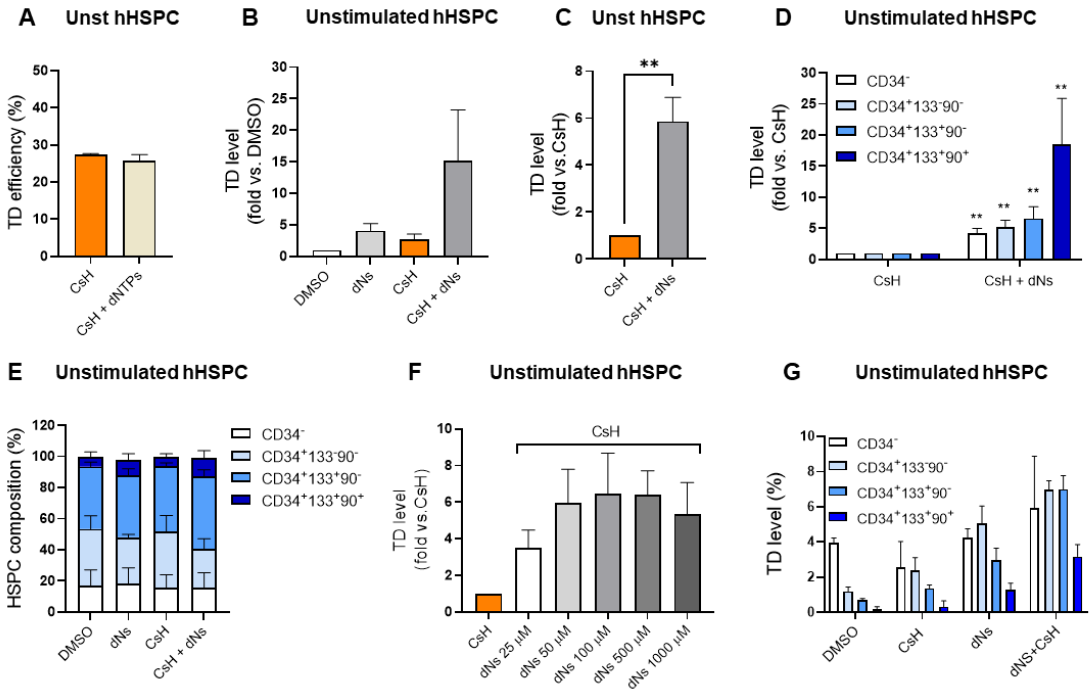

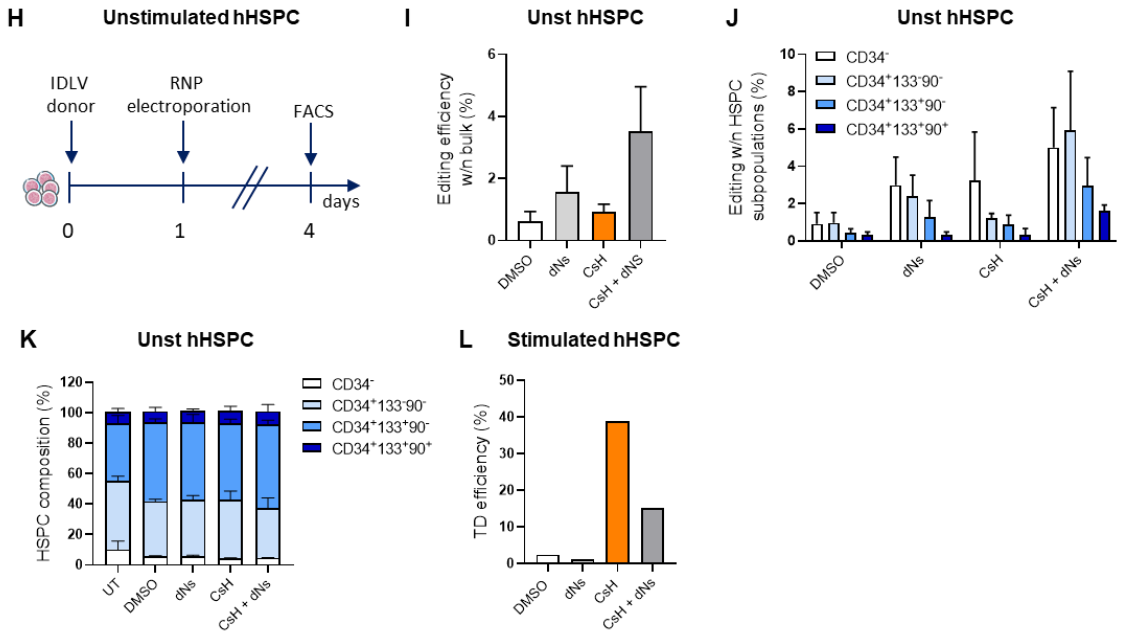

Figure 17. Exogenous deoxynucleosides synergize with CsH to significantly enhance lentiviral transduction in quiescent HSPC. A) *Unstimulated hHSPC were pre-treated with dNTPs before transduction with LV in presence of CsH. Percentages of transduced cells were assessed at 5 days by FACS (mean ± SEM, n=2).* ***B)*** *Unstimulated hHSPC were pre-treated with a mixture of the 4 dNs at a final concentration of 500 µM each before transduction with a LV in presence or not of CsH. Percentages of transduced cells were assessed at 5 days post-transduction and expressed as fold increase vs DMSO (mean ± SEM, n =4).* ***C)*** *Transduction efficiency in unstimulated hHSPC ± dNs in presence of CsH, expressed as fold increase vs CsH control (mean ± SEM, n=8, Wilcoxon signed rank test versus CsH=1, **p = 0.0078).* ***D)*** *Transduction efficiencies in the different subpopulations of unstimulated hHSPC expressed as fold increase vs CsH control (mean ± SEM, n=8, Wilcoxon signed rank test versus each CsH=1 **p = 0.0078).* ***E)*** *The composition of unstimulated hHSPC was evaluated 5 days post transduction.* ***F)*** *Transduction efficiency in unstimulated hHSPC in presence of different concentrations of dNs and expressed as fold increase versus CsH control (mean ± SEM, n ≥2).* ***G)*** *Unstimulated hHSPC were transduced with IDLV at MOI=200 ± CsH in presence or not of dNs. Transduction efficiency was evaluated in the different HSPC subsets 3 days post transduction (mean ± SEM, n=2).* ***H)*** *Scheme of the gene editing protocol for unstimulated hHSPC.* ***I-J)*** *Percentage of edited cells at AAVS1 locus measured within the bulk (I) or within the indicated HSPC subpopulations (J) 3 days post editing (n=2).* ***K)*** *The composition of unstimulated hHSPC was evaluated 3 days post editing.* ***L)*** *Transduction efficiencies in stimulated hHSPC ± dNs ± CsH (n=1)*

6.2.3. Combination of CsH and exogenous deoxynucleosides improves transduction across species and in multiple quiescent hematopoietic cell types

To test whether the combination of CsH and dNs could improve transduction efficiency across species, we tested our protocol in unstimulated murine HSPC. We confirmed also in this context a dNs-mediated enhancement of transduction. Although a slightly higher

basal level of transduction was observed in murine HSPC from SAMHD1 KO mice (**Figure 18A**), the effect of dNs was independent from SAMHD1-mediated LV restriction (**Figure 18A**). This data suggest that the intracellular dNTP pools may be a limiting factor also in the murine context and that lack of SAMHD1 is not sufficient to fully remove this block. Vpx-mediated degradation of SAMHD1 promotes HIV infection in resting T cells (Baldauf *et al*, 2012). Since we did not see any benefit in terms of transduction efficiencies with our Vpx-incorporating LV in resting T cells (**Figure 18B**), we decided to evaluate the effect of dNs delivery in combination or not with CsH on the transduction rate of T cells. While activated $CD3^+$ T cells did not benefit of dNs addition (**Figure 18C**), we observed a significant benefit in gene transfer efficacy in quiescent $CD3^+$ T cells, within the $CD14^-$ peripheral blood mononuclear cells (PBMC) population, in particular in combination with CsH (**Figure 18D**). This effect was maintained within the $CD4^+$ and $CD8^+$ T cell subsets (**Figure 18E**), with no alteration observed on their frequency upon dNs addition (**Figure 18F**). Importantly, the dNs and CsH combination did not alter the T cell composition and significantly improved LV transduction also in the quiescent stem memory T cells (TSCM) (**Figure 18G-H**).

Taken together, these data suggested that addition of exogenous dNs together with CsH-mediated removal of IFITM3 restriction enables efficient gene modification of difficult to transduce quiescent targets of gene therapy.

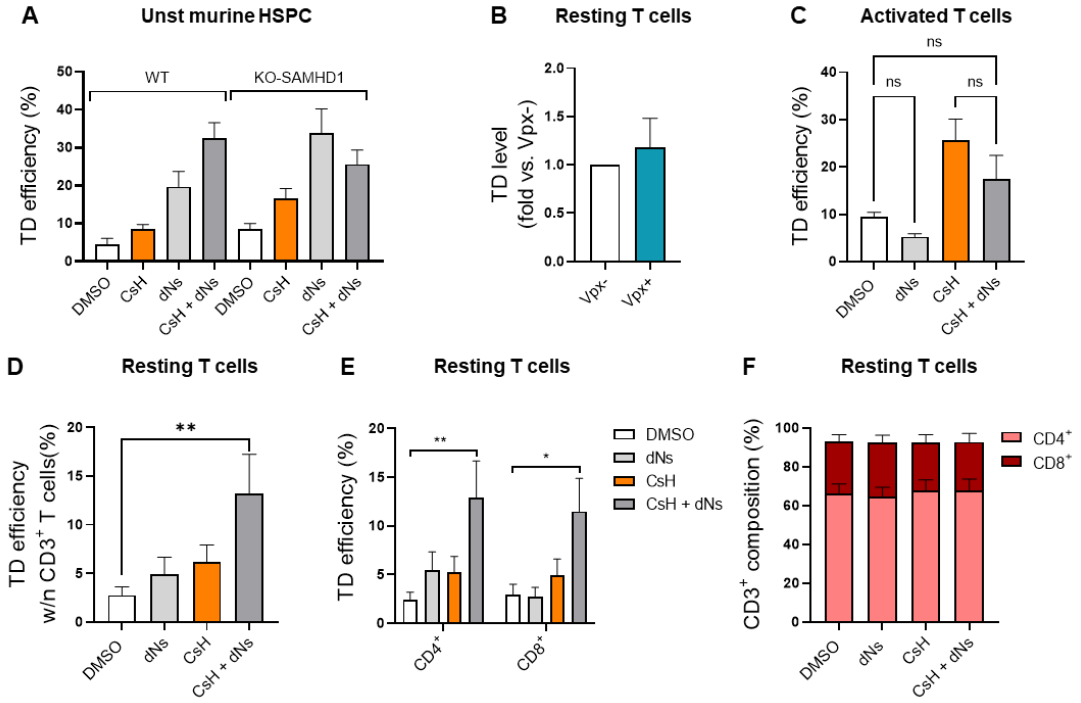

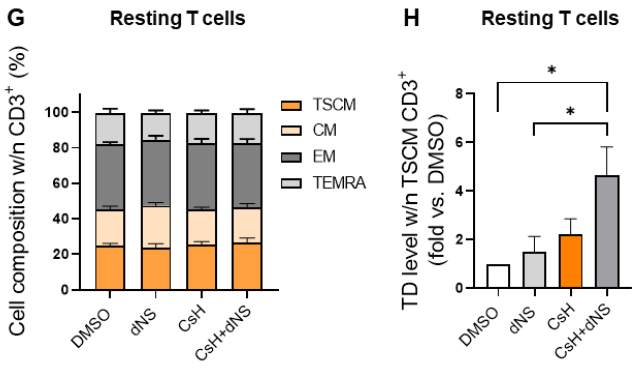

Figure 18. Combination of CsH and exogenous deoxynucleosides improves transduction across species and in multiple quiescent hematopoietic cell types. A) *Unstimulated murine HSPC from WT or SAMHD1 KO mice were transduced with LV (MOI=10) ± 8 μM CsH ± dNs. Percentages of transduced cells were assessed at 5 days post-transduction (mean ± SEM, n=3).* ***B)*** *Resting T cells were transduced with LV ± Vpx. Percentages of transduced cells were assessed 3 days post-transduction and expressed as fold versus Vpx- (mean ± SEM, n=6).* ***C)*** *Activated primary CD3⁺ T cells were transduced with LV (MOI=1) ± CsH ± dNs. Percentages of transduced cells were assessed at 5 days post-transduction (mean ± SEM, n=4, Dunn's adjusted Kruskal-Wallis test; ns, not significant).* ***D)*** *PBMC depleted of the CD14⁺ subset, were transduced with LV (MOI=25-50) ± CsH ± dNs. Transduction efficiency was evaluated within the CD3⁺ T cells subset 3 days post transduction (mean ± SEM, n=4, Dunn's adjusted Kruskal-Wallis test, **for p<0.01).* ***E)*** *Transduction efficiency within the CD4⁺ and CD8⁺ T cells subsets (mean ± SEM, n=4, Dunn's adjusted Kruskal-Wallis test,*for p<0.05, **for p<0.01).* ***F)*** *The proportion of CD4⁺ and CD8⁺ within the CD3⁺ T cells was evaluated 3 days post transduction.* ***G)*** *Subsets composition of resting CD3⁺ T cells was evaluated 3 days post transduction. TSCM, Stem Memory T Cells; CM, Central Memory; EM, Effector Memory; TEMRA, Terminally differentiated effector memory.* ***H)*** *Transduction efficiency within the TSCM CD3⁺ T cell subset expressed as fold increase versus DMSO control (mean ± SEM, n=2, Tukey's adjusted Kruskal-Wallis test, *for p<0.05).*

6.2.4. Exogenous pyrimidines mediate lentiviral transduction enhancement in quiescent HSPC

Given the advantage observed in transduction when adding dNs, we wanted to better address the role of the different dNTPs in mediating the increase in viral reverse-transcription. For this purpose, we transduced quiescent HSPC in presence of CsH and the single deoxynucleosides or the combination of purines (dA and dG) or pyrimidines (dC and dT) dNTP precursors. Remarkably, we observed no or minor impact on the transduction rate of quiescent HSPC upon addition of dA or dG or of the combination of the two purine dNTP precursors (**Figure 19A**). Instead, the transduction increase was mainly mediated by the addition of the two pyrimidines dNTP precursors, with dC alone leading to gene marking levels comparable to the combination of all dNs (**Figure 19B**).

To further dissect the mechanism behind pyrimidines-mediated improvement of transduction in quiescent cells we evaluated how addition of exogenous dNs to the culture media influenced the intracellular pools of single dNTPs. We did not observe homogeneous increase in all dNTP 24h after dNs delivery. The major changes occurred in the levels of deoxyadenosine triphosphate (dATP), while minor differences were observed for deoxythymidine triphosphate (dTTP) and very little or no effect was present in deoxyguanosine triphosphate (dGTP) and deoxycytidine triphosphate (dCTP) levels (**Figure 19C**). Of note, CsH *per se* did not alter intracellular dNTP pools in quiescent HSPC (**Figure 19C**).

Although these results are somewhat unexpected, we cannot exclude that the timing can be a critical factor to detect subtle changes in the levels of intracellular dNTPs and that the consumption rate may vary across the different dNTPs, making it difficult for us to conclude on the lack of an effective increase in all dNTPs. Of note, the increase in intracellular dATP demonstrated that the lack of dA-mediated effect on transduction was not due to limited entry or usage of this deoxynucleoside in the cells, while confirming that the purine pool is not the limiting one.

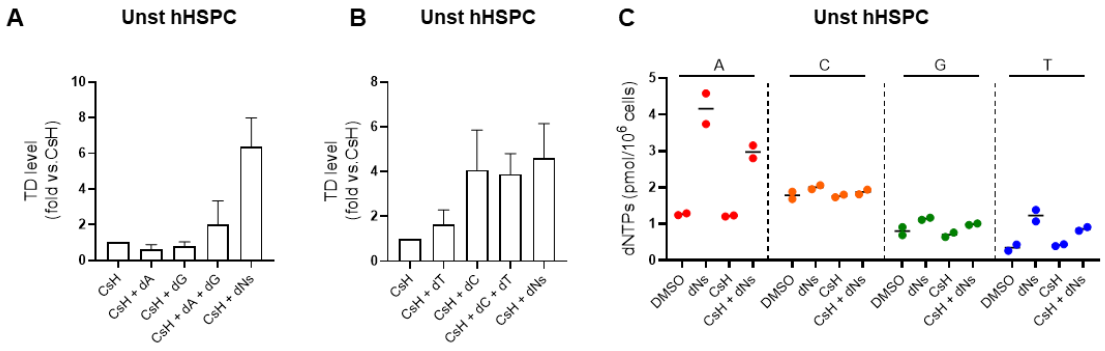

Figure 19. Exogenous pyrimidines mediate lentiviral transduction enhancement in quiescent HSPC. A) *Unstimulated hHSPC were transduced in presence of CsH upon exposure to dA, dG or dA+dG mix. Percentages of transduced cells were evaluated 5 days post transduction and expressed as fold increase versus CsH control (mean ± SEM, n=2-3).* ***B)*** *Unstimulated hHSPC were transduced in presence of CsH upon exposure to dC, dT or dC+dT mix. Percentages of transduced cells expressed as fold increase versus CsH control (mean ± SEM, n=3-4).* ***C)*** *Intracellular dNTP levels were measured in unstimulated hHSPC 24h post exposure to dNs in presence or absence of CsH (n=1).*

6.2.5. Fueling the pyrimidine *de novo* biosynthesis enhances lentiviral vector transduction in quiescent HSPC

Since our data suggested that pyrimidines are the limiting dNTPs in quiescent HSPC, we decided to further investigate the role of pyrimidines to exclude potential dNTP-independent effects of exogenous dNs addition on LV transduction. We thus exploited publicly available datasets to look at the endogenous levels of the two rate limiting enzymes of the '*the novo* pyrimidine synthesis' pathway, in quiescent versus activated HSPC (García-Prat *et al*, 2021). As expected for low metabolically active cells, in quiescent LT-HSCs the expression levels of carbamoyl-P synthetase (CPS) and dihydroorotate dehydrogenase (DHODH) was significantly lower as compared to their activated counterpart (García-Prat *et al*, 2021) (**Figure 20A**), which instead actively proliferate and require precursors for DNA synthesis. We validated these data in our experimental context by checking the expression levels of these two key genes in stimulated and unstimulated HSPC derived from the same donors (**Figure 20B-C**). We thus hypothesized that fueling the *de novo* pathway with precursors of the pyrimidines could have similar effects as providing exogenous dC and dT that fuel the 'salvage pathway' of the pyrimidine synthesis. In line with this hypothesis, orotic acid (OA) addition or uridine 5'-monophosphate (UMP) addition enhanced LV transduction in quiescent cells, with significant increase when the two compounds were combined with CsH (**Figure 20D-E**).

To determine if and how this increase was specific to the pyrimidine pools, we interrogated the same published database (García-Prat *et al*, 2021) to check the levels of phosphoribosyl pyrophosphate amidotransferase (PPAT), the first enzyme of '*de novo* purine synthesis' pathway, in quiescent versus activated HSPC. As expected, also PPAT appeared to be downregulated in unstimulated HSPC versus the stimulated counterpart (**Figure 20A**). However, when we tried to fuel the purine biosynthetic pathway providing the inosine monophosphate (IMP) precursor, no effect was observed on the transduction level of quiescent HSPC, alone or in combination with CsH (**Figure 20F**). These results are in accordance with our previous data showing that dA and/or dG addition did not increase LV transduction (**Figure 19A**) despite increased levels of dATP upon dNs delivery (**Figure 19E**).

Moreover, to further exclude dNTP-independent effects of exogenous dNs on LV transduction, we confirmed that dNs addition improved transduction only of vectors that

retro-transcribed their genome. Indeed, while dNs alone or in combination with CsH increased transduction of unstimulated human HSPC with γRV (**Figure 20G**) or SIV (**Figure 20H**) vectors, we did not observed any effect when dNs were added during transduction with AAV (**Figure 20I**) or SENDAI (**Figure 20J**) vectors, which have single strand DNA and RNA genome respectively.

Overall, these findings support the idea that dNs addition enhances LV transduction in unstimulated HSPC by directly increasing the intracellular pools of pyrimidines thus allowing an efficient reverse transcription, and suggest that minor increases in dNTPs upon dNs delivery could be explained by timing and/or consumption reasons.

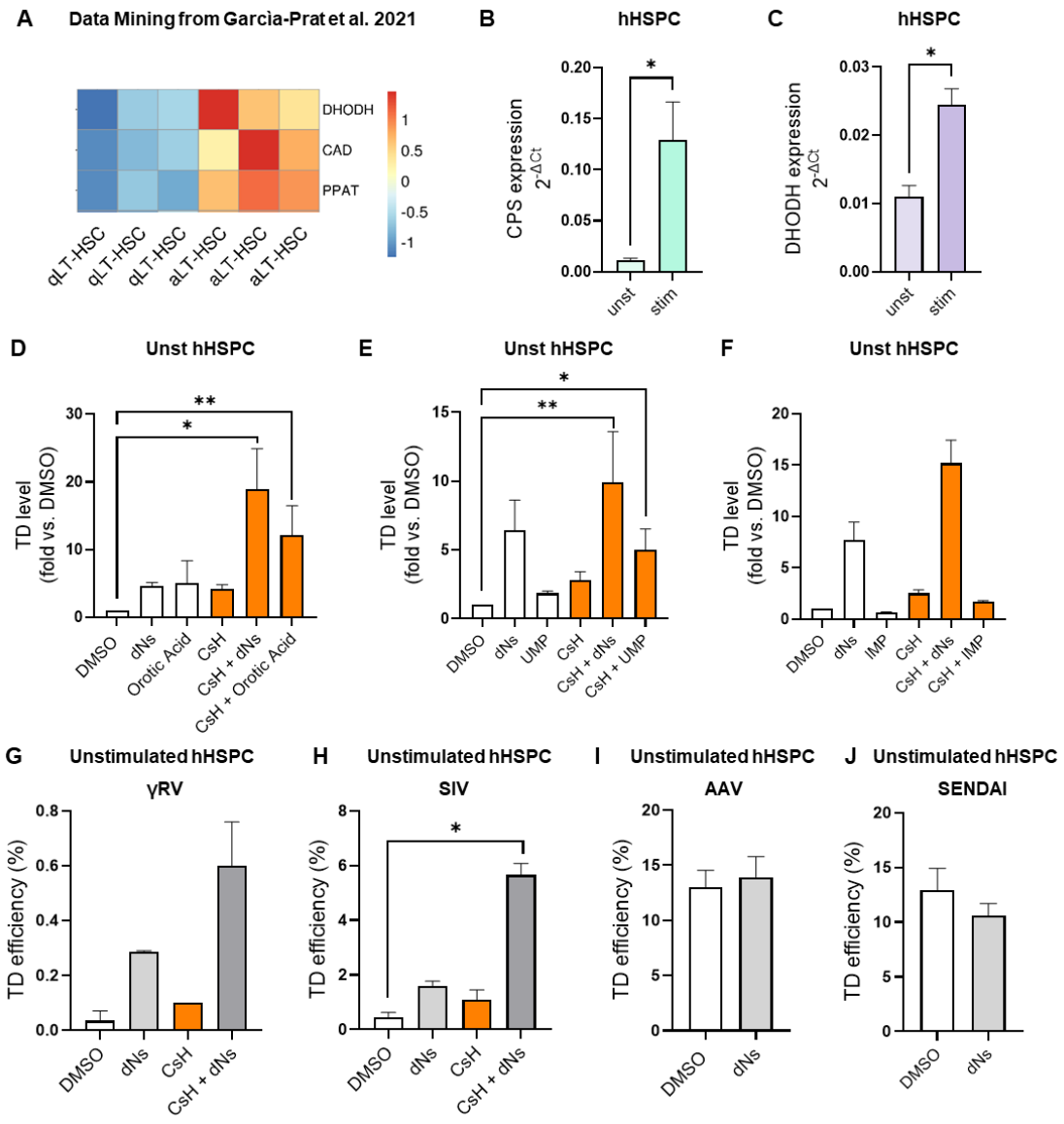

Figure 20. Fueling the pyrimidine de novo biosynthesis enhances lentiviral vector transduction in quiescent HSPC. A) *Heatmaps showing the expression levels of carbamoyl-P synthetase and dihydroorotate dehydrogenase analyzed from publicly available dataset (García-Prat et al, 2021) where the gene expression profile of quiescent long-term-HSC is compared to the one of activated long term-HSC.* ***B-C)*** *Relative gene expression levels of CPS (B) and DHODH (C) in unstimulated and stimulated hHSPC from the same donors (mean ± SEM, n=4, Mann Whitney test, *for p<0.05).* ***D)*** *Unstimulated hHSPC were transduced with LV ± 8 µM CsH after exposure or not to dNs or 7.5 µM Orotic Acid. Percentages of transduced cells expressed as fold increase versus DMSO control (mean ± SEM, n=4, Dunn's adjusted Kruskal-Wallis test,*for p<0.05, **for p<0.01).* ***E)*** *Unstimulated hHSPC were transduced with LV ± CsH after exposure or not to dNs or 1 mM UMP. Percentages of transduced cells expressed as fold increase versus DMSO control (mean ± SEM, n=4, Dunn's adjusted Kruskal-Wallis test,*for p<0.05, **for p<0.01).* ***F)*** *Unstimulated hHSPC were transduced with LV ± CsH after exposure or not to dNs or 5 mM IMP. Percentages of transduced cells expressed as fold increase versus DMSO control (mean ± SEM, n=3).* ***G-H)*** *Unstimulated hHSPC were transduced with γRV or SIV (MOI=10) ± CsH after exposure or not to dNs (mean ± SEM, n=2 per γRV, n=3 per SIV, Dunn's adjusted Kruskal-Wallis test, *for p<0.05).* ***I-J)*** *Unstimulated hHSPC were transduced with AAV6 (MOI=10000) or SENDAI vector (MOI=10) after exposure or not to dNs (mean ± SEM, n=3 AAV, n=4 SENDAI).*

6.2.6. dNs and CsH increase transduction of more complex, clinical-like vectors

Having demonstrated that our combinatorial transduction protocol in unstimulated cells is highly efficient with canonical pgk-GFP lentiviral vector used so far, we decided to validate the performance of the protocol with a more complex, clinical-like vector. To this end, we used a vector derived from the therapeutic GLOBE LV that is currently used in the clinics for treatment of β-thalassemia (Marktel *et al*, 2019). This vector retains the β-globin promoter and locus control region (LCR) elements, while having GFP instead of globin as transgene, allowing an easier tracking of transduced cells while maintaining the complexity of a clinical grade vector. As the transgene expression is dependent on an erythroid specific promoter, GFP can be visualized specifically in the erythroid lineage. We thus evaluated the transduction efficiencies by vector copy number in the liquid culture and performed colony-forming unit (CFU) assay to assess transduction specifically in erythroid colonies (**Figure 21A**). Vector copy number (VCN) analysis confirmed the synergistic effect of CsH and dNs in potently increasing transduction of Globe-like LV, with 44-fold increase as compared to the DMSO vehicle control (**Figure 21B**). Similar results were obtained from the CFU assay both in terms of VCN (**Figure 21C**) and transgene expression in Burst Forming Units-Erythroid (BFU-E) colonies (**Figure 21D**), in which the combination of CsH and dNs resulted in a significant enhancement of transduction.

Overall, these data suggest that the potential of our combinatorial protocol is not limited to simple lentiviral expression vectors with strong promoters, but can be broadly extended to more complex, clinical-like vectors with lineage-restricted promoter and bulky regulatory regions.

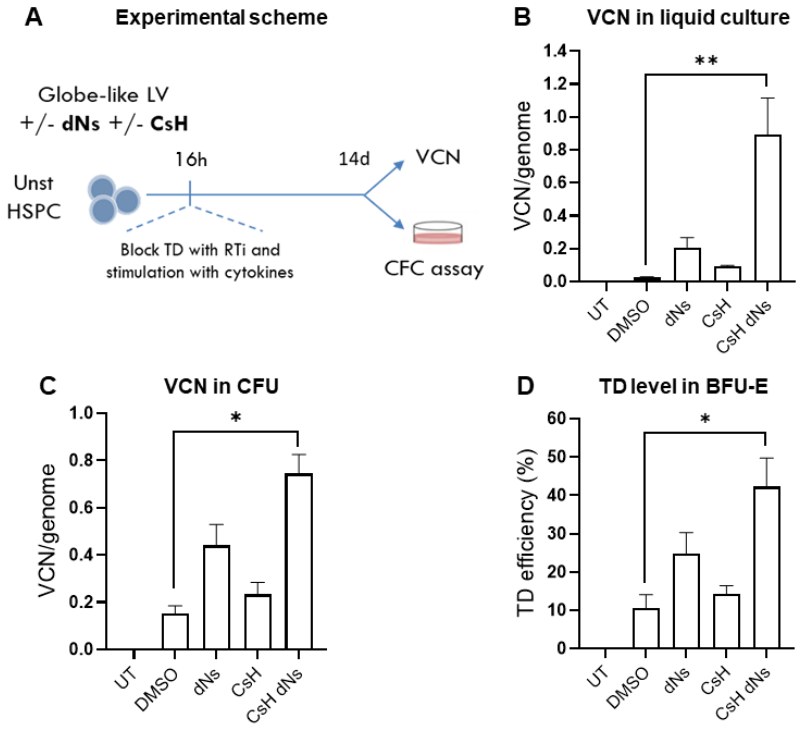

Figure 21. dNs and CsH increase transduction of more complex, clinical-like vectors. A) *Schematic representation of the transduction experiment with LV Globe-like vector in unstimulated HSPC.* ***B)*** *hHSPC were transduced with Globe-like LV (MOI=25-50) ± CsH ± dNs. Vector copy numbers were evaluated 14 days post-transduction (mean ± SEM, n=4, Dunn's adjusted Kruskal-Wallis test, **for p<0.01).* ***C-D)*** *hHSPC from figure B were plated the day after transduction in methocult to perform colony-forming unit assay. Vector copy numbers were evaluated in total colonies 14 days after plating (A). Percentages of transduced cells were evaluated in Burst Forming Units-Erythroid (BFU-E) by FACS 14 days after plating (Mean ± SEM, n=4, Dunn's adjusted Kruskal-Wallis test, *for p<0.05).*

6.2.7. dNs delivery does not impact on proliferation, apoptosis, and cell cycle status of unstimulated hHSPC

To next determine the impact of dNs on HSC biological properties, we performed *in vitro* assays to evaluate potential effects of dNs on proliferation, apoptosis or cell cycle status of unstimulated HSPC. HSPC were stained immediately after thawing with a fluorescent dye to monitor cell division at different time points. The proliferation of

transduced or untransduced cells , upon exposure to dNs was compared to the one of cells that did not receive the treatment. dNs addition did not cause any proliferation change, at any of the time points analyzed, with LV transduction having no impact on the proliferation rate of unstimulated HSPC (**Figure 22A**). We next checked by gene expression analysis the levels of p21 at 48h post transduction, as surrogate marker of DNA damage response. Importantly, we did not detect any strong p21 upregulation, with the combination of CsH and dNs reaching less than two-fold of induction, probably due to the increased vector copy numbers as reported for stimulated HSPC (Piras *et al*, 2017; Petrillo *et al*, 2018) (**Figure 22B**). In line with absence of DNA damage, dNs were not toxic, as no signs of apoptosis were detected in unstimulated HSPC 48h after dNs exposure both in transduced and untransduced cells (**Figure 22C**).

As preservation of HSPC quiescent phenotype may allow maintaining their stem-cell features, we evaluated whether dNs could alter the quiescent cell-cycle status of unstimulated HSPC. As expected, at 24h unstimulated cells showed a greater percentage of cells in G0 in respect to their stimulated counterpart, with almost complete absence of cycling cells (**Figure 22D**). dNs delivery did not alter the quiescence status of these cells, neither at 24h (**Figure 22D**) nor at longer time points (**Figure 22E**) both in transduced and untransduced conditions, suggesting that their stem-cell properties are preserved upon dNs addition. We next investigated whether dNs addition could affect the clonogenic potential of hematopoietic stem cells. We observed a small reduction in the number of colonies of unstimulated HSPC, which may be ascribed to the shorter culture time and thus a reduced number of progenitors (**Figure 22F**). Importantly we did not detect any difference in the clonogenic potential of unstimulated cells that received or not dNs (**Figure 22F**).

Overall, our data highlights a safe profile for dNs delivery in unstimulated HSPC, prompting us to consider dNs as a valid option to reach good levels of transduction while preserving the quiescence and stem cell properties of HSPC, potentially promoting higher engraftment *in vivo.*

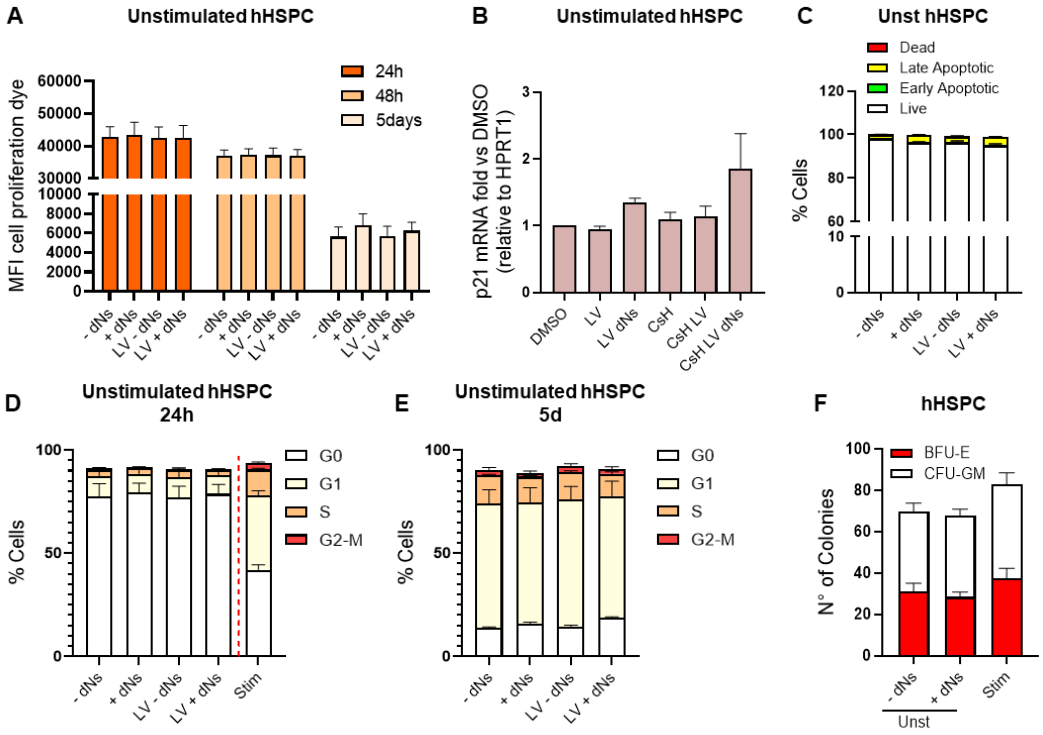

Figure 22. dNs delivery does not impact on proliferation, apoptosis, and cell cycle status of unstimulated hHSPC. A) *Impact of dNs on cell proliferation was assessed in transduced or untransduced quiescent hHSPC. Mean fluorescent intensity of cell proliferation dye was evaluated at the indicated time points by FACS (mean ± SEM; n=4).* ***B)*** *p21 mRNA levels were evaluated by qPCR in unstimulated HSPC 48h post transduction (mean ± SEM; n=3).* ***C)*** *Impact of dNs on apoptosis was assessed in unstimulated hHSPC 48h after dNs delivery during or not LV transduction (mean ± SEM; n=2-3).* ***D-E)*** *Impact of dNs on cell-cycle status of unstimulated hHSPC was evaluated at 24h (D) and at 5 days (E) after dNs delivery during or not of LV transduction (mean ± SEM; n=4).* ***F)*** *Colony-forming unit output of unstimulated hHSPC ± dNs versus stimulated hHSPC (mean ± SEM; n=4).*

6.2.8. Unstimulated HSPC engraft similarly to their pre-stimulated counterpart, despite lower cellular input

Ex vivo culture of HSPC impacts on their engraftment potential, due to cell cycle progression that drives lineage commitment and differentiation, as well as loss of adhesion molecules, which impact on their homing capacity in the BM (Kallinikou *et al*, 2012; Larochelle *et al*, 2012; Glimm *et al*, 2000). On these premises, we reasoned that an efficient gene transfer into quiescent HSPC should allow better preservation of their biological properties, including long-term repopulation capacity. Therefore, we decided to directly assess the HSC engraftment potential of unstimulated cells transduced with our combinatorial transduction protocol, using gold-standard xenograft assay.

Unstimulated human cord blood-derived $CD34^+$ cells were transduced with LV at MOI 25 with addition of CsH and dNs. As a control, HSPC were pre-stimulated over-night with human cytokines and transduced in presence of CsH only at the same MOI. We then transplanted HSPC into NOD scid gamma (NSG) mice by t_0 equivalent and engraftment and transduction efficiency were followed *in vivo* over time. Additional control conditions were kept for the *in vitro* analysis only (**Figure 23A**). Importantly, from the *in vitro* data of this experiment we observed that our combinatorial strategy in unstimulated HSPC yielded higher gene marking levels compared to stimulated HSPC transduced in presence of dimethyl sulfoxide (DMSO) alone, reaching 60% of GFP^+ cells at the moderate MOI used (**Figure 23B**). The enhanced transduction was maintained across the different HSPC subsets (**Figure 23C**), confirming no impact on their composition (**Figure 23D**). The transduction increase was confirmed in terms of integrated viral copies, with CsH and dNs in unstimulated HSPC leading to more than twice the copies observed in DMSO-stimulated HSPC (**Figure 23E**). Overall integrated copies in unstimulated cells remained lower compared to CsH-stimulated HSPC (**Figure 23E**), in line with the expected strong enhancement mediated by CsH in these cells (Petrillo *et al*, 2018).

Importantly, despite lower initial cellular input (**Figure 23F**), unstimulated HSPC showed similar engraftment compared to their stimulated counterpart at longer time points (**Figure 23G**). This was confirmed by the analysis of BM at 20 weeks where a similar percentage of $hCD45^+$ cells was observed between unstimulated and stimulated HSPC (**Figure 23H**). Moreover, similar percentages of $hCD34^+$ cells were observed in the BM of the two groups (**Figure 23I**) with similar composition of primitive $CD34^+CD38^-$ and more committed $CD34^+$ $CD38^+$ fractions (**Figure 23J**). Similar engraftment between the two groups was confirmed in other hematopoietic organs (**Figure 23K-23M**), with no differences in lineage composition of the spleen of primary recipients (**Figure 23L**) and similar frequency of $hCD3^+$ cells observed in the thymus from the two groups (**Figure 23N**).

Remarkably, the high transduction level achieved with the combination of dNs and CsH in unstimulated cells was maintained *in vivo* and remained stable among all the time points analyzed (**Figure 23O**). Similar gene marking levels were also confirmed in the different organs at 20 weeks post-transplantation (**Figure 23P-Q-R**). While the difference in transduction between unstimulated and stimulated HSPC was not strong in terms of percentages of GFP^+ cells, the number of integrated copies *in vivo* remained significantly lower in the unstimulated group in bone marrow, spleen and thymus

(**Figure 23S-T-U**). This reflects the strong enhancement effect of CsH in stimulated HSPC, as we have shown in the past that a I-hit CsH protocol outperforms the reference II-hit clinical protocol in terms of long term gene marking levels (Petrillo *et al*, 2018).

Indeed, although lower, we obtained around 2-3 copies *in vivo* in the non-stimulated group, which may allow reaching physiological expression levels of a desired transgene and is well within a safe and efficient target copy range for most gene therapy applications currently tested (Tucci *et al*, 2022).

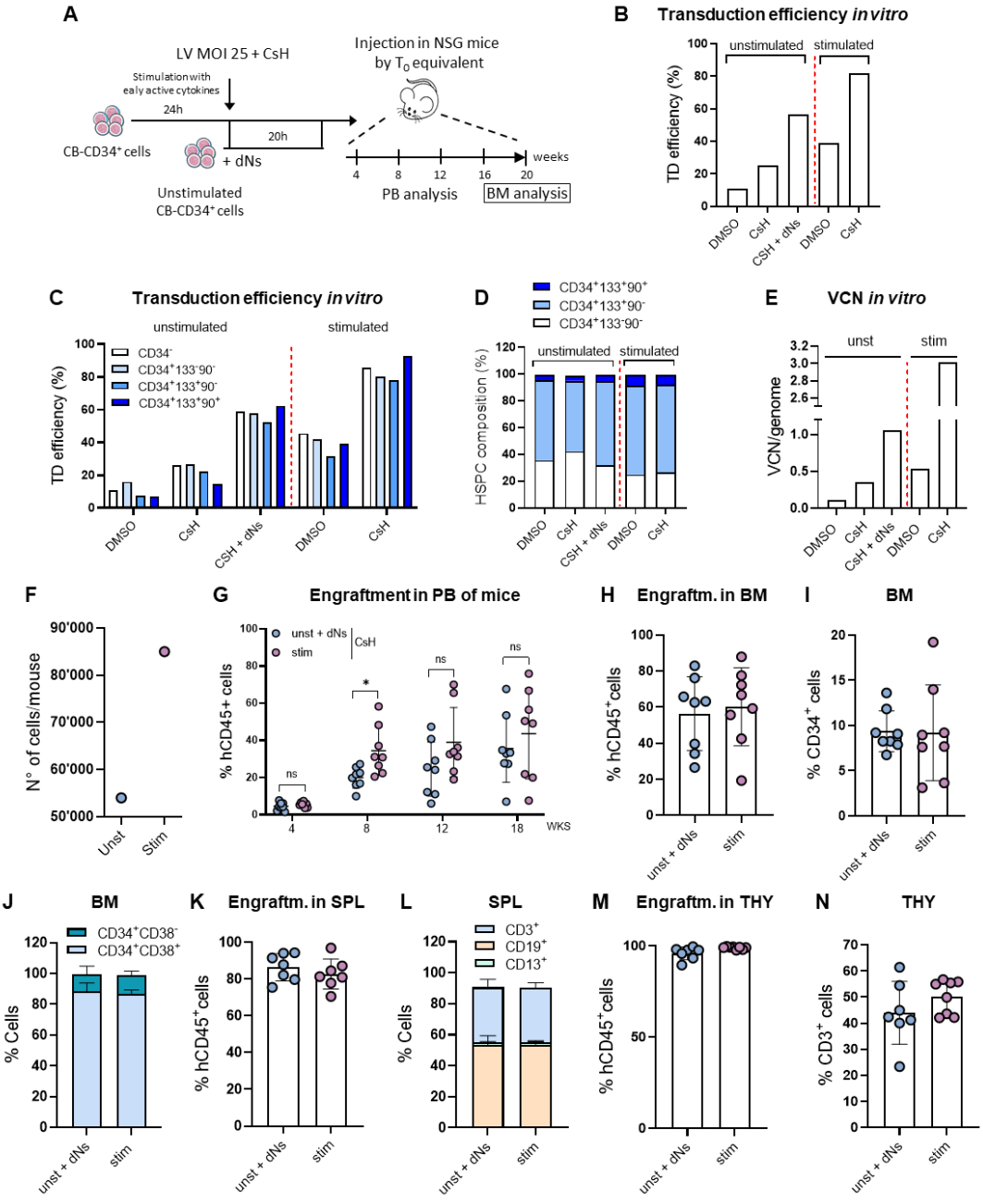

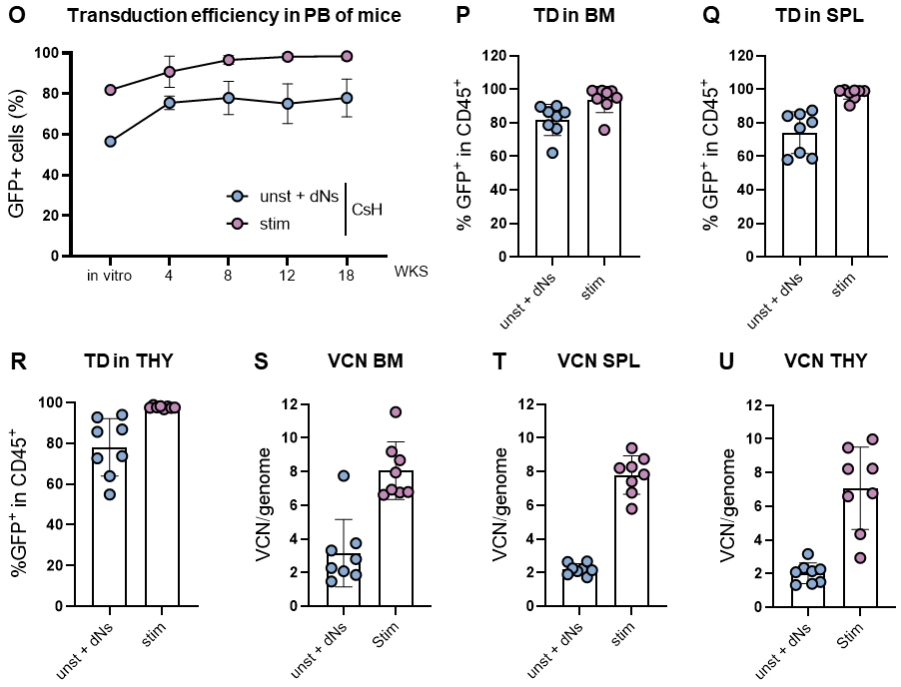

Figure 23. Unstimulated HSPC engraft similarly to their pre-stimulated counterpart, despite lower cellular input. A) *Experimental scheme of the transplant experiment. Human CD34⁺ cells from cord blood were pre-stimulated 24h with a cocktail of early active cytokines before transduction with LV (MOI=25) in presence of 8 µM CsH or kept unstimulated and transduced immediately with LV (MOI=25) in presence of CsH and 500 uM mix of dNs. Cells were then injected 20h post transduction by T_0 equivalent into NSG mice.* ***B-C)*** *In vitro transduction efficiency of the in vivo experiment was assessed 5 days post transduction in the bulk population of HSPC (B) and in the indicated subpopulations (C) by FACS.* ***D)*** *The composition of hHSPC was evaluated 5 days post transduction by FACS.* ***E)*** *In vitro VCN/genome were measured 5 days post transduction.* ***F)*** *N° of cells injected into mice for each experimental group was counted immediately before transplantation.* ***G)*** *Engraftment levels in the peripheral blood of mice from the two experimental groups (mean ± SD; n=8 mice per group, t-test,*for p<0.05, ns=non significant).* ***H)*** *Engraftment levels in the bone marrow at 20 weeks post-transplant (mean ± SD; n=8).* ***I)*** *Percentages of hCD34⁺ cells within hCD45⁺ in the bone marrow at 20 weeks (mean ± SD; n=8).* ***J)*** *Cell composition of the hCD34⁺ fraction in the bone marrow (mean ± SD; n=8).* ***K)*** *Engraftment levels in the spleen at 20 weeks post-transplant (mean ± SD; n=8).* ***L)*** *Percentages of different cell subpopulations of the spleen (mean ± SD; n=8).* ***M)*** *Engraftment levels in the thymus at 20 weeks post-transplant (mean ± SD; n=8).* ***N)*** *Percentages of hCD3⁺ cells within hCD45⁺ in the thymus at 20 weeks (mean ± SD; n=8).* ***O)*** *Transduction efficiencies in the peripheral blood of mice from the two experimental groups measured as % of GFP⁺ cells within hCD45⁺ cells (mean ± SD; n=8 mice per group).* ***P-Q-R)*** *Transduction efficiencies measured as % of GFP⁺ cells within hCD45⁺ cells in bone marrow (P), spleen (Q) and thymus (R) at 20 weeks post-transplant (mean ± SEM; n=8).* ***S-T-U)*** *VCN/genome were measured in the bone marrow (S), spleen (T) and thymus (U) at 20 weeks (mean ± SEM; n=8).*

6.2.9. dNs and CsH in unstimulated mPB HSPC allow reaching good levels of transduction while preserving their repopulation capacity

On these premises, we decided to confirm the potential of our combinatorial transduction protocol in a clinically relevant source, transplanting mobilized peripheral blood-derived hHSPC. We transduced unstimulated mPB-derived HSPC at MOI 50 with CsH and dNs. As a control, HSPC were pre-stimulated for 24h and transduced in presence of CsH alone. We then injected cells into NSG mice by t_0 equivalent and we follow engraftment and transduction efficiency *in vivo* over time (**Figure 24A**). From the *in vitro* analysis we confirmed that we can achieve high gene marking levels in unstimulated mPB-CD34$^+$ cells by combining dNs and CsH, reaching 60% of GFP$^+$ cells in the bulk and in the different HSPC subpopulations (**Figure 24B-24C**), with no major impact observed on HSPC composition (**Figure 24D**). The transduction level was confirmed in terms of integrated viral copies despite overall integrated copies in unstimulated cells remained much lower compared to CsH-stimulated HSPC, as previously observed in CB-CD34$^+$ cells (**Figure 24E**). Importantly, we confirmed similar engraftment capacity for unstimulated mPB-CD34$^+$ (**Figure 24G**) despite lower initial cellular input (**Figure 24F**). Similar levels of engraftment were confirmed in the BM at 20 weeks post-transplantation (**Figure 24H**), with similar cell composition observed for the two groups (**Figure 24I**). We also evaluated absolute counts to highlight potential differences between the two groups. Indeed, while percentages were similar, we observed a slight increase in human CD45$^+$ cells counts in the unstimulated group (**Figure 24J**), with consequent higher counts of human CD33$^+$, CD19$^+$ and CD34$^+$ cells (**Figure 24K**).

Importantly, we confirmed that with our transduction protocol we could achieve and maintain high level of transduction *in vivo* also in the more clinically relevant mPB source of unstimulated HSPC (**Figure 24L**). The high transduction levels were confirmed in the different hematopoietic organs at 20 weeks post-transplantation (**Figure 24M-N-O**). As previously observed, the difference in terms of integrated copies *in vivo* remained strong if comparing our unstimulated group to the CsH-stimulated one (**Figure 24P-Q-R**). This again reflects the fact that we are using as a reference for stimulated cells a protocol which have been demonstrated to be superior to the current clinical reference protocol (Petrillo *et al*, 2018). Indeed, we reasoned that the difference in vector copy number between the two groups would be less if the VCN from the unstimulated HSPC is compared to those usually retrieved from a standard II-hit clinical protocol in stimulated HSPC (Petrillo *et al*, 2018). For this reason, we decided to perform an additional *in vivo* experiment to compare our combinatorial approach in unstimulated HSPC with the

current gold-standard reference II-hit transduction protocol used in the clinics for stimulated HSPC.

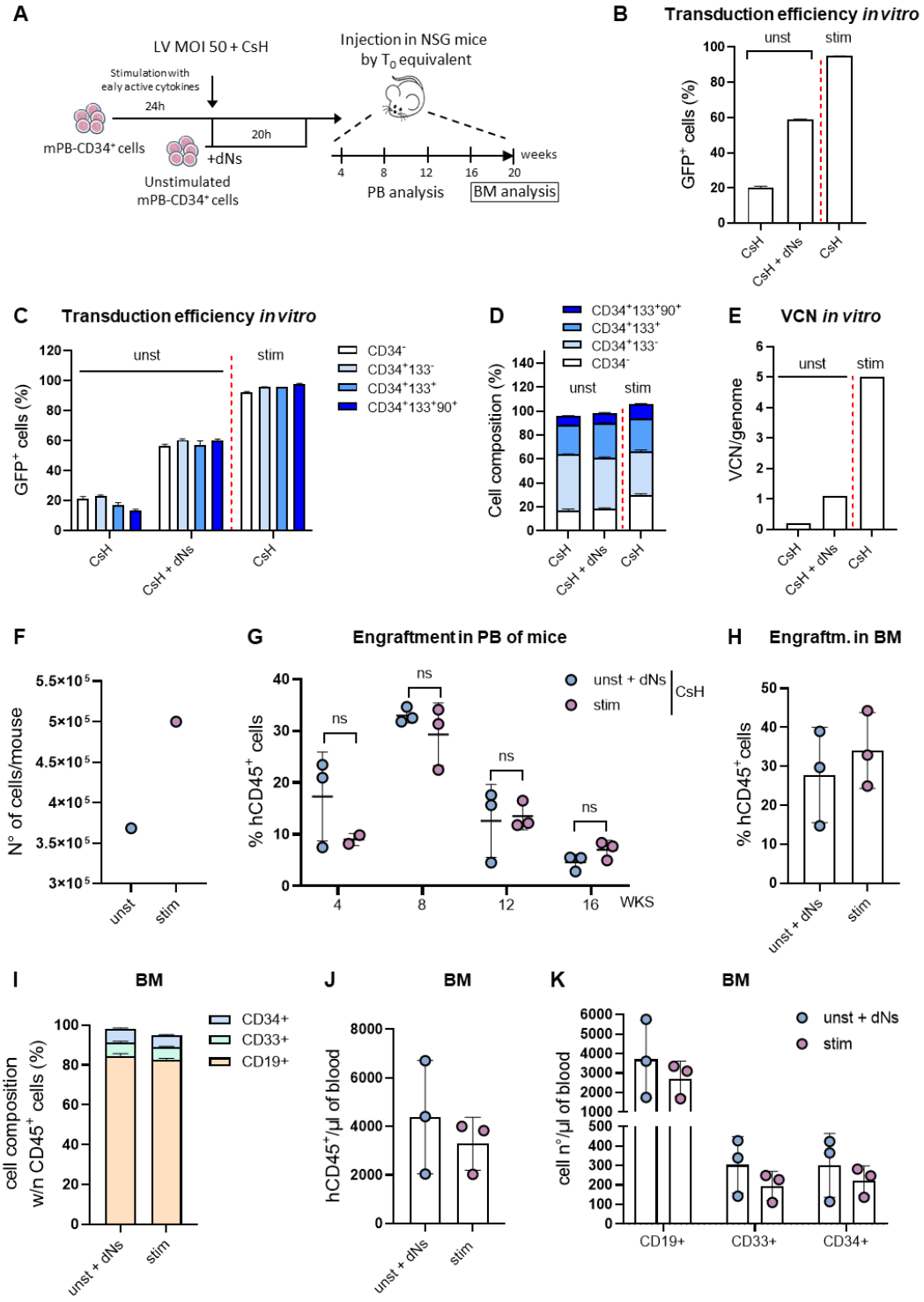

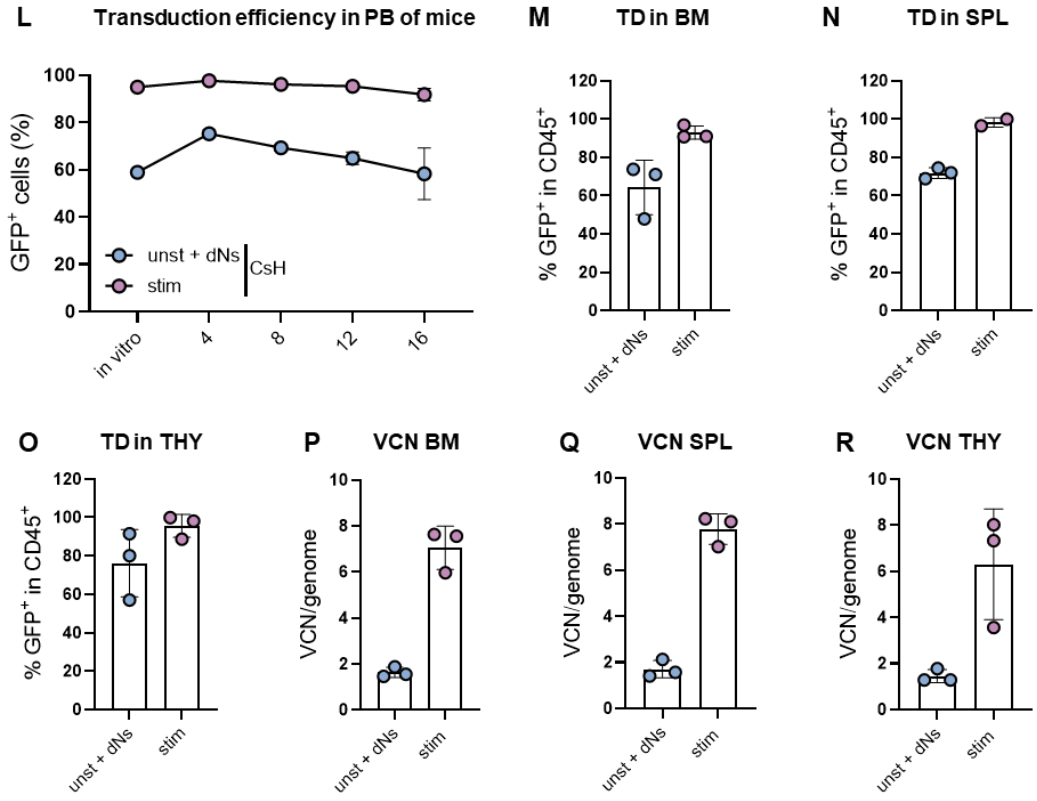

Figure 24. dNs and CsH in unstimulated mPB HSPC allow reaching good levels of transduction while preserving their repopulation capacity. A) *Experimental scheme of the transplant experiment. Human CD34⁺ cells from mobilized peripheral blood were pre-stimulated 24h with a cocktail of early active cytokines before transduction with LV (MOI=50) in presence of 8 µM CsH or kept unstimulated and transduced immediately with LV (MOI=50) in presence of CsH and 500 uM mix of dNs. Cells were then injected 20h post transduction by T_0 equivalent into NSG mice.* ***B-C)*** *In vitro transduction efficiency of the in vivo experiment was assessed 5 days post transduction by FACS in the bulk population of HSPC (B) and in the indicated subpopulations (C).* ***D)*** *The composition of hHSPC was evaluated 5 days post transduction by FACS.* ***E)*** *In vitro VCN/genome were measured 5 days post transduction.* ***F)*** *N° of cells injected into mice for each experimental group was counted immediately before transplantation.* ***G)*** *Engraftment levels in the peripheral blood of mice from the two experimental groups as percentages of hCD45⁺ cells (mean ± SD; n=3 mice per group, t-test, ns=non significant).* ***H)*** *Engraftment levels in the bone marrow at 20 weeks post-transplant as percentages of hCD45⁺ cells (mean ± SD; n=3).* ***I)*** *Cell composition of the bone marrow at 20 weeks (mean ± SEM; n=3).* ***J)*** *Absolute counts of hCD45⁺ cells in the bone marrow at 20 weeks (mean ± SD; n=3).* ***K)*** *Absolute counts of hCD33⁺, hCD19⁺, hCD34⁺ cells in the bone marrow at 20 weeks (mean ± SD; n=3).* ***L)*** *Transduction efficiencies in the peripheral blood of mice from the two experimental groups measured as % of GFP⁺ cells within hCD45⁺ cells (mean ± SD; n=3 mice per group).* ***M-N-O)*** *Transduction efficiencies, measured as % of GFP⁺ cells within hCD45⁺ cells, in bone marrow (M), spleen (N) and thymus (O) at 20 weeks post-transplant (mean ± SD; n=3).* ***P-Q-R)*** *VCN/genome were measured in the bone marrow (P), spleen (Q) and thymus (R) at 20 weeks post-transplant (mean ± SD; n=3).*

6.2.10. CsH+dNs-transduced unstimulated HSPC show great superiority in engraftment capacity as compared to HSPC transduced with the gold-standard II-hit protocol

We thus decided to compare our combinatorial transduction protocol in unstimulated cells to the reference II-hit protocol of transduction, in which mPB-CD34$^+$ cells are pre-stimulated for 24h with early active cytokines and transduced twice (after 20 hours) in the absence of CsH with LV at MOI 100. 20h after the second hit of transduction (for stimulated cells) or the single hit (for unstimulated cells) we transplanted an equal number of cells into NSG mice, to compare side by side the engraftment potential of the two groups (**Figure 25A-B**). The *in vitro* data confirmed our previous observations, with unstimulated cells reaching around 70% of transgene expression within all the different HSPC subsets (**Figure 25C-D**). As hypothesized, the difference in terms of integrated viral copies between the two groups was still present (**Figure 25F**) but was lower as compared to our previous experiment (**Figure 24E**). FACS analysis performed 5 days after the last hit of transduction highlighted a strong decrease in CD34$^+$ percentages in stimulated cells as compared to unstimulated ones, with a consequent reduction of the most primitive CD34$^+$CD133$^+$CD90$^+$ HSPC subset (**Figure 25E**), highlighting the negative impact of the longer *ex-vivo culture* on stemness properties. The most striking observation was the significantly enhanced engraftment potential *in vivo* of the unstimulated cells as compared to their stimulated counterpart at all the time points analyzed (**Figure 25G**). The engraftment was significantly improved also in BM at 13 weeks after transplant, both in terms of percentages (**Figure 25H**) and absolute counts (**Figure 25I**) of hCD45$^+$ cells. The advantage of unstimulated cells in engraftment was not only quantitative but also qualitative, as demonstrated by the analysis of cellular composition of the BM (**Figure 25J**). Unstimulated cells showed increased percentage of hCD34$^+$ cells (**Figure 25J-K**), which corresponded to a significant increase in their total number (**Figure 25L**). Moreover, CD34$^+$ cells from unstimulated group were slightly enriched in the more primitive CD34$^+$38$^-$ fraction (**Figure 25M**), which appeared significantly higher when looking at the total counts (**Figure 25N**). In addition, the proportion of myeloid progenitors was enriched (**Figure 25J**) in unstimulated versus stimulated group with overall higher total number of both myeloid (CD33$^+$) and lymphoid (CD19$^+$) cells (**Figure 25O-P**). Analysis of the thymus 13 weeks post transplantation revealed high and comparable engraftment for both groups (**Figure 25Q**), with a

significantly higher proportion of hCD3^{+} cells in the unstimulated condition (**Figure 25R**).

In terms of gene marking levels, unstimulated cells maintained around 70-60% of GFP^{+} cells *in vivo* across all the time points analyzed (**Figure 25S**), and in the bone marrow (**Figure 25T**). This was confirmed by VCN analysis in the BM, where we detected at least one vector copy per cell as previously observed *in vitro* (**Figure 25U)**. Unexpectedly, in the stimulated condition we observed a huge increase in total VCN from the *in vitro* condition to the *in vivo* (**Figure 25U**). Consequently, while the *in vitro* data confirmed a smaller gap in transduction between unstimulated and stimulated cells, we could not confirm the same from the *in vivo* data. However, we confirmed good transduction levels for the unstimulated cells and since the engraftment data were promising, we decided to evaluate long-term HSC function performing secondary transplant experiment. This on-going experiment will allow us to better evaluate and compare the fitness of the two groups and their ability to sustain hematopoietic reconstitution long-term.

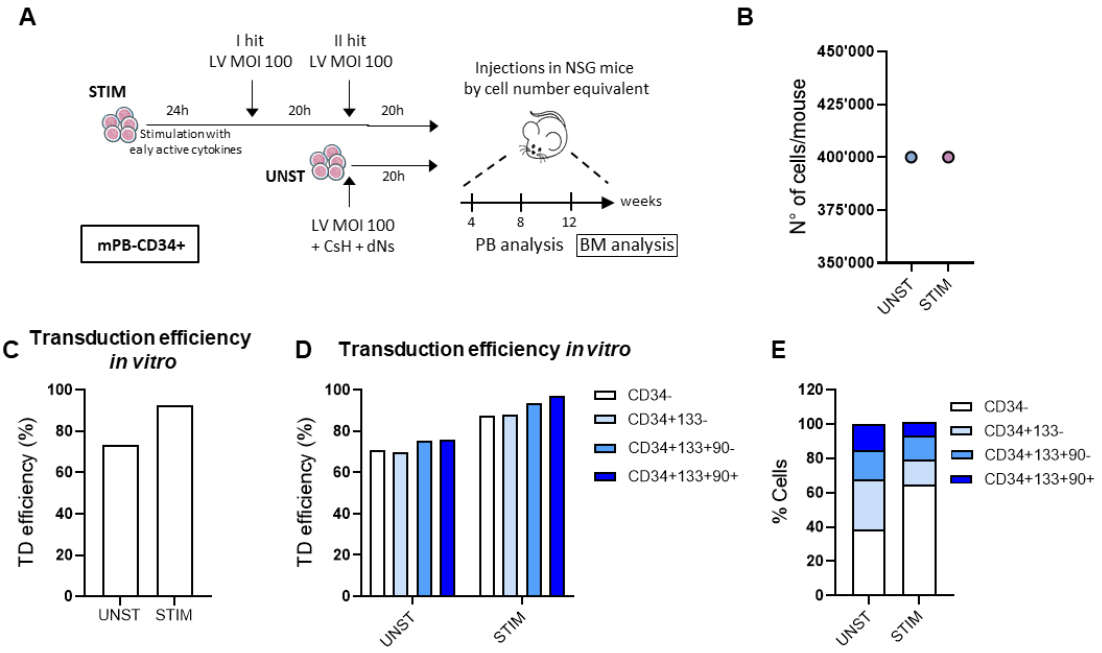

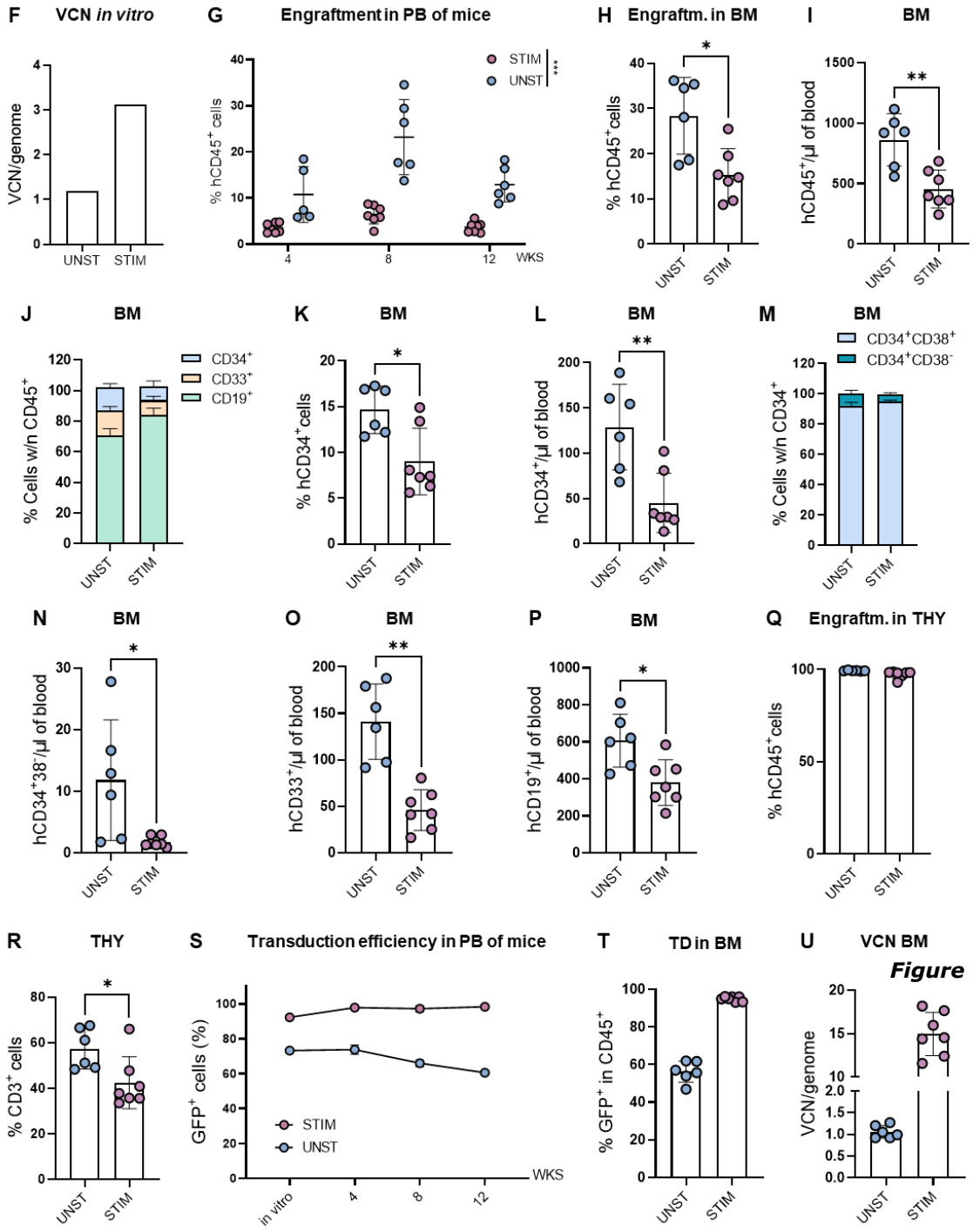

Figure 25. CsH+dNs-transduced unstimulated HSPC show great superiority in engraftment capacity as compared to HSPC transduced with the gold-standard II-hit protocol. A) *Experimental scheme of the transplant experiment. Human CD34⁺ cells from mPB were pre-stimulated 24h with a cocktail of early active cytokines and transduced twice with LV (MOI=100) or kept unstimulated and transduced immediately with LV (MOI=100) in presence of CsH and 500*

uM mix of dNs. Cells were then injected 20h post transduction by cell number equivalent into NSG mice. ***B)*** *N° of cells injected into mice for each experimental group.* ***C-D)*** *In vitro transduction efficiency of the in vivo experiment was assessed 5 days post transduction in the bulk population of HSPC (C) and in the indicated subpopulations (D) by FACS.* ***E)*** *The composition of hHSPC was evaluated 5 days post transduction by FACS.* ***F)*** *In vitro VCN/genome were measured 5 days post transduction.* ***G)*** *Engraftment levels in the peripheral blood of mice from the two experimental groups as percentages of human $CD45^+$ cells (mean ± SD; n=7 mice for stimulated group, n=6 mice for unstimulated group, Mann-Whitney test, ***for p<0.001).* ***H)*** *Engraftment levels in the bone marrow at 13 weeks post-transplant as percentages of human $CD45^+$ cells (mean ± SD; n=6-7, Mann-Whitney test,*for p<0.05).* ***I)*** *Absolute counts of $hCD45^+$ cells in the bone marrow at 13 weeks post-transplant (mean ± SD; n=6-7, Mann-Whitney test, **for p<0.01).* ***J)*** *Cell composition of the bone marrow at 13 weeks (mean ± SEM; n=).* ***K)*** *Percentages of $hCD34^+$ cells within $hCD45^+$ in the bone marrow at 13 weeks (mean ± SD; n=6-7, Mann-Whitney test, *for p<0.05).* ***L)*** *Absolute counts of $hCD34^+$ cells in the bone marrow at 13 weeks (mean ± SD; n=3, Mann-Whitney test, **for p<0.01).* ***M)*** *Cell composition of the $hCD34^+$ fraction in the bone marrow (mean ± SEM; n=6-7).* ***N)*** *Absolute counts of the $hCD34^+38^-$ fraction in the bone marrow at 13 weeks (mean ± SD; n=6-7, Mann-Whitney test, *for p<0.05).* ***O-P)*** *Absolute counts of $hCD33^+$ (O) and $hCD19^+$ (P) cells in the bone marrow at 13 weeks (mean ± SD; n=6-7, Mann-Whitney test, *for p<0.05, **for p<0.01).* ***Q)*** *Engraftment levels in the thymus at 13 weeks post-transplant as percentages of human $CD45^+$ cells (mean ± SD; n=6-7).* ***R)*** *Percentages of $hCD3^+$ cells in the thymus at 13 weeks post-transplant (mean ± SD; n=6-7, Mann-Whitney test, *for p<0.05).* ***R)*** *Transduction efficiencies in the peripheral blood of mice from the two experimental groups as percentages of GFP^+ cells within $hCD45^+$ cells (mean ± SD; n=6-7 mice per group).* ***T)*** *Transduction efficiencies, measured as % of GFP^+ cells within $hCD45^+$ cells, in bone marrow at 13 weeks post-transplant (mean ± SD; n=6-7).* ***U)*** *VCN/genome were measured in the bone marrow at 13 weeks post-transplant (mean ± SD; n=6-7).*

7. DISCUSSION

Hematopoietic stem cell gene therapy has demonstrated a great potential for treating blood monogenic disorders with several clinical successes highlighting the potency and safety of this application (Ferrari *et al*, 2021a). Still, prolonged *ex vivo* culture and multiple rounds of transduction are required to achieve clinically relevant gene marking levels. Both culture conditions and vector manipulation may negatively impact HSC biology with harmful consequences on their repopulation capacity and overall gene therapy efficacy. One of the reasons behind poor permissivity to transduction is the viral origin of the vectors (Piras & Kajaste-Rudnitski, 2021). Thus, an improved understanding of the interactions between HSC and viral vectors may support the improvement of gene therapy protocols.

In this thesis, we focused on the two aspects of vector-host interactions. On one side, we expanded our study of innate immune mechanisms of gene therapy vectors recognition, focusing on γRV-induced signaling. On the other side, we investigated the restriction mechanisms underlying the low permissivity of HSPC to viral transduction, from SAMHD1 role in stimulated and unstimulated HSPC to the design of a protocol for efficient LV manipulation of quiescent HSPC.

7.1. Investigating innate immune responses to viral vectors in human hematopoietic stem cells

We have previously shown that viral gene therapy vectors are differently recognized by HSPC (Piras *et al*, 2017). While LV and AAV6 trigger p21 response, γRV induce strong upregulation of type I IFN responses, through mechanisms there are still unclear.

Here we show that human monocyte-derived macrophages (MDM) recapitulate the response to γRV and we used them as a model to investigate the molecular mechanisms behind vector recognition. We show that γRV transduction leads to upregulation of different ISG that raise from 6h to 24h after transduction, indicating that early steps of the retroviral cycle lead to IFN production. Moreover, ISG induction can be prevented by using a neutralizing antibody against the IFNα receptor.

Early recognition may suggest the involvement of nucleic acid sensing. While LV do not trigger type I IFN responses, we hypothesized that recognition of γRV may be due to a lower rate of nuclear entry in non-cycling cells, with accumulation of reverse-

transcribed products within the cytosol that become accessible to cytosolic sensors, differently from LV that actively enter the nucleus. Indeed, MLV DNA is recognized by cGAS-STING in macrophage cells and primary macrophages, triggering activation of type I IFN responses (Gao *et al*, 2013). However, the recognition occurs if mechanisms that prevent the accumulation of viral DNA are lost, such as in the absence of the TREX1 endonuclease. Furthermore, different gammaretroviruses, including MoMLV, code for a glycosylated Gag, named glyco-Gag, which originates from an earlier start codon (Stavrou *et al*, 2013). The absence of glyco-Gag affects the stability of the capsid, which induces strong antiviral responses due to increased detection of reverse-transcribed products from cytosolic sensors (Stavrou *et al*, 2013, 2015). MoMLV-derived γRV used in gene therapy lacks the upstream initiation codon for the production of glyco-Gag rendering plausible the possibility that the low capsid stability could be the cause of vector recognition in primary HSPC and MDM. Differences in core stability could also explain why only γRV and not LV trigger IFN responses in these cells (Piras *et al*, 2017). Indeed, HIV-1-derived LV exploit cellular cofactors to tightly orchestrate reverse transcription, uncoating, and nuclear entry, thus avoiding detection of viral DNA in the cytoplasm (Rasaiyaah *et al*, 2013). Nevertheless, the reverse-transcribed DNA is not the trigger of γRV recognition, neither in HSPC (Piras *et al*, 2017) nor in MDM, as shown here. Experiments in which cells are exposed to γRV with addition of the RT inhibitor AZT demonstrate that lack of RT does not prevent induction of the antiviral response. Moreover, knockouts of the cytosolic DNA sensors cGAS and STING, confirm that these factors are dispensable for activation of immune responses upon γRV transduction.

Several TLRs are involved in immune responses against murine retroviral infections in mice. TLR7-deficient mice display higher infection levels due to the inability of mounting an effective immune response (Browne, 2013). TLR3 as well can limit viral infection in mice with induction of type I interferon responses (Gibbert *et al*, 2014). TLR3 likely detects endosomal dsRNA that generates from ssRNA secondary structures or dimerization of the two genomic ssRNA molecules. Nevertheless, little is reported about the mechanisms of murine retroviral nucleic acids recognition in human primary cells. We show here that endosomal TLRs are not activated upon γRV entry into the cell, and in line with a lack of endosomal recognition, vectors that are pseudotyped with plasma membrane-fusing envelope continue to be recognized, suggesting a possible cytosolic mechanism of RNA detection. It has been shown that RIG-I can sense purified genomic RNA from HIV-1, which instead does not activate MDA5 (Solis *et al*, 2011). In addition,

RIG-I can mediate innate immune responses upon recognition of secondary structured HIV-derived RNA (Berg *et al*, 2012), leading us to test its potential involvement in γRV RNA sensing. However, we show that cells KO for RIG-I and MAVS retained the ability to respond to the vector. While RIG-I is not the unique cytosolic RNA sensor, the MAVS KO cell lines allow us to broaden our conclusions to other RLR members as all of them recruit MAVS for downstream activation of type I IFN responses (Rehwinkel & Gack, 2020). Importantly, we show that transduction with empty particles devoided of the viral RNA genome, induces similar induction of ISG in primary macrophages, suggesting a mechanism of structural rather than nucleic acid sensing.

Viral vectors employed in this work were produced transfecting HEK293T from which the supernatant is collected, filtered, and concentrated by ultracentrifugation. It is known that this procedure for lab-grade vector production often leads to the incorporation of contaminants within the stocks, which may cause toxicity and activation of immune responses, as observed in *in vivo* setting (Baekelandt *et al*, 2003; Soldi *et al*, 2020). Since γRV undergoes two rounds of ultracentrifugation, we hypothesized that a higher amount of contaminants could be present in the vector stocks becoming a source of innate immune activation. Nevertheless, we show that similar amounts of contaminants are present in both LV and γRV productions. Moreover, treatment of vectors with DNase does not impair the recognition of γRV, suggesting that ISG induction is not due to plasmid contaminants.

Based on the observation that empty particles retain immune triggering phenotype, we made different hypotheses about the nature of the PAMP that can be sensed in MDM. VLP lack viral nucleic acids but retain the structural components that derive from the Gag gene, and viral enzymes from the Pol sequence. The viral structural core represents an interaction platform for many different host proteins (Fletcher *et al*, 2018). Sensing of the retroviral capsid by TRIM5α is unexpected, as hTRIM5α is unable to restrict NB-tropic MLV strains such as MoMLV, from which γRV derive (Stremlau *et al*, 2006; Perron *et al*, 2007). In addition, TRIM5α signaling involves NF-κB rather than IFN (Pertel *et al*, 2011; Fletcher *et al*, 2018). In line, we show that cells KO for TRIM5α continue to recognize γRV, inducing ISG upregulation. Nevertheless, despite we have not been successful in constructing MLV capsid chimeric LV, our data with the other structural chimeric LV suggest that the γRV capsid represents the putative source of vector recognition. As it is known that interfering with the retroviral core structure may affect

its stability (Burdick *et al*, 2020), it will be important to evaluate capsid stability of the chimeric constructs by either sucrose-gradient fractionation or electron microscopy.

Capsid sequence and three-dimensional structure may be fundamental in determining interaction with host factors, as occurring with TRIM5α, where single amino acid substitutions within the capsid sequence can promote or limit viral restriction (Maillard *et al*, 2007). Thus, we are currently producing and testing retroviral vectors derived from N- or B-tropic MLV, to determine whether they retain the immune-triggering phenotype in primary macrophages. The alignment and comparison of the capsid sequence of NB-, N-, and B-tropic MLV will allow us to better identify domains that are important for viral recognition. In the capsid region that faces outside the core, only 11 amino acids differ between the three viruses. In the case of an NB-tropic specific immune response, site-directed mutagenesis will allow us to identify critical residues for capsid recognition.

While the host sensors that detect ɣRV in HSPC and MDM remain to be determined, we highlight the involvement of the TBK1 kinase in mediating the downstream response to the vector. While TBK1 role in canonical nucleic acid sensor-mediated responses is extensively studied, less is known about other factors that engage TBK1. Of note, our observations are based on the use of a chemical compound, BX795, described to inhibit TBK1 phosphorylation and activation. Thus, the generation of U937 KO cell lines for TBK1 will be important to confirm the central role of this kinase. Indeed, despite we observe early TBK1 phosphorylation, we cannot exclude that this may be an indirect consequence of immune activation of the cells, rather than a direct engagement by host sensors. Moreover, both our antibody and the BX795 inhibitor recognize and target also the close homolog of TBK1, IKKε. It is known that the two kinases have overlapping functions, with IKKε being able to phosphorylate IRF3 and IRF7 to mediate IFN production (Fitzgerald *et al*, 2003; Perry *et al*, 2004; tenOever *et al*, 2004). In addition, TBK1-deficient cells develop compensatory strategies, where IKKε upregulation may remedy TBK1 loss (tenOever *et al*, 2004; Taft *et al*, 2021; Balka *et al*, 2020). We are currently generating IKKε KO and double KO cell lines to better dissect the contribution of the two kinases in orchestrating antiviral responses to the vector.

Genome-wide screening may allow us to identify host factors involved in vector sensing in an unbiased way. However, some limits, such as the requirement of high vector doses, exist in our experimental model rendering it difficult to work with very large cell numbers to maintain the high coverage of genome-wide libraries. Thus, we decided to exploit a CRISPR/Cas9 library targeting 1902 interferon-stimulated genes to

search for candidate factors (OhAinle *et al*, 2018). cGAS, STING, RIG-I, MDA5, MAVS, TRL3 and 7, and the structural sensor TRIM5α are all examples of innate immune sensors that are ISG family members. Moreover, we observed that U937 cells are competent for structural γRV sensing only when differentiated in macrophage-like cells with PMA treatment. Interestingly, analyzing publicly available datasets we found that the many ISG are upregulated upon PMA exposure (Baek *et al*, 2009), suggesting that the viral immune phenotype may be linked to the upregulation of some specific factors in PMA-treated cells. Together, these observations support our rationale for screening for ISG in the search for the immune sensor recognizing the γRV core. Importantly, among the highest-ranking genes, we found expected genes related to the IFNα signaling pathway, thus confirming the success of our screening. Among others, many regulators of transcription came out, which can broadly influence the expression of different genes including interferon-stimulated genes, thus being potentially less relevant for our purposes. We are currently focusing on less general and more interesting candidate factors to assess their role in the response to γRV transduction in the U937 cell line model.

Overall, the data presented in my work underline the existence of a novel immune mechanism of viral structural recognition, shedding light on molecular mechanisms that control innate immune defenses in HSPC and primary macrophages. The same mechanisms may potentially apply to other primary cell types. This is relevant for future gene therapy applications. Indeed, γRV are no longer considered the first choice as gene transfer vehicle in current gene therapy approaches due to their genotoxic profile and evidence of LV as a safer and more efficient platform (Ferrari *et al*, 2021a). Nevertheless, virus-like particles, including those derived from murine retroviruses, are emerging as promising delivery vehicles for the new gene editing platforms, as well as for the delivery of RNP *in vivo* (Gee *et al*, 2020; Banskota *et al*, 2022). As we have highlighted a nucleic-acid independent recognition of the vector, it will be critical to evaluate possible activation of immune responses to viral structural components that are retained in the VLP in the target cells, either HSPC or other organ cell types. Indeed, while we have not observed similar activation of type I IFN responses upon γRV exposure in T cells (data not shown), it remains to be evaluated whether the recognition mechanisms are conserved among other cell types that are targeted for *in vivo* gene therapy applications, such as hepatocytes, neurons, or retinal cells. In addition, several CAR T cell products are still produced using MLV-based γRV (Watanabe & McKenna, 2022). Current and

future work will be important to identify the host sensor involved in the detection of retroviral cores. This may allow identifying novel immune factors that despite being involved in the recognition of murine retroviruses may be important for the recognition of other viruses, including relevant human pathogens.

7.2. Investigating antiviral restriction mechanisms in human hematopoietic stem cells

Genetic engineering of quiescent HSPC represents a challenge for gene therapy as they are highly refractory to transduction and constraints inherent to their quiescent cell cycle status impair efficient HDR-based gene editing approaches (Shin *et al*, 2020). However, *ex vivo* manipulation of HSPC negatively impacts their fitness and repopulation capacity (Larochelle *et al*, 2012; Kallinikou *et al*, 2012). The possibility to efficiently transduce quiescent HSPC would therefore allow to preserve their biological properties such as stemness and engraftment. With this in mind, we have developed here a novel lentiviral transduction protocol that allows efficient gene manipulation of quiescent HSPC, reaching good levels of transduction while promoting high engraftment *in vivo*.

Several attempts to increase transduction of *ex vivo* cultured HSPC have guided the development of several transduction enhancers (Heffner *et al*, 2018; Ozog *et al*, 2019; Petrillo *et al*, 2015, 2018; Wang *et al*, 2014). However, few studies have addressed the poor permissiveness of quiescent HSPC. We have previously shown that CsH enhances LV transduction also in quiescent HSPC (Petrillo *et al*, 2018). However, the overall transduction levels are too low for clinical translation, suggesting that additional blocks exist beyond the IFITM3-mediated restriction of LV entry.

The role of SAMHD1 restriction in human HSPC has been explored in pre-stimulated cells exploiting Vpx-incorporating LV, without significant improvements observed on their transduction efficiency, despite stimulated HSPC display high levels of SAMHD1 (Li *et al*, 2015). SAHMD1 phosphorylation is known to regulate its restriction against HIV (Ryoo *et al*, 2014). The functional antiviral form of SAMHD1 may be less abundant in HSPC despite the overall high expression of the protein. Indeed, increased levels of the phosphorylated form have been observed in HSPC in respect to MDM, with Vpx slightly reducing p-SAMHD1 in HSPC (Li *et al*, 2015). This may be the reason why Vpx delivery does not affect transduction in pre-stimulated HSPC, although total SAMHD1 levels decreased. Despite expressing lower levels of SAMHD1 protein (Li *et al*, 2015), we show

here that Vpx can modestly improve LV transduction in freshly isolated HSPC. This benefit is additive with CsH, in agreement with the removal of sequential antiviral blocks mediated by IFITM3 and SAMHD1 on the lentiviral life cycle.

In agreement with SAMHD1-mediated effects on LV reverse transcription through regulation of the cellular dNTP levels (Lahouassa *et al*, 2012), the addition of exogenous dNTPs moderately enhance LV transduction in quiescent murine HSPC (Mikkola *et al*, 2000). No impact instead has been observed in stimulated human HSPC, in line with the lack of benefit from Vpx (Li *et al*, 2015). While we observe that dNTPs addition fails to improve transduction in quiescent human HSPC, the delivery of exogenous dNs significantly improves LV transduction, similarly to CsH, probably due their better penetration in the cells as compared to dNTPs (Shepard *et al*, 2019). Moreover, combining dNs and CsH has a potent synergistic enhancement effect on LV transduction, with a more prominent effect observed in the most primitive HSPC compartment.

Interestingly, we show that dC is almost exclusively responsible for improving transduction, highlighting a prominent role of the pyrimidines in quiescent HSPC restriction. However, measurement of intracellular dNTP levels in quiescent HSPC after exposure to exogenous dNs revealed variable changes in the levels of the four dNTPs, with no impact on dCTP levels. The discrepancy between the levels of intracellular dNTPs and the role of the different dNs may suggest a more complex mechanism behind the dNs-mediated enhancement of transduction than simple additive removal of IFITM3 and SAMHD1 mediated blocks. Nevertheless, we cannot exclude limitations in the sensitivity of the assay, as well as variables that may affect the final readout such as timing or differential dNTPs consumption rate (Rampazzo *et al*, 2010). Of note, dNs addition leads to an intracellular increase in dATP levels, despite dA alone having no effect on the transduction rate of quiescent HSPC, further highlighting the differential importance of the purine and pyrimidines pools.

The levels of intracellular dNTPs are tuned according to the replication rate of the cells. Since quiescent cells are mainly in G0-G1 phase, they require low dNTPs supply. dNTPs production during the S phase is sustained by the *de novo* synthesis pathway, which is an energetically expensive process. Quiescent cells rely mainly on the salvage pathway to recycle nucleic acids to regenerate dNTPs. The expression levels of synthetic enzymes are induced or upregulated at the G1-S transition (Rampazzo *et al*, 2010). In line, we show and confirm that key enzymes of the *de novo* pathway are strongly downregulated in quiescent versus activated HSC (García-Prat *et al*, 2021). Interestingly

rescue of pyrimidines synthesis but not of purines, through the addition of exogenous key intermediates molecules, has a similar effect of providing exogenous dNs, further confirming a major role of the pyrimidine pool in restricting quiescent HSPC. The observation that dNs specifically and solely enhance the transduction of vectors that undergo reverse transcription is another indication of a specific effect on the intracellular dNTP pools rather than a general and non-specific mechanism of enhanced transduction.

In the context of T cells, SAMHD1 has been suggested to play an important role in restricting HIV reverse transcription in resting $CD4^+$ T cells (Baldauf *et al*, 2012). Nevertheless, Vpx-mediated depletion of SAMHD1 did not lead to improved LV transduction in the context of VSV-G pseudotyped vectors in resting T cells. We show here that dNs and even more their combination with CsH may enhance transduction also in resting T cells.

Chimeric antigen receptor (CAR)-T cells are a promising tool for treating cancers and viral infections (Sadelain *et al*, 2017; Seif *et al*, 2019; Kuhlmann *et al*, 2018). However, prolonged *ex vivo* culture, usually ranging from 7 to 14 days, is required to expand CAR T cells, with potential progression towards cells with a terminally differentiated effector memory phenotype and loss of the central memory phenotype (Lu *et al*, 2016; Coeshott *et al*, 2019; Pampusch *et al*, 2020; Sudarsanam *et al*, 2022). Clinical studies have highlighted the importance of having T lymphocytes with a less differentiated phenotype as they better engraft and persist long-term (Klebanoff *et al*, 2012). Indeed, shorter culture protocols have highlighted a better preservation of T cell phenotype and function (Ghassemi *et al*, 2018). In this context, our CsH + dNs-based LV transduction protocol could offer the possibility to generate CAR-T cells from minimally manipulated PBMC as well as to achieve gene marking also in the relevant resting T cell populations including the T stem memory compartment (Gattinoni *et al*, 2011). Recently, it was developed a 24h short protocol for the generation of CAR T from non-activated cells. The authors demonstrated an improvement in killing capacity *in vivo* with respect to standardly produced CAR T (Ghassemi *et al*, 2022). Efficient transduction of unstimulated T cells was obtained by combining different factors including starvation, to enhance expression of the LDL receptor used by LV, the addition of dNs, and by incrementing the ratio between the surface area and the volume of the culture plate. Although they are the first to show how dNs can be exploited to generate CAR T from non-activated cells, we believe that inclusion of CsH can represent a strength of our protocol as with the unique combination of dNs and CsH we reach around 5-fold higher transduction without starving

the cells. Thus different elements, including the use of alternative glycoproteins envelope for LV, such as the measles virus glycoproteins (Frecha *et al*, 2008), can be evaluated together to further ameliorate resting T cells manipulation.

The design of lentiviral vectors may take into account the need of maintaining the physiological expression of the transgene to reach the therapeutic benefit while avoiding toxic effects. This may include the incorporation of large genomic sequences and regulatory elements, as observed for CGD and β-thalassemia (Kohn *et al*, 2020; Morgan *et al*, 2020), representing a limit for the design and manufacturing of high-titer vectors. We show here that vector complexity does not limit the applicability of our protocol in quiescent HSPC. Indeed, the combination of dNs and CsH strongly enhances transduction with a GLOBE-like LV (Marktel *et al*, 2019) that has a lineage-restricted promoter and locus control region elements.

It has been shown that purine or pyrimidine imbalances may negatively impact on cell proliferation (Diehl *et al*, 2022) and cellular pyrimidines deficiency has been linked to mitochondrial DNA-dependent innate immune activation (Sprenger *et al*, 2021). Thus, despite observing that pyrimidine precursors are sufficient to enhance LV transduction, we included all four precursors in our experiments to avoid unwanted harmful consequences on cellular biology. On the other hand, excess intracellular dNTPs has been linked to cell cycle progression and genomic instability (Kohnken *et al*, 2015). Imbalanced intracellular dNTP can cause uncontrolled and low-fidelity DNA replication contributing to mutagenesis and cancer development. DNA replication stress arising from increased mutation rate can contribute to genomic instability and trigger DDR activation (Gorgoulis *et al*, 2005). Importantly, we observe that exogenous dNs addition does not affect the proliferation rate of unstimulated HSPC nor alters their quiescent phenotype with cells remaining in the G0-G1 phases of the cell cycle. Moreover, we do not observe activation of the DDR response with only a slight increase in p21 expression levels when combining CsH and dNs, which may be explained by higher amounts of vector copies within the cells as previously observed for stimulated HSPC (Piras *et al*, 2017).

Overall, our *in vivo* data demonstrate that unstimulated HSPC engraft better and yield superior hematopoietic output compared to the stimulated counterpart. This suggests better preservation of their biological properties and repopulation capacity in line with the lack of *ex vivo* culture. We have previously shown that CsH potently enhances transduction in stimulated HSPC and that a I-hit CsH protocol can surpass the reference II-hit clinical protocol in term of long-term gene marking levels (Petrillo *et al*, 2018).

Since CsH is not currently used in the clinic, we compared our protocol also to the II-hit clinical protocol. Unluckily, we observe an unexpected increase in VCN *in vivo* in stimulated cells, which makes it difficult to compare the two groups. Nevertheless, we believe that this increase from the *in vitro* to the *in vivo* setting is not highlighting better intrinsic properties of stimulated HSPC, as we have never observed such an increase in our previous experiments or in other contexts (Petrillo *et al*, 2018), but is rather linked to the animal model employed in these experiments. Moreover, despite the demonstrated safety of LV as gene delivery platform, semi-random vector integration remains of concern. For instance, in clinical trials for beta-thalassemia, LV integration has been shown to cause transcriptional activation of HMGA2 leading to higher production of a truncated form of the RNA (Cavazzana-Calvo *et al*, 2010). As high vector copy numbers may promote oncogenic events, the FDA recommends less than five VCN per genome (Zhao *et al*, 2017).

Importantly, despite overall transduction levels remain lower with respect to stimulated HSPC, with our transduction protocol we reach high transgene expression and clinically relevant number of integrated copies long-term *in vivo* without affecting HSC function. While the levels of VCN achieved with our protocol will likely be insufficient for disease contexts in which supraphysiological expression of the transgene is required for clinical benefit, it may represent a safe strategy for diseases in which the gene-corrected cells acquire engraftment and proliferative advantages, such as in the context of Fanconi Anemia (Río *et al*, 2019). Moreover, the possibility to reduce the culture time is extremely important if we consider some of the limitations encountered in current clinical trials. Thus far, X-CGD LV gene therapy has failed to fully restore functional defects and several patients have lost engraftment of gene-marked HSC (Kohn *et al*, 2020; Magnani *et al*, 2014). While the etiology of graft loss remains unclear, increased oxidative DNA damage and inflammation have been suggested to compromise X-CGD HSC (Weisser *et al*, 2016; Yahata *et al*, 2011). Similarly, current gene therapy protocols for Fanconi Anemia disease rely on short transduction protocols aimed at limiting the *ex vivo* manipulation of these extremely fragile cells (Río *et al*, 2019). On these premises, we predict that our CsH+dNs transduction protocol that does not require prolonged *ex vivo* culture of HSPC will provide a significant improvement for such settings in which the disease background impacts HSC biological properties.

Secondary transplant experiments will allow us to evaluate and compare the ability of HSPC, from unstimulated or stimulated sources, to sustain hematopoietic

reconstitution long-term. Finally, studies aimed at evaluating the integration profile of LV in unstimulated HSPC are ongoing. It will be important to highlight a benign integration profile. Moreover, whether transduction of quiescent cells may lead to benefits in terms of graft clonality remains to be addressed.

Overall, our data support the existence of multiple innate immune blocks to efficient transduction of unstimulated HSPC and other quiescent cell sources, paving the way for new genetic engineering strategies directly in unstimulated targets of cell and gene therapies.

Together, my thesis work provides examples of how investigating the innate immune mechanisms of cell-vector interactions can provide relevant insight into the biology and innate defenses of clinically relevant primary cells and can fuel the development of improved cell and gene therapies.

8. MATERIALS AND METHODS

8.1. Vectors

Lentiviral and γ-retroviral vectors were produced and titered as described (Dull *et al*, 1998; Follenzi & Naldini, 2002; Montini *et al*, 2006). To produce IDLV the packaging construct was replaced by the pMD.Lg/pRRE.D64VInt, as already reported (Lombardo *et al*, 2007). Bald vectors were generated eliminating the use of the envelope plasmid; empty vectors were generated eliminating the use of the transfer plasmid as previously reported (Piras *et al*, 2017). To produce vectors pseudotyped with the baboon envelope, the envelope plasmid was substituted with the BaEV-TR plasmid (Girard-Gagnepain *et al*, 2014). To produce vectors with the RD114 envelope, the envelope plasmid was replaced with the endogenous feline viral envelope RD114. Vpx-incorporating LV were produced as described (Bobadilla *et al*, 2013). SIV vectors were generated transfecting the SIVmacGFP transfer plasmid, the SIVmac packaging construct and usual envelope plasmid (Mangeot *et al*, 2002). Globe-like vector was provided in collaboration by Giuliana Ferrari group from SR-TIGET. Chimeric LV-γRV vectors were generated by replacing the packaging construct with modified packaging plasmids synthesized and purchased from GeneScript. All the chimeras were made by replacing HIV structural components with indicated MLV sequences maintaining HIV sequences at junctions between MLV and HIV sequences. AAV6 vectors were purchased from TIGEM Vector Core. The donor template for reporter cell line generation was built by cloning the donor cassette within a plasmid carrying AAV2 inverted terminal repeats, as described (Schiroli *et al*, 2019). The donor cassette was designed with homology arms adjacent to the selected gRNA cut site, the last portion of the ISG15 gene devoid of its stop codon, a 2A self-cleaving peptide, and the dTomato reporter sequence. The construct was design in collaboration with Angelo Lombardo group from ST-TIGET, synthesized, and cloned by GeneScript. SENDAI vector was kindly provided by Luigi Naldini group from SR-TIGET. Knock-out cells lines were generated transducing cells with LV produced with a transfer plasmid coding for the Cas9 nuclease and sgRNA targeting the desired genes (Shalem *et al*, 2014) (sgRNA STING: GTTAAACGGGGTCTGCAGCC; sgRNA cGAS: GCTTCCGCACGGAATGCCAG, sgRNA MAVS: ACAGGGTCAGTTGTATCTAC, sgRNA RIGI: AAAAGTGTGGCAGCCTCCAT, sgRNA TRIM5: CTCAAAATCTGCCAAGACGT). As control, LV

generated using a transfer plasmid coding for the mammalian codon-optimized Cas9 nuclease only was used.

8.2. Cells

Human HEK293T cells were maintained in IMDM medium (Sigma). Human U937 cells were cultured in RPMI medium (Lonza). All media were supplemented with 10% fetal bovine serum (FBS), 100 IU/ml of penicillin, 100 mg/ml of streptomycin, and 2% glutamine. For differentiation of U937 in macrophage-like cells, cells were kept in complete RPMI with phorbol 12myristate 13acetate (PMA) at 40 ng/mL. After 2 days, the medium was replaced with complete medium without PMA for one additional day. U937 KO cells lines were transduced with the previously described LV, and selected with puromycin. Human $CD34^+$ hematopoietic stem cells were isolated with Miltenyi MicroBead Kit from CB of healthy donors following to the Institutional Ethical Committee criteria (TIGET01/09). HSPC from different used sources were purchased from Lonza. $CD34^+$ cells from cord-blood were cultured in StemSpan medium (StemCell Technologies), BM and mPB-derived HSPC were maintained in CellGro medium (Cell Genix). Both media were supplemented with antibiotic and a mix of recombinant human cytokines as previously reported (Petrillo *et al*, 2018). Human $CD14^+$ monocytes were isolated with Miltenyi MicroBead Kit, following manufacturer's instructions from CB or PB. Primary macrophages were differentiated from $CD14^+$ cells culturing them for 7 days in complete DMEM medium supplemented with 5% of human serum (Lonza) (Petrillo *et al*, 2018). T cells were obtained from $CD14^+$-depleted peripheral blood mononuclear cells from healthy individuals and activated using Dynabeads human T-activator CD3/CD28 (Invitrogen) in complete IMDM supplemented with 1 mM non-essential amino acids and sodium pyruvate (GIBCO-BRL), 5 ng/ml of IL-7 and IL-15 (PeproTech) as previously reported (Provasi *et al*, 2012). For resting T cells culture, $CD14^+$-depleted mononuclear cells were maintained in the same medium without addition of IL-7 and IL-5 cytokines. Frozen BM samples from WT or SAMHD1 KO mice were kindly provided by Rayk Behrendt's group. BM samples from WT, MYD88, TLR4, and IFNAR KO mice were a gift from Francesca Granucci's group. Murine hematopoietic stem cells were isolated using the mouse Lineage Cell Depletion Kit (Miltenyi Biotec). Cells were cultured in StemSpan supplemented with penicillin and streptomycin. For stimulation of murine Lin- cells, a mix of murine cytokines was added to the medium as described (Petrillo *et al*, 2018).

8.3. Transduction

Cells were transduced at the reported MOI according to vector titers, which were evaluated as previously described (Follenzi & Naldini, 2002). Human HSPC were transduced after 24h of cytokines stimulation and washed 16-20 hours after transduction. The same medium described above was added for additional 5 days after which they were maintained in complete IMDM without cytokines. Quiescent $CD34^+$ cells were transduced immediately after isolation or thawing for 16-24 hours. After washing, human cytokines and 10μM of the reverse-transcriptase inhibitor 3TC (SIGMA) were added to the medium as reported (Petrillo *et al*, 2018). Primary macrophages were transduced at the end of the differentiation. After 24h, cells were washed and maintained in the same medium. Activated T lymphocytes were transduced after 3 days of stimulation with Dynabeads and washed after 16-20h, and maintained in the same medium. Total $CD14^-$ PBMC were transduced freshly isolated and washed after 16-20h. Lin- cells were transduced after 6h of cytokines stimulation. After 16-24h, cells were maintained in StemSpam as described above. For transduction of unstimulated murine Lin- cells, cells were transduced immediately after thawing or isolation and washed and put in medium with cytokines after 20h.

8.4. Gene editing

The best gRNA for editing experiment in U937 cells was selected by electroporation (SF Cell Line 4D-Nucleofector, Lonza) of 1.25 mM of RNP assembled as reported (Ferrari *et al*, 2020). Cut efficiency was evaluated by NHEJ assay. The sequence recognized by the selected gRNA targeting the IS15 gene is the following: TTCATGAATCTGCGCCTGCG. For gene editing, cells were electroporated as before. 15 minutes after electroporation, cells were transduced with AAV6 donor template described in section 8.1 at MOI 10000. Editing efficiency was evaluated at 4 days by FACS looking at the percentages of $dTomato^+$ cells. For gene editing experiments in quiescent hHSPC, cells were immediately transduced with IDLV (Genovese *et al*, 2014) at MOI 100, with or without addition of dNs and CsH. After 24 hours, cells were electroporated (P3 Primary Cell 4D-Nucleofector, Lonza) as before. The sequence recognized by the gRNA for AAVS1 locus is the following: TCACCAATCCTGTCCCTAG. After electroporation cells were cultured in their medium supplemented with cytokines and 3TC. Editing efficiency was evaluated by

FACS looking at percentages of GFP^+ cells, 3 days after electroporation. For the NHEJ assay, the Surveyor assay (IDT 706020) was performed on PCR amplified fragments covering the sgRNA recognized region, according to manufacturer's instruction. The resulting digested amplicons were analyzed with the Tape Station Instrument (Agilent).

8.5. Compounds

All drugs were handled according to manufacturer's instructions. All inhibitory drugs were put in culture media during or prior to transduction according to the timing specified in the products datasheet. The mouse monoclonal antibody against the human IFN α/β receptor (PBL assay science 21385) was used at 1000x. TLR3 inhibitor (Calbiochem 614310) was used at 5 μM. Azidothymidine (Sigma 30516-87-1), Myd88 inhibitory peptide (Invivogen tlrl-pimyd), and TRIF inhibitory peptide (Invivogen tlrl-pitrif) were used at 25 μM. TRL4 inhibitor (Invivogen tlrl-cli95) was used at 1 μg/mL. STING inhibitor H151 (Invivogen inh-h151), TLR9 inhibitor (Invivogen tlrl-2088), and TBK1 inhibitor BX795 (Invivogen tlrl-bx7) were used at 5 μM. Poly(I:C) (Invivogen tlrl-pic) was used at 50 ng/μl. LPS (Enzo life science ALX-581-010-L001) was used at 10 ng/mL. 2'3'cGAMP (Invivogen tlrl-nacga23) was used at 5-10 ng/μl. Human IFNα (PBL assay science 11105-1) was used at 1000x. Cyclosporine H (Sigma SML1575) was added during transduction at 8 μM. dNTPs (NEB N1201AA) were added during transduction at 10uM. dA (D8668), dC (D0776), dG (D0901) and dT (T1895) were all purchased from Sigma (Li *et al*, 2015). dNs mix, single dNs or combinations of dNs were used at the reported concentrations (500-1000 μM) 2h before transduction. For dosage experiment 25 μM to 1000 μM concentrations of each dN was tested. Uridine 5'-monophosphate (UMP) (Selleckchem S9451), orotic acid (OA) (Sigma O2750), inosine 5'-monophosphate (IMP) (Sigma PHR1475) were added to the media 4h before transduction at 1mM, 7.5 uM, and 5 mM concentration respectively. All drugs were washed away 16-24h after transduction/stimulation.

8.6. Gene expression analysis

RNA was extracted with the RNeasy Plus micro Kit (Qiagen 74034) and reverse-transcribed using the SuperScript™ IV VILO™ Master Mix (Invitrogen 11766050) as described (Petrillo *et al*, 2018). TaqMan probes (Applied Biosystems) were used to

perform RT-qPCR. The Viia 7 instrument and software were used for the analysis. The following Taqman probes were used: HPRT1 (Hs01003267_m1), ISG15 (Hs01921425_s1), IRF7 (Hs01014809_g1), OAS1 (Hs00973637_m1), IFNA1 (Hs00256882_s1), cGAS (Hs00403553_m1), IL6 (Hs00174131_m1), DHODH (Hs00361406_m1); CPS II (Hs00983188_m1), p21 (Hs00355782_m1).

8.7. Immunofluorescence

Macrophages were differentiated directly on round coverslip in 48 multiwell plates. 24h after transduction cells were washed and fixed with 1% paraformaldehyde in PBS for 10 minutes at room temperature (RT). Permeabilization was done with pure cold methanol for 10 minutes at RT. After washing, blocking was performed with 5% BSA in 0.3% Triton X-100/PBS. Staining was done overnight at 4°C with rabbit anti-phospho-TBK1 polyclonal antibody (Cell Signaling 5483) at 1:50 dilution. Cells were then stained with Alexa Fluor 555 αRabbit antibody (1:2000, 2 hours RT), incubated 10 minutes with DAPI (1:10000) and mounted upside down on a drop of FluorSave reagent. Images were acquired with TCS SP5 Leica confocal microscope at Almebic core facility.

8.8. Western Blot

Protein extraction and WB were performed as previously reported (Petrillo *et al*, 2018). The following primary antibody were used: STING rabbit monoclonal antibody (1:1000, Cell Signaling 13647); Rig-I rabbit monoclonal antibody (1:500, Cell Signaling 3743); MAVS mouse monoclonal antibody (1:1000, Santa Cruz 166583); TRIM5α goat polyclonal antibody (1:500, Abcam ab4389); MLV p30 Gag rabbit polyclonal antibody (1:1000, Acris Antibodies AP33447PU-N); HIV-1 p24 mouse monoclonal antibody (1:2000, Acris 603-420). β-Actin (1:5000, Sigma-Aldrich A2228) or α-tubulin (1:1000, Cell Signaling 2125) were used as normalizers.

8.9. DNA extraction and VCN analysis

DNA was extracted using the QIAamp DNA micro kit (Qiagen). VCN in transduced cells were measured by droplet digital PCR using the following primers: RT-RV ΔU3 sense: CGAGCTCAATAAAAGAGCCCAC, PBS antisense: GAGTCCTGCGTCGGAGAGAG as

previously described (Piras *et al*, 2017). Normalization was done as reported, using the human TERT gene as reference (Piras *et al*, 2017; Lombardo *et al*, 2007). The QuantaSoft software was used for the analysis.

8.10. Contaminants evaluation

Total DNA content within vector stocks was quantified with Quant-iT PicoGreen dsDNA Assay Kit (Invitrogen) as previously reported (Soldi *et al*, 2020). For quantification of residual plasmids contained within vector stocks, the VSV-G construct copies were amplified by droplet digital PCR using primers and probe previously designed (Soldi *et al*, 2020). For DNaseI treatment, 50 ul of vectors stocks were incubated with 4 Units of Ambion DNase I (Invitrogen AM2222) (2 hours, 37°C). As control, undigested vectors were incubated in the same way.

8.11. CRISPR-Cas9 screening analysis

Libraries were prepared starting from amplicons with partial Illumina adaptors. Sequencing was done on a MiSeq flowcell to produce 250bp-long reads in paired-end mode and obtain a minimum coverage of 300x per sample. Model-based Analysis of Genome-wide CRISPR-Cas9 Knockout (MAGeCK) software v 0.5.5 (Li *et al*, 2014) was applied to analyze the CRISPR screen output starting from raw fastq files. The quantification of sgRNAs was done with count function normalizing by the amount of control guides included. Then, the differentially enriched sgRNAs/genes were identified using the test function (rra method) with the following parameters: --paired --norm-method control --adjust-method fdr --sort-criteria pos --remove-zero both --gene-lfc-method median. sgRNAs/genes were considered differentially enriched if the FDR was less than 0.05.

8.12. Markers expression analysis

Expression analysis of quiescent and activated HSC markers genes for pyrimidines (CAD; DHODH) and purines (PPAT) was performed by exploiting the publicly available RNA-Seq dataset (GSE153911) from the Gene Expression Ominbus (GEO) database. In

brief, the raw counts from qLT-HSCs and aLT-HSCs samples were retrieved and normalized by calculating the relative CPM (Counts per million mapped reads) values. Then, the CPM values for the marker genes were scaled by computing the z-scores. Heatmap was generated with the pheatmap R package 1.0.12.

8.13. Colony-forming cell assay

Colony-forming cell assays was performed as previously described (Petrillo *et al*, 2018). Briefly, 800 hHSPC were plated in triplicate in a methylcellulose-based medium (Methocult GF4434 Stem Cell Technologies). After 15 days colonies were counted and erythroid and myeloid colonies were distinguished according to their morphology. Triplicates of colonies were then pooled and either analyzed by flow cytometry or kept for VCN analysis.

8.14. Apoptosis, cell cycle and proliferation

The apoptosis assay was performed with the Annexin V Apoptosis Detection Kit I (BD Pharmigen 559763) 48 hours after dNs addition and/or transduction of hHSPC. Cell cycle analysis was performed at the indicated time points with Ki67 (BD Pharmingen) and Hoechst (Invitrogen) as previously described (Piras *et al*, 2017). For evaluating cellular proliferation, the cell proliferation dye eFluor®670 (eBioscience 65-0840-85) was added to the cells immediately after thawing and analyzed by FACS at the indicated time points.

8.15. dNTPs measurements

For dNTPs measurements, samples were prepared and processed following the published protocol (Hollenbaugh & Kim, 2016).

8.16. Mice

NOD-SCID-IL2Rg−/− (NSG) mice were purchased from Jackson laboratory. All procedures were performed according to protocols approved by the Animal Care and Use Committee of the San Raffaele Hospital (IACUC 1220) and authorized by the Ministry of

Health and local authorities according to the Italian law. For transplant experiments hHSPC (CB or mPB-derived) were kept unstimulated or pre-stimulated for 24h and transduced with one or two hit of LV at the indicated MOI with or without CsH and dNs. After transduction, cells were injected in sublethally irradiated (200 cGy) 8-10 week-old female mice (Petrillo *et al*, 2018). Peripheral blood samples were analyzed at the indicated time points. At 15-20 weeks, mice were sacrificed by carbon dioxide and different organs were collected and analyzed.

8.17. Flow cytometry

FACS Canto IV instrument and Cytoflex S instrument were used for the cytometric analysis. For sorting experiments, the FACS Aria Fusion instrument was used. Downstream analysis were performed using the FACS Express De Novo Software. **Table 1** show the list of antibodies used. 7-Aminoactinomycin D was used to exclude dead cells from the analysis.

8.17.1. Transduced cells

To evaluate transduction efficiency, the expression of the GFP was measured 3-5 days post-transduction. dTomato expression was measured 24 hours after transduction. Cells were detached by Tripsin-EDTA if adherent, or simply collected, centrifuged and resuspended in PBS 2% FBS. To evaluate HSPC and T cells subpopulations composition, cells were collected according to the reported timing, blocked with anti-human Fc-receptor antibody (5 minutes, RT), and stained with indicated antibodies for 15 minutes at RT. For HSPC anti-human CD34, CD133, CD90 antibodies were used. For T cells anti-human CD3, CD4, CD8, CD45RA, and CD62L antibodies were used.

8.17.2. Colonies

Triplicates of each condition were pooled and resuspended at single cells. After washing, anti-human Fc-receptor blocking antibody was added (5 minutes, RT), and then cells were incubated (15 minutes, RT) with anti-human CD235a and anti-human CD33 antibodies as previously reported (Petrillo *et al*, 2019).

8.17.3. Peripheral blood and organs of mice

For engraftment analysis in the periphery of mice, 100 µL of blood isolated from the vein of mice was mixed with 20µL of PBS with 45 mg/mL EDTA. For the analysis of BM, femurs were flushed in PBS 2% FBS, washed, and 10^6 cells were analyzed. The spleens and thymus were smashed and passed through 40 µm nylon mesh filter in PBS 2% FBS. After washing, 10^6 cells were analyzed. All the samples were blocked with anti-human and anti-mouse Fc receptor blocking antibodies (5 minutes, RT) and then stained with indicated antibodies (15 minutes, RT). For peripheral blood samples, erythrocytes were lysed using the TQ-Prep workstation (Beckman-Coulter) after addition of 100µL of FBS (Petrillo *et al*, 2018).

Table 1. List of FACS antibodies

Antibody	**Fluorochrome**	**Dilution**	**Company**	**Code**
Human FcR Blocking Reagent		1:50	Miltenyi Biotec	130-059-901
Anti-Mouse CD16/CD32		1:100	BD Biosciences	553142
hCD34	PeCy7	1:30	BD Biosciences	348811
hCD133/2	PE	1:25	Miltenyi Biotec	130-113-186
hCD90	APC	1:25	BD Biosciences	559869
hCD235a	APC	1:25	BD Biosciences	551336
hCD33	BV421	1:25	BD Biosciences	562854
hCD45	APCh7	1:30	eBioscience	47-0459-42
hCD45 PerCP	PerCP/Cy5.5	1:30	BioLegend	304028
hCD19	PE	1:50	BD Biosciences	345789
hCD3	APC	1:50	BD Biosciences	555335
hCD13	BV	1:50	BD Biosciences	562596

hCD33	PeCy7	1:25	BD Biosciences	333952
hCD4	BV421	1:50	BD Biosciences	558116
hCD8	APCh7	1:50	Biosciences	641400
hCD38	PerCP/Cy5.5	1:25	BioLegend	356614
hCD45RA	APC	1:25	BD Biosciences	550855
hCD62L	PE	1:25	BioLegend	304822

8.18. Statistical analysis

Values in the presented figures are expressed as mean ± standard error of the mean (SEM) or mean ± standard deviation (SD), as reported in the legends. Mann Whitney or Wilcoxon Signed Rank tests were used to compare the mean of 2 groups, while Dunn's adjusted Kruskal–Wallis test was used to compare the mean when more than two groups were present, as reported in the figure legends. The number of biological replicates and the statistic applied are reported in the captions.

9. REFERENCES

Aboud M, Shoor R & Salzberg S (1979) Adsorption, Penetration, and Uncoating of Murine Leukemia Virus Studied by Using Its Reverse Transcriptase. *J Virol* 30: 32–37

Ahn J, Hao C, Yan J, DeLucia M, Mehrens J, Wang C, Gronenborn AM & Skowronski J (2012) HIV/Simian Immunodeficiency Virus (SIV) Accessory Virulence Factor Vpx Loads the Host Cell Restriction Factor SAMHD1 onto the E3 Ubiquitin Ligase Complex CRL4DCAF1. *J Biol Chem* 287: 12550–12558

Ailles L, Schmidt M, Santoni de Sio FR, Glimm H, Cavalieri S, Bruno S, Piacibello W, Von Kalle C & Naldini L (2002) Molecular evidence of lentiviral vector-mediated gene transfer into human self-renewing, multi-potent, long-term NOD/SCID repopulating hematopoietic cells. *Mol Ther* 6: 615–26

Aiuti A, Roncarolo MG & Naldini L (2017) Gene therapy for ADA-SCID, the first marketing approval of an *ex vivo* gene therapy in Europe: paving the road for the next generation of advanced therapy medicinal products. *EMBO Mol Med* 9: 737–740

Akashi K, Traver D, Miyamoto T & Weissman IL (2000) A clonogenic common myeloid progenitor that gives rise to all myeloid lineages. *Nature* 404: 193–197

Almine JF, O'Hare CAJ, Dunphy G, Haga IR, Naik RJ, Atrih A, Connolly DJ, Taylor J, Kelsall IR, Bowie AG, *et al* (2017) IFI16 and cGAS cooperate in the activation of STING during DNA sensing in human keratinocytes. *Nat Commun* 8: 14392

Amarante-Mendes GP, Adjemian S, Branco LM, Zanetti LC, Weinlich R & Bortoluci KR (2018) Pattern Recognition Receptors and the Host Cell Death Molecular Machinery. *Front Immunol* 9

Amini-Bavil-Olyaee S, Choi YJ, Lee JH, Shi M, Huang I-C, Farzan M & Jung JU (2013) The Antiviral Effector IFITM3 Disrupts Intracellular Cholesterol Homeostasis to Block Viral Entry. *Cell Host Microbe* 13: 452–464

Antonucci JM, Kim SH, St. Gelais C, Bonifati S, Li T-W, Buzovetsky O, Knecht KM, Duchon AA, Xiong Y, Musier-Forsyth K, *et al* (2018) SAMHD1 Impairs HIV-1 Gene Expression and Negatively Modulates Reactivation of Viral Latency in CD4 $^{+}$ T Cells. *J Virol* 92

Anzalone A V., Randolph PB, Davis JR, Sousa AA, Koblan LW, Levy JM, Chen PJ, Wilson C, Newby GA, Raguram A, *et al* (2019) Search-and-replace genome editing without double-strand breaks or donor DNA. *Nature* 576: 149–157

Armant MA & Fenton MJ (2002) Toll-like receptors: a family of pattern-recognition receptors in mammals. *Genome Biol* 3: reviews3011.1

Baek Y-S, Haas S, Hackstein H, Bein G, Hernandez-Santana M, Lehrach H, Sauer S & Seitz H (2009) Identification of novel transcriptional regulators involved in macrophage differentiation and activation in U937 cells. *BMC Immunol* 10: 18

Baekelandt V, Eggermont K, Michiels M, Nuttin B & Debyser Z (2003) Optimized lentiviral vector production and purification procedure prevents immune response after transduction of mouse brain. *Gene Ther* 10: 1933–1940

Bailey CC, Zhong G, Huang I-C & Farzan M (2014) IFITM-Family Proteins: The Cell's First Line of Antiviral Defense. *Annu Rev Virol* 1: 261–283

Baldauf H-M, Pan X, Erikson E, Schmidt S, Daddacha W, Burggraf M, Schenkova K, Ambiel I, Wabnitz G, Gramberg T, *et al* (2012) SAMHD1 restricts HIV-1 infection in resting CD4+ T

cells. *Nat Med* 18: 1682–1688

Balka KR, Louis C, Saunders TL, Smith AM, Calleja DJ, D'Silva DB, Moghaddas F, Tailler M, Lawlor KE, Zhan Y, *et al* (2020) TBK1 and IKKε Act Redundantly to Mediate STING-Induced NF-κB Responses in Myeloid Cells. *Cell Rep* 31: 107492

Ballana E & Esté JA (2015) SAMHD1: At the Crossroads of Cell Proliferation, Immune Responses, and Virus Restriction. *Trends Microbiol* 23: 680–692

Banskota S, Raguram A, Suh S, Du SW, Davis JR, Choi EH, Wang X, Nielsen SC, Newby GA, Randolph PB, *et al* (2022) Engineered virus-like particles for efficient in vivo delivery of therapeutic proteins. *Cell* 185: 250-265.e16

Basmaciogullari S & Pizzato M (2014) The activity of Nef on HIV-1 infectivity. *Front Microbiol* 5

Battivelli E, Migraine J, Lecossier D, Matsuoka S, Perez-Bercoff D, Saragosti S, Clavel F & Hance AJ (2011) Modulation of TRIM5α Activity in Human Cells by Alternatively Spliced TRIM5 Isoforms. *J Virol* 85: 7828–7835

Beasley BE & Hu W-S (2002) cis-Acting Elements Important for Retroviral RNA Packaging Specificity. *J Virol* 76: 4950–4960

BECKER AJ, McCULLOCH EA & TILL JE (1963) Cytological Demonstration of the Clonal Nature of Spleen Colonies Derived from Transplanted Mouse Marrow Cells. *Nature* 197: 452–454

Berg RK, Melchjorsen J, Rintahaka J, Diget E, Søby S, Horan KA, Gorelick RJ, Matikainen S, Larsen CS, Ostergaard L, *et al* (2012) Genomic HIV RNA Induces Innate Immune Responses through RIG-I-Dependent Sensing of Secondary-Structured RNA. *PLoS One* 7: e29291

Biasco L, Pellin D, Scala S, Dionisio F, Basso-Ricci L, Leonardelli L, Scaramuzza S, Baricordi C, Ferrua F, Cicalese MP, *et al* (2016) In Vivo Tracking of Human Hematopoiesis Reveals Patterns of Clonal Dynamics during Early and Steady-State Reconstitution Phases. *Cell Stem Cell* 19: 107–119

Bieniasz PD, Grdina TA, Bogerd HP & Cullen BR (1999) Recruitment of cyclin T1/P-TEFb to an HIV type 1 long terminal repeat promoter proximal RNA target is both necessary and sufficient for full activation of transcription. *Proc Natl Acad Sci U S A* 96: 7791–6

Biffi A, Bartolomae CC, Cesana D, Cartier N, Aubourg P, Ranzani M, Cesani M, Benedicenti F, Plati T, Rubagotti E, *et al* (2011) Lentiviral vector common integration sites in preclinical models and a clinical trial reflect a benign integration bias and not oncogenic selection. *Blood* 117: 5332–5339

Billon P, Bryant EE, Joseph SA, Nambiar TS, Hayward SB, Rothstein R & Ciccia A (2017) CRISPR-Mediated Base Editing Enables Efficient Disruption of Eukaryotic Genes through Induction of STOP Codons. *Mol Cell* 67: 1068-1079.e4

Bobadilla S, Sunseri N & Landau NR (2013) Efficient transduction of myeloid cells by an HIV-1-derived lentiviral vector that packages the Vpx accessory protein. *Gene Ther* 20: 514–520

Boitano AE, Wang J, Romeo R, Bouchez LC, Parker AE, Sutton SE, Walker JR, Flaveny CA, Perdew GH, Denison MS, *et al* (2010) Aryl Hydrocarbon Receptor Antagonists Promote the Expansion of Human Hematopoietic Stem Cells. *Science (80-)* 329: 1345–1348

Bowman T V. & Trompouki E (2021) Sensing Stemness. *Curr Stem Cell Reports* 7: 219–228

Brass AL, Huang I-C, Benita Y, John SP, Krishnan MN, Feeley EM, Ryan BJ, Weyer JL, van der Weyden L, Fikrig E, *et al* (2009) The IFITM Proteins Mediate Cellular Resistance to Influenza A H1N1 Virus, West Nile Virus, and Dengue Virus. *Cell* 139: 1243–1254

Braun CJ, Boztug K, Paruzynski A, Witzel M, Schwarzer A, Rothe M, Modlich U, Beier R, Göhring G, Steinemann D, *et al* (2014) Gene Therapy for Wiskott-Aldrich Syndrome—Long-Term Efficacy and Genotoxicity. *Sci Transl Med* 6

Browne EP (2013) Toll-Like Receptor 7 Inhibits Early Acute Retroviral Infection through Rapid Lymphocyte Responses. *J Virol* 87: 7357–7366

Bryant CE, Gay NJ, Heymans S, Sacre S, Schaefer L & Midwood KS (2015) Advances in Toll-like receptor biology: Modes of activation by diverse stimuli. *Crit Rev Biochem Mol Biol* 50: 359–379

Bukrinsky MI, Sharova N, Dempsey MP, Stanwick TL, Bukrinskaya AG, Haggerty S & Stevenson M (1992) Active nuclear import of human immunodeficiency virus type 1 preintegration complexes. *Proc Natl Acad Sci* 89: 6580–6584

Burdick RC, Li C, Munshi M, Rawson JMO, Nagashima K, Hu W-S & Pathak VK (2020) HIV-1 uncoats in the nucleus near sites of integration. *Proc Natl Acad Sci* 117: 5486–5493

Burns JC, Friedmann T, Driever W, Burrascano M & Yee JK (1993) Vesicular stomatitis virus G glycoprotein pseudotyped retroviral vectors: concentration to very high titer and efficient gene transfer into mammalian and nonmammalian cells. *Proc Natl Acad Sci* 90: 8033–8037

Cavazzana-Calvo M, Payen E, Negre O, Wang G, Hehir K, Fusil F, Down J, Denaro M, Brady T, Westerman K, *et al* (2010) Transfusion independence and HMGA2 activation after gene therapy of human β-thalassaemia. *Nature* 467: 318–322

Cavazzana M, Six E, Lagresle-Peyrou C, André-Schmutz I & Hacein-Bey-Abina S (2016) Gene Therapy for X-Linked Severe Combined Immunodeficiency: Where Do We Stand? *Hum Gene Ther* 27: 108–116

Cesana D, Sgualdino J, Rudilosso L, Merella S, Naldini L & Montini E (2012) Whole transcriptome characterization of aberrant splicing events induced by lentiviral vector integrations. *J Clin Invest* 122: 1667–1676

Chabannon C, Kuball J, Bondanza A, Dazzi F, Pedrazzoli P, Toubert A, Ruggeri A, Fleischhauer K & Bonini C (2018) Hematopoietic stem cell transplantation in its 60s: A platform for cellular therapies. *Sci Transl Med* 10

Charlesworth CT, Camarena J, Cromer MK, Vaidyanathan S, Bak RO, Carte JM, Potter J, Dever DP & Porteus MH (2018) Priming Human Repopulating Hematopoietic Stem and Progenitor Cells for Cas9/sgRNA Gene Targeting. *Mol Ther - Nucleic Acids* 12: 89–104

Chen Q, Sun L & Chen ZJ (2016) Regulation and function of the cGAS–STING pathway of cytosolic DNA sensing. *Nat Immunol* 17: 1142–1149

Chesarino NM, McMichael TM, Hach JC & Yount JS (2014a) Phosphorylation of the Antiviral Protein Interferon-inducible Transmembrane Protein 3 (IFITM3) Dually Regulates Its Endocytosis and Ubiquitination. *J Biol Chem* 289: 11986–11992

Chesarino NM, McMichael TM & Yount JS (2014b) Regulation of the trafficking and antiviral activity of IFITM3 by post-translational modifications. *Future Microbiol* 9: 1151–1163

Chiriaco M, Farinelli G, Capo V, Zonari E, Scaramuzza S, Di Matteo G, Sergi LS, Migliavacca M, Hernandez RJ, Bombelli F, *et al* (2014) Dual-regulated Lentiviral Vector for Gene Therapy of X-linked Chronic Granulomatosis. *Mol Ther* 22: 1472–1483

Chiu Y-L, Ho CK, Saha N, Schwer B, Shuman S & Rana TM (2002) Tat Stimulates Cotranscriptional Capping of HIV mRNA. *Mol Cell* 10: 585–597

Coeshott C, Vang B, Jones M & Nankervis B (2019) Large-scale expansion and characterization of CD3+ T-cells in the Quantum® Cell Expansion System. *J Transl Med* 17: 258

Coffin JM, Hughes SH & Varmus HE (1997) retroviral virions and genome

Cosnefroy O, Murray PJ & Bishop KN (2016) HIV-1 capsid uncoating initiates after the first strand transfer of reverse transcription. *Retrovirology* 13: 58

Cribier A, Descours B, Valadão ALC, Laguette N & Benkirane M (2013) Phosphorylation of SAMHD1 by Cyclin A2/CDK1 Regulates Its Restriction Activity toward HIV-1. *Cell Rep* 3: 1036–1043

Cronin J, Zhang X-Y & Reiser J (2005) Altering the Tropism of Lentiviral Vectors through Pseudotyping. *Curr Gene Ther* 5: 387–398

D'Souza V & Summers MF (2005) How retroviruses select their genomes. *Nat Rev Microbiol* 3: 643–655

Deddouche S, Goubau D, Rehwinkel J, Chakravarty P, Begum S, Maillard P V, Borg A, Matthews N, Feng Q, van Kuppeveld FJM, *et al* (2014) Identification of an LGP2-associated MDA5 agonist in picornavirus-infected cells. *Elife* 3

Diebold SS, Kaisho T, Hemmi H, Akira S & Reis e Sousa C (2004) Innate Antiviral Responses by Means of TLR7-Mediated Recognition of Single-Stranded RNA. *Science (80-)* 303: 1529–1531

Diehl FF, Miettinen TP, Elbashir R, Nabel CS, Darnell AM, Do BT, Manalis SR, Lewis CA & Vander Heiden MG (2022) Nucleotide imbalance decouples cell growth from cell proliferation. *Nat Cell Biol* 24: 1252–1264

DiGiusto DL, Krishnan A, Li L, Li H, Li S, Rao A, Mi S, Yam P, Stinson S, Kalos M, *et al* (2010) RNA-Based Gene Therapy for HIV with Lentiviral Vector–Modified CD34 $^{+}$ Cells in Patients Undergoing Transplantation for AIDS-Related Lymphoma. *Sci Transl Med* 2

Doman JL, Raguram A, Newby GA & Liu DR (2020) Evaluation and minimization of Cas9-independent off-target DNA editing by cytosine base editors. *Nat Biotechnol* 38: 620–628

Donello JE, Loeb JE & Hope TJ (1998) Woodchuck Hepatitis Virus Contains a Tripartite Posttranscriptional Regulatory Element. *J Virol* 72: 5085–5092

Doudna JA & Charpentier E (2014) The new frontier of genome engineering with CRISPR-Cas9. *Science (80-)* 346

Doulatov S, Notta F, Laurenti E & Dick JE (2012) Hematopoiesis: A Human Perspective. *Cell Stem Cell* 10: 120–136

Duggal NK & Emerman M (2012) Evolutionary conflicts between viruses and restriction factors shape immunity. *Nat Rev Immunol* 12: 687–695

Dull T, Zufferey R, Kelly M, Mandel RJ, Nguyen M, Trono D & Naldini L (1998) A Third-Generation Lentivirus Vector with a Conditional Packaging System. *J Virol* 72: 8463–8471

Dunphy G, Flannery SM, Almine JF, Connolly DJ, Paulus C, Jønsson KL, Jakobsen MR, Nevels MM, Bowie AG & Unterholzner L (2018) Non-canonical Activation of the DNA Sensing Adaptor STING by ATM and IFI16 Mediates NF-κB Signaling after Nuclear DNA Damage. *Mol Cell* 71: 745-760.e5

Eaves CJ (2015) Hematopoietic stem cells: concepts, definitions, and the new reality. *Blood* 125: 2605–2613

Eichler F, Duncan C, Musolino PL, Orchard PJ, De Oliveira S, Thrasher AJ, Armant M, Dansereau C, Lund TC, Miller WP, *et al* (2017) Hematopoietic Stem-Cell Gene Therapy for Cerebral Adrenoleukodystrophy. *N Engl J Med* 377: 1630–1638

El-Zayat SR, Sibaii H & Mannaa FA (2019) Toll-like receptors activation, signaling, and targeting: an overview. *Bull Natl Res Cent* 43: 187

Escobar G, Moi D, Ranghetti A, Ozkal-Baydin P, Squadrito ML, Kajaste-Rudnitski A, Bondanza A, Gentner B, De Palma M, Mazzieri R, *et al* (2014) Genetic Engineering of Hematopoiesis for Targeted IFN-α Delivery Inhibits Breast Cancer Progression. *Sci Transl Med* 6

Esplin BL, Shimazu T, Welner RS, Garrett KP, Nie L, Zhang Q, Humphrey MB, Yang Q, Borghesi LA & Kincade PW (2011) Chronic Exposure to a TLR Ligand Injures Hematopoietic Stem Cells. *J Immunol* 186: 5367–5375

Evans ME, Kumkhaek C, Hsieh MM, Donahue RE, Tisdale JF & Uchida N (2014) TRIM5α Variations Influence Transduction Efficiency With Lentiviral Vectors in Both Human and Rhesus CD34+ Cells In Vitro and In Vivo. *Mol Ther* 22: 348–358

Fares I, Chagraoui J, Gareau Y, Gingras S, Ruel R, Mayotte N, Csaszar E, Knapp DJHF, Miller P, Ngom M, *et al* (2014) Pyrimidoindole derivatives are agonists of human hematopoietic stem cell self-renewal. *Science (80-)* 345: 1509–1512

Fernandez J, Machado AK, Lyonnais S, Chamontin C, Gärtner K, Léger T, Henriquet C, Garcia C, Portilho DM, Pugnière M, *et al* (2019) Transportin-1 binds to the HIV-1 capsid via a nuclear localization signal and triggers uncoating. *Nat Microbiol* 4: 1840–1850

Ferrara JL, Levine JE, Reddy P & Holler E (2009) Graft-versus-host disease. *Lancet* 373: 1550–1561

Ferrari G, Thrasher AJ & Aiuti A (2021a) Gene therapy using haematopoietic stem and progenitor cells. *Nat Rev Genet* 22: 216–234

Ferrari S, Jacob A, Beretta S, Unali G, Albano L, Vavassori V, Cittaro D, Lazarevic D, Brombin C, Cugnata F, *et al* (2020) Efficient gene editing of human long-term hematopoietic stem cells validated by clonal tracking. *Nat Biotechnol* 38: 1298–1308

Ferrari S, Jacob A, Cesana D, Laugel M, Beretta S, Varesi A, Unali G, Conti A, Canarutto D, Albano L, *et al* (2022) Choice of template delivery mitigates the genotoxic risk and adverse impact of editing in human hematopoietic stem cells. *Cell Stem Cell* 29: 1428-1444.e9

Ferrari S, Vavassori V, Canarutto D, Jacob A, Castiello MC, Javed AO & Genovese P (2021b) Gene Editing of Hematopoietic Stem Cells: Hopes and Hurdles Toward Clinical Translation. *Front Genome Ed* 3

Ferrua F & Aiuti A (2017) Twenty-Five Years of Gene Therapy for ADA-SCID: From *Bubble Babies* to an Approved Drug. *Hum Gene Ther* 28: 972–981

Ferrua F, Cicalese MP, Galimberti S, Giannelli S, Dionisio F, Barzaghi F, Migliavacca M, Bernardo ME, Calbi V, Assanelli AA, *et al* (2019) Lentiviral haemopoietic stem/progenitor cell gene therapy for treatment of Wiskott-Aldrich syndrome: interim results of a non-randomised, open-label, phase 1/2 clinical study. *Lancet Haematol* 6: e239–e253

Fischer A, Hacein-Bey Abina S, Touzot F & Cavazzana M (2015) Gene therapy for primary immunodeficiencies. *Clin Genet* 88: 507–515

Fitzgerald KA, McWhirter SM, Faia KL, Rowe DC, Latz E, Golenbock DT, Coyle AJ, Liao S-M & Maniatis T (2003) IKKε and TBK1 are essential components of the IRF3 signaling pathway. *Nat Immunol* 4: 491–496

Fletcher AJ, Vaysburd M, Maslen S, Zeng J, Skehel JM, Towers GJ & James LC (2018) Trivalent RING Assembly on Retroviral Capsids Activates TRIM5 Ubiquitination and Innate Immune Signaling. *Cell Host Microbe* 24: 761-775.e6

Follenzi A, Ailles LE, Bakovic S, Geuna M & Naldini L (2000) Gene transfer by lentiviral vectors is

limited by nuclear translocation and rescued by HIV-1 pol sequences. *Nat Genet* 25: 217–222

Follenzi A & Naldini L (2002) [26] Generation of HIV-1 derived lentiviral vectors. In pp 454–465.

Francis AC & Melikyan GB (2018) Single HIV-1 Imaging Reveals Progression of Infection through CA-Dependent Steps of Docking at the Nuclear Pore, Uncoating, and Nuclear Transport. *Cell Host Microbe* 23: 536-548.e6

Frangoul H, Altshuler D, Cappellini MD, Chen Y-S, Domm J, Eustace BK, Foell J, de la Fuente J, Grupp S, Handgretinger R, *et al* (2021) CRISPR-Cas9 Gene Editing for Sickle Cell Disease and β-Thalassemia. *N Engl J Med* 384: 252–260

Franzolin E, Pontarin G, Rampazzo C, Miazzi C, Ferraro P, Palumbo E, Reichard P & Bianchi V (2013) The deoxynucleotide triphosphohydrolase SAMHD1 is a major regulator of DNA precursor pools in mammalian cells. *Proc Natl Acad Sci* 110: 14272–14277

Frecha C, Costa C, Nègre D, Gauthier E, Russell SJ, Cosset F-L & Verhoeyen E (2008) Stable transduction of quiescent T cells without induction of cycle progression by a novel lentiviral vector pseudotyped with measles virus glycoproteins. *Blood* 112: 4843–4852

Ganser-Pornillos BK, Chandrasekaran V, Pornillos O, Sodroski JG, Sundquist WI & Yeager M (2011) Hexagonal assembly of a restricting TRIM5α protein. *Proc Natl Acad Sci* 108: 534–539

Gao D, Wu J, Wu Y-T, Du F, Aroh C, Yan N, Sun L & Chen ZJ (2013) Cyclic GMP-AMP Synthase Is an Innate Immune Sensor of HIV and Other Retroviruses. *Science (80-)* 341: 903–906

García-Prat L, Kaufmann KB, Schneiter F, Voisin V, Murison A, Chen J, Chan-Seng-Yue M, Gan OI, McLeod JL, Smith SA, *et al* (2021) TFEB-mediated endolysosomal activity controls human hematopoietic stem cell fate. *Cell Stem Cell* 28: 1838-1850.e10

Gasiewicz TA, Singh KP & Bennett JA (2014) The Ah receptor in stem cell cycling, regulation, and quiescence. *Ann N Y Acad Sci* 1310: 44–50

Gatti R, Meuwissen H, Allen H, Hong R & Good R (1968) IMMUNOLOGICAL RECONSTITUTION OF SEX-LINKED LYMPHOPENIC IMMUNOLOGICAL DEFICIENCY. *Lancet* 292: 1366–1369

Gattinoni L, Lugli E, Ji Y, Pos Z, Paulos CM, Quigley MF, Almeida JR, Gostick E, Yu Z, Carpenito C, *et al* (2011) A human memory T cell subset with stem cell-like properties. *Nat Med* 17: 1290–7

Gaudelli NM, Komor AC, Rees HA, Packer MS, Badran AH, Bryson DI & Liu DR (2017) Programmable base editing of A•T to G•C in genomic DNA without DNA cleavage. *Nature* 551: 464–471

Gee P, Lung MSY, Okuzaki Y, Sasakawa N, Iguchi T, Makita Y, Hozumi H, Miura Y, Yang LF, Iwasaki M, *et al* (2020) Extracellular nanovesicles for packaging of CRISPR-Cas9 protein and sgRNA to induce therapeutic exon skipping. *Nat Commun* 11: 1334

Genovese P, Schiroli G, Escobar G, Di Tomaso T, Firrito C, Calabria A, Moi D, Mazzieri R, Bonini C, Holmes MC, *et al* (2014) Targeted genome editing in human repopulating haematopoietic stem cells. *Nature* 510: 235–240

Gentner B, Bernardo ME, Tucci F, Zonari E, Fumagalli F, Pontesilli S, Acquati S, Silvani P, Ciceri F, Rovelli A, *et al* (2019) Extensive Metabolic Correction of Hurler Disease By Hematopoietic Stem Cell-Based Gene Therapy: Preliminary Results from a Phase I/II Trial. *Blood* 134: 607–607

Georgel P, Jiang Z, Kunz S, Janssen E, Mols J, Hoebe K, Bahram S, Oldstone MBA & Beutler B (2007) Vesicular stomatitis virus glycoprotein G activates a specific antiviral Toll-like

receptor 4-dependent pathway. *Virology* 362: 304–313

Gertz MA (2010) review: Current status of stem cell mobilization. *Br J Haematol* 150: 647–662

Ghassemi S, Durgin JS, Nunez-Cruz S, Patel J, Leferovich J, Pinzone M, Shen F, Cummins KD, Plesa G, Cantu VA, *et al* (2022) Rapid manufacturing of non-activated potent CAR T cells. *Nat Biomed Eng* 6: 118–128

Ghassemi S, Nunez-Cruz S, O'Connor RS, Fraietta JA, Patel PR, Scholler J, Barrett DM, Lundh SM, Davis MM, Bedoya F, *et al* (2018) Reducing *Ex Vivo* Culture Improves the Antileukemic Activity of Chimeric Antigen Receptor (CAR) T Cells. *Cancer Immunol Res* 6: 1100–1109

Gibbert K, Francois S, Sigmund AM, Harper MS, Barrett BS, Kirchning CJ, Lu M, Santiago ML & Dittmer U (2014) Friend retrovirus drives cytotoxic effectors through Toll-like receptor 3. *Retrovirology* 11: 126

Girard-Gagnepain A, Amirache F, Costa C, Lévy C, Frecha C, Fusil F, Nègre D, Lavillette D, Cosset F-L & Verhoeyen E (2014) Baboon envelope pseudotyped LVs outperform VSV-G-LVs for gene transfer into early-cytokine-stimulated and resting HSCs. *Blood* 124: 1221–1231

Glimm H, Oh IH & Eaves CJ (2000) Human hematopoietic stem cells stimulated to proliferate in vitro lose engraftment potential during their S/G(2)/M transit and do not reenter G(0). *Blood* 96: 4185–93

Goldstone DC, Ennis-Adeniran V, Hedden JJ, Groom HCT, Rice GI, Christodoulou E, Walker PA, Kelly G, Haire LF, Yap MW, *et al* (2011) HIV-1 restriction factor SAMHD1 is a deoxynucleoside triphosphate triphosphohydrolase. *Nature* 480: 379–382

Gorgoulis VG, Vassiliou L-VF, Karakaidos P, Zacharatos P, Kotsinas A, Liloglou T, Venere M, DiTullio RA, Kastrinakis NG, Levy B, *et al* (2005) Activation of the DNA damage checkpoint and genomic instability in human precancerous lesions. *Nature* 434: 907–913

Goubau D, Deddouche S & Reis e Sousa C (2013) Cytosolic Sensing of Viruses. *Immunity* 38: 855–869

Goujon C, Arfi V, Pertel T, Luban J, Lienard J, Rigal D, Darlix J-L & Cimarelli A (2008) Characterization of Simian Immunodeficiency Virus SIV $_{SM}$ /Human Immunodeficiency Virus Type 2 Vpx Function in Human Myeloid Cells. *J Virol* 82: 12335–12345

Grünewald J, Zhou R, Garcia SP, Iyer S, Lareau CA, Aryee MJ & Joung JK (2019) Transcriptome-wide off-target RNA editing induced by CRISPR-guided DNA base editors. *Nature* 569: 433–437

Gupta RM & Musunuru K (2014) Expanding the genetic editing tool kit: ZFNs, TALENs, and CRISPR-Cas9. *J Clin Invest* 124: 4154–4161

Habjan M & Pichlmair A (2015) Cytoplasmic sensing of viral nucleic acids. *Curr Opin Virol* 11: 31–37

Hacein-Bey-Abina S, Garrigue A, Wang GP, Soulier J, Lim A, Morillon E, Clappier E, Caccavelli L, Delabesse E, Beldjord K, *et al* (2008) Insertional oncogenesis in 4 patients after retrovirus-mediated gene therapy of SCID-X1. *J Clin Invest* 118: 3132–3142

Han K, Lou DI & Sawyer SL (2011) Identification of a Genomic Reservoir for New TRIM Genes in Primate Genomes. *PLoS Genet* 7: e1002388

Hartmann G (2017) Nucleic Acid Immunity. *Adv Immunol* 133: 121–169

Hatakeyama S (2017) TRIM Family Proteins: Roles in Autophagy, Immunity, and Carcinogenesis. *Trends Biochem Sci* 42: 297–311

Hayward JA, Mathur A, Ngo C & Man SM (2018) Cytosolic Recognition of Microbes and Pathogens: Inflammasomes in Action. *Microbiol Mol Biol Rev* 82

Heffner GC, Bonner M, Christiansen L, Pierciey FJ, Campbell D, Smurnyy Y, Zhang W, Hamel A, Shaw S, Lewis G, *et al* (2018) Prostaglandin E2 Increases Lentiviral Vector Transduction Efficiency of Adult Human Hematopoietic Stem and Progenitor Cells. *Mol Ther* 26: 320–328

Heil F, Hemmi H, Hochrein H, Ampenberger F, Kirschning C, Akira S, Lipford G, Wagner H & Bauer S (2004) Species-Specific Recognition of Single-Stranded RNA via Toll-like Receptor 7 and 8. *Science (80-)* 303: 1526–1529

Höfig I, Atkinson MJ, Mall S, Krackhardt AM, Thirion C & Anastasov N (2012) Poloxamer synperonic F108 improves cellular transduction with lentiviral vectors. *J Gene Med* 14: 549–560

Hofmann H, Logue EC, Bloch N, Daddacha W, Polsky SB, Schultz ML, Kim B & Landau NR (2012) The Vpx Lentiviral Accessory Protein Targets SAMHD1 for Degradation in the Nucleus. *J Virol* 86: 12552–12560

Hollenbaugh JA & Kim B (2016) HIV-1 Reverse Transcriptase-Based Assay to Determine Cellular dNTP Concentrations. In pp 61–70.

Hornung V, Ellegast J, Kim S, Brzózka K, Jung A, Kato H, Poeck H, Akira S, Conzelmann K-K, Schlee M, *et al* (2006) 5′-Triphosphate RNA Is the Ligand for RIG-I. *Science (80-)* 314: 994–997

Horwitz ME, Chao NJ, Rizzieri DA, Long GD, Sullivan KM, Gasparetto C, Chute JP, Morris A, McDonald C, Waters-Pick B, *et al* (2014) Umbilical cord blood expansion with nicotinamide provides long-term multilineage engraftment. *J Clin Invest* 124: 3121–3128

Hoshino K, Takeuchi O, Kawai T, Sanjo H, Ogawa T, Takeda Y, Takeda K & Akira S (1999) Cutting edge: Toll-like receptor 4 (TLR4)-deficient mice are hyporesponsive to lipopolysaccharide: evidence for TLR4 as the Lps gene product. *J Immunol* 162: 3749–52

Hou B, Reizis B & DeFranco AL (2008) Toll-like Receptors Activate Innate and Adaptive Immunity by using Dendritic Cell-Intrinsic and -Extrinsic Mechanisms. *Immunity* 29: 272–282

Howe SJ, Mansour MR, Schwarzwaelder K, Bartholomae C, Hubank M, Kempski H, Brugman MH, Pike-Overzet K, Chatters SJ, de Ridder D, *et al* (2008) Insertional mutagenesis combined with acquired somatic mutations causes leukemogenesis following gene therapy of SCID-X1 patients. *J Clin Invest* 118: 3143–3150

Hrecka K, Hao C, Gierszewska M, Swanson SK, Kesik-Brodacka M, Srivastava S, Florens L, Washburn MP & Skowronski J (2011) Vpx relieves inhibition of HIV-1 infection of macrophages mediated by the SAMHD1 protein. *Nature* 474: 658–661

Huang I-C, Bailey CC, Weyer JL, Radoshitzky SR, Becker MM, Chiang JJ, Brass AL, Ahmed AA, Chi X, Dong L, *et al* (2011) Distinct Patterns of IFITM-Mediated Restriction of Filoviruses, SARS Coronavirus, and Influenza A Virus. *PLoS Pathog* 7: e1001258

Hulme AE, Perez O & Hope TJ (2011) Complementary assays reveal a relationship between HIV-1 uncoating and reverse transcription. *Proc Natl Acad Sci* 108: 9975–9980

Jacobson LO, Simmons EL, Marks EK & Eldredge JH (1951) Recovery from Radiation Injury. *Science (80-)* 113: 510–511

Jakobsen MR, Bak RO, Andersen A, Berg RK, Jensen SB, Jin T, Laustsen A, Hansen K, Østergaard L, Fitzgerald KA, *et al* (2013) IFI16 senses DNA forms of the lentiviral replication cycle and controls HIV-1 replication. *Proc Natl Acad Sci* 110

Jiang H, Xue X, Panda S, Kawale A, Hooy RM, Liang F, Sohn J, Sung P & Gekara NO (2019)

Chromatin-bound <scp>cGAS</scp> is an inhibitor of DNA repair and hence accelerates genome destabilization and cell death. *EMBO J* 38

Jimenez-Guardeño JM, Apolonia L, Betancor G & Malim MH (2019) Immunoproteasome activation enables human TRIM5α restriction of HIV-1. *Nat Microbiol* 4: 933–940

Kajaste-Rudnitski A & Naldini L (2015) Cellular Innate Immunity and Restriction of Viral Infection: Implications for Lentiviral Gene Therapy in Human Hematopoietic Cells. *Hum Gene Ther* 26: 201–209

Kallinikou K, Anjos-Afonso F, Blundell MP, Ings SJ, Watts MJ, Thrasher AJ, Linch DC, Bonnet D & Yong KL (2012) Engraftment defect of cytokine-cultured adult human mobilized CD34+ cells is related to reduced adhesion to bone marrow niche elements. *Br J Haematol* 158: 778–787

Kane M, Case LK, Wang C, Yurkovetskiy L, Dikiy S & Golovkina TV (2011) Innate Immune Sensing of Retroviral Infection via Toll-like Receptor 7 Occurs upon Viral Entry. *Immunity* 35: 135–145

Kanter J, Tisdale JF, Mapara MY, Kwiatkowski JL, Krishnamurti L, Schmidt M, Miller AL, Pierciey FJ, Huang W, Ribeil J-A, *et al* (2019) Resolution of Sickle Cell Disease Manifestations in Patients Treated with Lentiglobin Gene Therapy: Updated Results from the Phase 1/2 Hgb-206 Group C Study. *Blood* 134: 990–990

Kantor A, McClements M & MacLaren R (2020) CRISPR-Cas9 DNA Base-Editing and Prime-Editing. *Int J Mol Sci* 21: 6240

Kato H, Takeuchi O, Mikamo-Satoh E, Hirai R, Kawai T, Matsushita K, Hiiragi A, Dermody TS, Fujita T & Akira S (2008) Length-dependent recognition of double-stranded ribonucleic acids by retinoic acid–inducible gene-I and melanoma differentiation–associated gene 5. *J Exp Med* 205: 1601–1610

Kay MA, Glorioso JC & Naldini L (2001) Viral vectors for gene therapy: the art of turning infectious agents into vehicles of therapeutics. *Nat Med* 7: 33–40

Keckesova Z, Ylinen LMJ & Towers GJ (2004) The human and African green monkey TRIM5α genes encode Ref1 and Lv1 retroviral restriction factor activities. *Proc Natl Acad Sci* 101: 10780–10785

Kim K, Dauphin A, Komurlu S, McCauley SM, Yurkovetskiy L, Carbone C, Diehl WE, Strambio-De-Castillia C, Campbell EM & Luban J (2019) Cyclophilin A protects HIV-1 from restriction by human TRIM5α. *Nat Microbiol* 4: 2044–2051

Kim VN, Mitrophanous K, Kingsman SM & Kingsman AJ (1998) Minimal Requirement for a Lentivirus Vector Based on Human Immunodeficiency Virus Type 1. *J Virol* 72: 811–816

Klages N, Zufferey R & Trono D (2000) A Stable System for the High-Titer Production of Multiply Attenuated Lentiviral Vectors. *Mol Ther* 2: 170–176

Klebanoff CA, Gattinoni L & Restifo NP (2012) Sorting Through Subsets. *J Immunother* 35: 651–660

Kleinstiver BP, Pattanayak V, Prew MS, Tsai SQ, Nguyen NT, Zheng Z & Joung JK (2016) High-fidelity CRISPR–Cas9 nucleases with no detectable genome-wide off-target effects. *Nature* 529: 490–495

Kleinstiver BP, Prew MS, Tsai SQ, Topkar V V., Nguyen NT, Zheng Z, Gonzales APW, Li Z, Peterson RT, Yeh J-RJ, *et al* (2015) Engineered CRISPR-Cas9 nucleases with altered PAM specificities. *Nature* 523: 481–485

Kohn DB, Booth C, Kang EM, Pai S-Y, Shaw KL, Santilli G, Armant M, Buckland KF, Choi U, De

Ravin SS, *et al* (2020) Lentiviral gene therapy for X-linked chronic granulomatous disease. *Nat Med* 26: 200–206

Kohnken R, Kodigepalli KM & Wu L (2015) Regulation of deoxynucleotide metabolism in cancer: novel mechanisms and therapeutic implications. *Mol Cancer* 14: 176

Komor AC, Kim YB, Packer MS, Zuris JA & Liu DR (2016) Programmable editing of a target base in genomic DNA without double-stranded DNA cleavage. *Nature* 533: 420–424

Kondo M, Weissman IL & Akashi K (1997) Identification of Clonogenic Common Lymphoid Progenitors in Mouse Bone Marrow. *Cell* 91: 661–672

Kootstra NA, Zwart BM & Schuitemaker H (2000) Diminished Human Immunodeficiency Virus Type 1 Reverse Transcription and Nuclear Transport in Primary Macrophages Arrested in Early G_1 Phase of the Cell Cycle. *J Virol* 74: 1712–1717

Korin YD & Zack JA (1999) Nonproductive Human Immunodeficiency Virus Type 1 Infection in Nucleoside-Treated G_0 Lymphocytes. *J Virol* 73: 6526–6532

Kuhlmann A-S, Peterson CW & Kiem H-P (2018) Chimeric antigen receptor T-cell approaches to HIV cure. *Curr Opin HIV AIDS* 13: 446–453

Kujirai T, Zierhut C, Takizawa Y, Kim R, Negishi L, Uruma N, Hirai S, Funabiki H & Kurumizaka H (2020) Structural basis for the inhibition of cGAS by nucleosomes. *Science (80-)* 370: 455–458

Kurt IC, Zhou R, Iyer S, Garcia SP, Miller BR, Langner LM, Grünewald J & Joung JK (2021) CRISPR C-to-G base editors for inducing targeted DNA transversions in human cells. *Nat Biotechnol* 39: 41–46

Kuscu C, Parlak M, Tufan T, Yang J, Szlachta K, Wei X, Mammadov R & Adli M (2017) CRISPR-STOP: gene silencing through base-editing-induced nonsense mutations. *Nat Methods* 14: 710–712

Kutluay SB, Perez-Caballero D & Bieniasz PD (2013) Fates of Retroviral Core Components during Unrestricted and TRIM5-Restricted Infection. *PLoS Pathog* 9: e1003214

Laguette N, Sobhian B, Casartelli N, Ringeard M, Chable-Bessia C, Ségéral E, Yatim A, Emiliani S, Schwartz O & Benkirane M (2011) SAMHD1 is the dendritic- and myeloid-cell-specific HIV-1 restriction factor counteracted by Vpx. *Nature* 474: 654–657

Lahouassa H, Daddacha W, Hofmann H, Ayinde D, Logue EC, Dragin L, Bloch N, Maudet C, Bertrand M, Gramberg T, *et al* (2012) SAMHD1 restricts the replication of human immunodeficiency virus type 1 by depleting the intracellular pool of deoxynucleoside triphosphates. *Nat Immunol* 13: 223–228

Larochelle A, Gillette JM, Desmond R, Ichwan B, Cantilena A, Cerf A, Barrett AJ, Wayne AS, Lippincott-Schwartz J & Dunbar CE (2012) Bone marrow homing and engraftment of human hematopoietic stem and progenitor cells is mediated by a polarized membrane domain. *Blood* 119: 1848–1855

Laurenti E & Göttgens B (2018) From haematopoietic stem cells to complex differentiation landscapes. *Nature* 553: 418–426

Lefkopoulos S, Polyzou A, Derecka M, Bergo V, Clapes T, Cauchy P, Jerez-Longres C, Onishi-Seebacher M, Yin N, Martagon-Calderón N-A, *et al* (2020) Repetitive Elements Trigger RIG-I-like Receptor Signaling that Regulates the Emergence of Hematopoietic Stem and Progenitor Cells. *Immunity* 53: 934-951.e9

Lévy C, Amirache F, Girard-Gagnepain A, Frecha C, Roman-Rodríguez FJ, Bernadin O, Costa C, Nègre D, Gutierrez-Guerrero A, Vranckx LS, *et al* (2017) Measles virus envelope

pseudotyped lentiviral vectors transduce quiescent human HSCs at an efficiency without precedent. *Blood Adv* 1: 2088–2104

Li D, Schlaepfer E, Audigé A, Rochat M-A, Ivic S, Knowlton CN, Kim B, Keppler OT & Speck RF (2015) Vpx mediated degradation of SAMHD1 has only a very limited effect on lentiviral transduction rate in ex vivo cultured HSPCs. *Stem Cell Res* 15: 271–280

Li H, Yang Y, Hong W, Huang M, Wu M & Zhao X (2020) Applications of genome editing technology in the targeted therapy of human diseases: mechanisms, advances and prospects. *Signal Transduct Target Ther* 5: 1

Li W, Xu H, Xiao T, Cong L, Love MI, Zhang F, Irizarry RA, Liu JS, Brown M & Liu XS (2014) MAGeCK enables robust identification of essential genes from genome-scale CRISPR/Cas9 knockout screens. *Genome Biol* 15: 554

Li Y-L, Chandrasekaran V, Carter SD, Woodward CL, Christensen DE, Dryden KA, Pornillos O, Yeager M, Ganser-Pornillos BK, Jensen GJ, *et al* (2016) Primate TRIM5 proteins form hexagonal nets on HIV-1 capsids. *Elife* 5

Liggett LA & Sankaran VG (2020) Unraveling Hematopoiesis through the Lens of Genomics. *Cell* 182: 1384–1400

Liu G & Gack MU (2020) Distinct and Orchestrated Functions of RNA Sensors in Innate Immunity. *Immunity* 53: 26–42

Lombardo A, Genovese P, Beausejour CM, Colleoni S, Lee Y-L, Kim KA, Ando D, Urnov FD, Galli C, Gregory PD, *et al* (2007) Gene editing in human stem cells using zinc finger nucleases and integrase-defective lentiviral vector delivery. *Nat Biotechnol* 25: 1298–1306

Lorenz E, Congdon C & Uphoff D (1952) Modification of Acute Irradiation Injury in Mice and Guinea-Pigs by Bone Marrow Injections. *Radiology* 58: 863–877

Loughran SJ, Haas S, Wilkinson AC, Klein AM & Brand M (2020) Lineage commitment of hematopoietic stem cells and progenitors: insights from recent single cell and lineage tracing technologies. *Exp Hematol* 88: 1–6

Lu TL, Pugach O, Somerville R, Rosenberg SA, Kochenderfer JN, Better M & Feldman SA (2016) A Rapid Cell Expansion Process for Production of Engineered Autologous CAR-T Cell Therapies. *Hum Gene Ther Methods* 27: 209–218

Lund JM, Alexopoulou L, Sato A, Karow M, Adams NC, Gale NW, Iwasaki A & Flavell RA (2004) Recognition of single-stranded RNA viruses by Toll-like receptor 7. *Proc Natl Acad Sci* 101: 5598–5603

Maetzig T, Galla M, Baum C & Schambach A (2011) Gammaretroviral Vectors: Biology, Technology and Application. *Viruses* 3: 677–713

Magnani A, Brosselin P, Beauté J, de Vergnes N, Mouy R, Debré M, Suarez F, Hermine O, Lortholary O, Blanche S, *et al* (2014) Inflammatory manifestations in a single-center cohort of patients with chronic granulomatous disease. *J Allergy Clin Immunol* 134: 655-662.e8

Maillard P V, Reynard S, Serhan F, Turelli P & Trono D (2007) Interfering Residues Narrow the Spectrum of MLV Restriction by Human TRIM5α. *PLoS Pathog* 3: e200

Mandell MA, Saha B & Thompson TA (2020) The Tripartite Nexus: Autophagy, Cancer, and Tripartite Motif-Containing Protein Family Members. *Front Pharmacol* 11

Mangeot P-E, Duperrier K, Nègre D, Boson B, Rigal D, Cosset F-L & Darlix J-L (2002) High Levels of Transduction of Human Dendritic Cells with Optimized SIV Vectors. *Mol Ther* 5: 283–290

Marktel S, Scaramuzza S, Cicalese MP, Giglio F, Galimberti S, Lidonnici MR, Calbi V, Assanelli A,

Bernardo ME, Rossi C, *et al* (2019) Intrabone hematopoietic stem cell gene therapy for adult and pediatric patients affected by transfusion-dependent ß-thalassemia. *Nat Med* 25: 234–241

Masiuk KE, Zhang R, Osborne K, Hollis RP, Campo-Fernandez B & Kohn DB (2019) PGE2 and Poloxamer Synperonic F108 Enhance Transduction of Human HSPCs with a β-Globin Lentiviral Vector. *Mol Ther - Methods Clin Dev* 13: 390–398

Mazurier F, Gan OI, McKenzie JL, Doedens M & Dick JE (2004) Lentivector-mediated clonal tracking reveals intrinsic heterogeneity in the human hematopoietic stem cell compartment and culture-induced stem cell impairment. *Blood* 103: 545–552

McClure MO, Marsh M & Weiss RA (1988) Human immunodeficiency virus infection of CD4-bearing cells occurs by a pH-independent mechanism. *EMBO J* 7: 513–518

McRae HM, Voss AK & Thomas T (2019) Are transplantable stem cells required for adult hematopoiesis? *Exp Hematol* 75: 1–10

Merten O-W, Hebben M & Bovolenta C (2016) Production of lentiviral vectors. *Mol Ther - Methods Clin Dev* 3: 16017

Mikkola H, Woods N-B, Sjögren M, Helgadottir H, Hamaguchi I, Jacobsen S-E, Trono D & Karlsson S (2000) Lentivirus Gene Transfer in Murine Hematopoietic Progenitor Cells Is Compromised by a Delay in Proviral Integration and Results in Transduction Mosaicism and Heterogeneous Gene Expression in Progeny Cells. *J Virol* 74: 11911–11918

Miyoshi H, Blömer U, Takahashi M, Gage FH & Verma IM (1998) Development of a Self-Inactivating Lentivirus Vector. *J Virol* 72: 8150–8157

Modlich U, Navarro S, Zychlinski D, Maetzig T, Knoess S, Brugman MH, Schambach A, Charrier S, Galy A, Thrasher AJ, *et al* (2009) Insertional Transformation of Hematopoietic Cells by Self-inactivating Lentiviral and Gammaretroviral Vectors. *Mol Ther* 17: 1919–1928

Montini E, Cesana D, Schmidt M, Sanvito F, Bartholomae CC, Ranzani M, Benedicenti F, Sergi LS, Ambrosi A, Ponzoni M, *et al* (2009) The genotoxic potential of retroviral vectors is strongly modulated by vector design and integration site selection in a mouse model of HSC gene therapy. *J Clin Invest* 119: 964–975

Montini E, Cesana D, Schmidt M, Sanvito F, Ponzoni M, Bartholomae C, Sergi LS, Benedicenti F, Ambrosi A, Di Serio C, *et al* (2006) Hematopoietic stem cell gene transfer in a tumor-prone mouse model uncovers low genotoxicity of lentiviral vector integration. *Nat Biotechnol* 24: 687–696

Morgan RA, Unti MJ, Aleshe B, Brown D, Osborne KS, Koziol C, Ayoub PG, Smith OB, O'Brien R, Tam C, *et al* (2020) Improved Titer and Gene Transfer by Lentiviral Vectors Using Novel, Small β-Globin Locus Control Region Elements. *Mol Ther* 28: 328–340

Morrison SJ & Weissman IL (1994) The long-term repopulating subset of hematopoietic stem cells is deterministic and isolatable by phenotype. *Immunity* 1: 661–673

Moussy A, Papili Gao N, Corre G, Poletti V, Majdoul S, Fenard D, Gunawan R, Stockholm D & Páldi A (2019) Constraints on Human CD34+ Cell Fate due to Lentiviral Vectors Can Be Relieved by Valproic Acid. *Hum Gene Ther* 30: 1023–1034

Mukai K, Konno H, Akiba T, Uemura T, Waguri S, Kobayashi T, Barber GN, Arai H & Taguchi T (2016) Activation of STING requires palmitoylation at the Golgi. *Nat Commun* 7: 11932

Müller M, Lee CM, Gasiunas G, Davis TH, Cradick TJ, Siksnys V, Bao G, Cathomen T & Mussolino C (2016) Streptococcus thermophilus CRISPR-Cas9 Systems Enable Specific Editing of the Human Genome. *Mol Ther* 24: 636–644

Müller U, Steinhoff U, Reis LFL, Hemmi S, Pavlovic J, Zinkernagel RM & Aguet M (1994) Functional Role of Type I and Type II Interferons in Antiviral Defense. *Science (80-)* 264: 1918–1921

Nagai Y, Garrett KP, Ohta S, Bahrun U, Kouro T, Akira S, Takatsu K & Kincade PW (2006) Toll-like Receptors on Hematopoietic Progenitor Cells Stimulate Innate Immune System Replenishment. *Immunity* 24: 801–812

Naldini L (2011) Ex vivo gene transfer and correction for cell-based therapies. *Nat Rev Genet* 12: 301–315

Naldini L (2019) Genetic engineering of hematopoiesis: current stage of clinical translation and future perspectives. *EMBO Mol Med* 11

Naldini L, Blömer U, Gallay P, Ory D, Mulligan R, Gage FH, Verma IM & Trono D (1996) In Vivo Gene Delivery and Stable Transduction of Nondividing Cells by a Lentiviral Vector. *Science (80-)* 272: 263–267

Neville M, Stutz F, Lee L, Davis LI & Rosbash M (1997) The importin-beta family member Crm1p bridges the interaction between Rev and the nuclear pore complex during nuclear export. *Curr Biol* 7: 767–775

Nishida K, Arazoe T, Yachie N, Banno S, Kakimoto M, Tabata M, Mochizuki M, Miyabe A, Araki M, Hara KY, *et al* (2016) Targeted nucleotide editing using hybrid prokaryotic and vertebrate adaptive immune systems. *Science (80-)* 353

O'Brien WA, Namazi A, Kalhor H, Mao SH, Zack JA & Chen IS (1994) Kinetics of human immunodeficiency virus type 1 reverse transcription in blood mononuclear phagocytes are slowed by limitations of nucleotide precursors. *J Virol* 68: 1258–1263

OhAinle M, Helms L, Vermeire J, Roesch F, Humes D, Basom R, Delrow JJ, Overbaugh J & Emerman M (2018) A virus-packageable CRISPR screen identifies host factors mediating interferon inhibition of HIV. *Elife* 7

Okude H, Ori D & Kawai T (2021) Signaling Through Nucleic Acid Sensors and Their Roles in Inflammatory Diseases. *Front Immunol* 11

Orkin SH & Zon LI (2008) Hematopoiesis: An Evolving Paradigm for Stem Cell Biology. *Cell* 132: 631–644

Ossovskaya VS, Mazo IA, Chernov M V, Chernova OB, Strezoska Z, Kondratov R, Stark GR, Chumakov PM & Gudkov A V (1996) Use of genetic suppressor elements to dissect distinct biological effects of separate p53 domains. *Proc Natl Acad Sci* 93: 10309–10314

Ozog S, Timberlake ND, Hermann K, Garijo O, Haworth KG, Shi G, Glinkerman CM, Schefter LE, D'Souza S, Simpson E, *et al* (2019) Resveratrol trimer enhances gene delivery to hematopoietic stem cells by reducing antiviral restriction at endosomes. *Blood* 134: 1298–1311

Pampusch MS, Haran KP, Hart GT, Rakasz EG, Rendahl AK, Berger EA, Connick E & Skinner PJ (2020) Rapid Transduction and Expansion of Transduced T Cells with Maintenance of Central Memory Populations. *Mol Ther - Methods Clin Dev* 16: 1–10

Pattabhi S, Lotti SN, Berger MP, Singh S, Lux CT, Jacoby K, Lee C, Negre O, Scharenberg AM & Rawlings DJ (2019) In Vivo Outcome of Homology-Directed Repair at the HBB Gene in HSC Using Alternative Donor Template Delivery Methods. *Mol Ther - Nucleic Acids* 17: 277–288

Pauls E, Ruiz A, Badia R, Permanyer M, Gubern A, Riveira-Muñoz E, Torres-Torronteras J, Álvarez M, Mothe B, Brander C, *et al* (2014) Cell Cycle Control and HIV-1 Susceptibility Are Linked by CDK6-Dependent CDK2 Phosphorylation of SAMHD1 in Myeloid and Lymphoid

Cells. *J Immunol* 193: 1988–1997

Pavani G & Amendola M (2021) Targeted Gene Delivery: Where to Land. *Front Genome Ed* 2

Pavel-Dinu M, Wiebking V, Dejene BT, Srifa W, Mantri S, Nicolas CE, Lee C, Bao G, Kildebeck EJ, Punjya N, *et al* (2019) Gene correction for SCID-X1 in long-term hematopoietic stem cells. *Nat Commun* 10: 1634

Perron MJ, Stremlau M, Lee M, Javanbakht H, Song B & Sodroski J (2007) The Human TRIM5α Restriction Factor Mediates Accelerated Uncoating of the N-Tropic Murine Leukemia Virus Capsid. *J Virol* 81: 2138–2148

Perron MJ, Stremlau M, Song B, Ulm W, Mulligan RC & Sodroski J (2004) TRIM5α mediates the postentry block to N-tropic murine leukemia viruses in human cells. *Proc Natl Acad Sci* 101: 11827–11832

Perry AK, Chow EK, Goodnough JB, Yeh W-C & Cheng G (2004) Differential Requirement for TANK-binding Kinase-1 in Type I Interferon Responses to Toll-like Receptor Activation and Viral Infection. *J Exp Med* 199: 1651–1658

Pertel T, Hausmann S, Morger D, Züger S, Guerra J, Lascano J, Reinhard C, Santoni FA, Uchil PD, Chatel L, *et al* (2011) TRIM5 is an innate immune sensor for the retrovirus capsid lattice. *Nature* 472: 361–365

Petrillo C, Calabria A, Piras F, Capotondo A, Spinozzi G, Cuccovillo I, Benedicenti F, Naldini L, Montini E, Biffi A, *et al* (2019) Assessing the Impact of Cyclosporin A on Lentiviral Transduction and Preservation of Human Hematopoietic Stem Cells in Clinically Relevant *Ex Vivo* Gene Therapy Settings. *Hum Gene Ther* 30: 1133–1146

Petrillo C, Cesana D, Piras F, Bartolaccini S, Naldini L, Montini E & Kajaste-Rudnitski A (2015) Cyclosporin A and Rapamycin Relieve Distinct Lentiviral Restriction Blocks in Hematopoietic Stem and Progenitor Cells. *Mol Ther* 23: 352–362

Petrillo C, Thorne LG, Unali G, Schiroli G, Giordano AMS, Piras F, Cuccovillo I, Petit SJ, Ahsan F, Noursadeghi M, *et al* (2018) Cyclosporine H Overcomes Innate Immune Restrictions to Improve Lentiviral Transduction and Gene Editing In Human Hematopoietic Stem Cells. *Cell Stem Cell* 23: 820-832.e9

Pichlmair A & Reis e Sousa C (2007) Innate Recognition of Viruses. *Immunity* 27: 370–383

Piras F & Kajaste-Rudnitski A (2021) Antiviral immunity and nucleic acid sensing in haematopoietic stem cell gene engineering. *Gene Ther* 28: 16–28

Piras F, Riba M, Petrillo C, Lazarevic D, Cuccovillo I, Bartolaccini S, Stupka E, Gentner B, Cittaro D, Naldini L, *et al* (2017) Lentiviral vectors escape innate sensing but trigger p53 in human hematopoietic stem and progenitor cells. *EMBO Mol Med* 9: 1198–1211

Prakash V, Moore M & Yáñez-Muñoz RJ (2016) Current Progress in Therapeutic Gene Editing for Monogenic Diseases. *Mol Ther* 24: 465–474

Provasi E, Genovese P, Lombardo A, Magnani Z, Liu P-Q, Reik A, Chu V, Paschon DE, Zhang L, Kuball J, *et al* (2012) Editing T cell specificity towards leukemia by zinc finger nucleases and lentiviral gene transfer. *Nat Med* 18: 807–815

Ragheb JA, Yu H, Hofmann T & Anderson WF (1995) The amphotropic and ecotropic murine leukemia virus envelope TM subunits are equivalent mediators of direct membrane fusion: implications for the role of the ecotropic envelope and receptor in syncytium formation and viral entry. *J Virol* 69: 7205–7215

Rai R, Romito M, Rivers E, Turchiano G, Blattner G, Vetharoy W, Ladon D, Andrieux G, Zhang F, Zinicola M, *et al* (2020) Targeted gene correction of human hematopoietic stem cells for

the treatment of Wiskott - Aldrich Syndrome. *Nat Commun* 11: 4034

Rajsbaum R, García-Sastre A & Versteeg GA (2014) TRIMmunity: The Roles of the TRIM E3-Ubiquitin Ligase Family in Innate Antiviral Immunity. *J Mol Biol* 426: 1265–1284

Ramdas P, Sahu AK, Mishra T, Bhardwaj V & Chande A (2020) From Entry to Egress: Strategic Exploitation of the Cellular Processes by HIV-1. *Front Microbiol* 11

Rampazzo C, Miazzi C, Franzolin E, Pontarin G, Ferraro P, Frangini M, Reichard P & Bianchi V (2010) Regulation by degradation, a cellular defense against deoxyribonucleotide pool imbalances. *Mutat Res Toxicol Environ Mutagen* 703: 2–10

Ran FA, Cong L, Yan WX, Scott DA, Gootenberg JS, Kriz AJ, Zetsche B, Shalem O, Wu X, Makarova KS, *et al* (2015) In vivo genome editing using Staphylococcus aureus Cas9. *Nature* 520: 186–191

Rasaiyaah J, Tan CP, Fletcher AJ, Price AJ, Blondeau C, Hilditch L, Jacques DA, Selwood DL, James LC, Noursadeghi M, *et al* (2013) HIV-1 evades innate immune recognition through specific cofactor recruitment. *Nature* 503: 402–405

De Ravin SS, Wu X, Moir S, Kardava L, Anaya-O'Brien S, Kwatemaa N, Littel P, Theobald N, Choi U, Su L, *et al* (2016) Lentiviral hematopoietic stem cell gene therapy for X-linked severe combined immunodeficiency. *Sci Transl Med* 8

Ravot E, Comolli G, Lori F & Lisziewicz J (2002) High efficiency lentiviral gene delivery in non-dividing cells by deoxynucleoside treatment. *J Gene Med* 4: 161–169

Rehwinkel J & Gack MU (2020) RIG-I-like receptors: their regulation and roles in RNA sensing. *Nat Rev Immunol* 20: 537–551

Le Rhun A, Escalera-Maurer A, Bratovič M & Charpentier E (2019) CRISPR-Cas in *Streptococcus pyogenes*. *RNA Biol* 16: 380–389

Ribeil J-A, Hacein-Bey-Abina S, Payen E, Magnani A, Semeraro M, Magrin E, Caccavelli L, Neven B, Bourget P, El Nemer W, *et al* (2017) Gene Therapy in a Patient with Sickle Cell Disease. *N Engl J Med* 376: 848–855

Río P, Navarro S, Wang W, Sánchez-Domínguez R, Pujol RM, Segovia JC, Bogliolo M, Merino E, Wu N, Salgado R, *et al* (2019) Successful engraftment of gene-corrected hematopoietic stem cells in non-conditioned patients with Fanconi anemia. *Nat Med* 25: 1396–1401

Rittiner JE, Moncalvo M, Chiba-Falek O & Kantor B (2020) Gene-Editing Technologies Paired With Viral Vectors for Translational Research Into Neurodegenerative Diseases. *Front Mol Neurosci* 13

Romero Z, Lomova A, Said S, Miggelbrink A, Kuo CY, Campo-Fernandez B, Hoban MD, Masiuk KE, Clark DN, Long J, *et al* (2019) Editing the Sickle Cell Disease Mutation in Human Hematopoietic Stem Cells: Comparison of Endonucleases and Homologous Donor Templates. *Mol Ther* 27: 1389–1406

Ruiz A, Pauls E, Badia R, Torres-Torronteras J, Riveira-Muñoz E, Clotet B, Martí R, Ballana E & Esté JA (2015) Cyclin D3-dependent control of the dNTP pool and HIV-1 replication in human macrophages. *Cell Cycle* 14: 1657–1665

Ryoo J, Choi J, Oh C, Kim S, Seo M, Kim S-Y, Seo D, Kim J, White TE, Brandariz-Nuñez A, *et al* (2014) The ribonuclease activity of SAMHD1 is required for HIV-1 restriction. *Nat Med* 20: 936–941

Sadelain M, Rivière I & Riddell S (2017) Therapeutic T cell engineering. *Nature* 545: 423–431

Sandrin V, Boson B, Salmon P, Gay W, Nègre D, Le Grand R, Trono D & Cosset F-L (2002)

Lentiviral vectors pseudotyped with a modified RD114 envelope glycoprotein show increased stability in sera and augmented transduction of primary lymphocytes and CD34+ cells derived from human and nonhuman primates. *Blood* 100: 823–832

Sawyer SL, Wu LI, Emerman M & Malik HS (2005) Positive selection of primate *TRIM5* ɑ identifies a critical species-specific retroviral restriction domain. *Proc Natl Acad Sci* 102: 2832–2837

Schiroli G, Conti A, Ferrari S, della Volpe L, Jacob A, Albano L, Beretta S, Calabria A, Vavassori V, Gasparini P, *et al* (2019) Precise Gene Editing Preserves Hematopoietic Stem Cell Function following Transient p53-Mediated DNA Damage Response. *Cell Stem Cell* 24: 551-565.e8

Schiroli G, Ferrari S, Conway A, Jacob A, Capo V, Albano L, Plati T, Castiello MC, Sanvito F, Gennery AR, *et al* (2017) Preclinical modeling highlights the therapeutic potential of hematopoietic stem cell gene editing for correction of SCID-X1. *Sci Transl Med* 9

Schlee M & Hartmann G (2016) Discriminating self from non-self in nucleic acid sensing. *Nat Rev Immunol* 16: 566–580

Schoggins JW (2019) Interferon-Stimulated Genes: What Do They All Do? *Annu Rev Virol* 6: 567–584

Schoggins JW & Rice CM (2011) Interferon-stimulated genes and their antiviral effector functions. *Curr Opin Virol* 1: 519–525

Schott JW, León-Rico D, Ferreira CB, Buckland KF, Santilli G, Armant MA, Schambach A, Cavazza A & Thrasher AJ (2019) Enhancing Lentiviral and Alpharetroviral Transduction of Human Hematopoietic Stem Cells for Clinical Application. *Mol Ther - Methods Clin Dev* 14: 134–147

Schuessler-Lenz M, Enzmann H & Vamvakas S (2020) Regulators' Advice Can Make a Difference: European Medicines Agency Approval of Zynteglo for Beta Thalassemia. *Clin Pharmacol Ther* 107: 492–494

Seif M, Einsele H & Löffler J (2019) CAR T Cells Beyond Cancer: Hope for Immunomodulatory Therapy of Infectious Diseases. *Front Immunol* 10

Seissler T, Marquet R & Paillart J-C (2017) Hijacking of the Ubiquitin/Proteasome Pathway by the HIV Auxiliary Proteins. *Viruses* 9: 322

Sessa M, Lorioli L, Fumagalli F, Acquati S, Redaelli D, Baldoli C, Canale S, Lopez ID, Morena F, Calabria A, *et al* (2016) Lentiviral haemopoietic stem-cell gene therapy in early-onset metachromatic leukodystrophy: an ad-hoc analysis of a non-randomised, open-label, phase 1/2 trial. *Lancet* 388: 476–487

Shalem O, Sanjana NE, Hartenian E, Shi X, Scott DA, Mikkelsen TS, Heckl D, Ebert BL, Root DE, Doench JG, *et al* (2014) Genome-Scale CRISPR-Cas9 Knockout Screening in Human Cells. *Science (80-)* 343: 84–87

Shaw A & Cornetta K (2014) Design and Potential of Non-Integrating Lentiviral Vectors. *Biomedicines* 2: 14–35

Shepard C, Xu J, Holler J, Kim D-H, Mansky LM, Schinazi RF & Kim B (2019) Effect of induced dNTP pool imbalance on HIV-1 reverse transcription in macrophages. *Retrovirology* 16: 29

Sheridan C (2011) Gene therapy finds its niche. *Nat Biotechnol* 29: 121–128

Shi G, Ozog S, Torbett BE & Compton AA (2018) mTOR inhibitors lower an intrinsic barrier to virus infection mediated by IFITM3. *Proc Natl Acad Sci* 115

Shin J & Oh J-W (2020) Development of CRISPR/Cas9 system for targeted DNA modifications

and recent improvements in modification efficiency and specificity. *BMB Rep* 53: 341–348

Shin JJ, Schröder MS, Caiado F, Wyman SK, Bray NL, Bordi M, Dewitt MA, Vu JT, Kim W-T, Hockemeyer D, *et al* (2020) Controlled Cycling and Quiescence Enables Efficient HDR in Engraftment-Enriched Adult Hematopoietic Stem and Progenitor Cells. *Cell Rep* 32: 108093

Shirley JL, de Jong YP, Terhorst C & Herzog RW (2020) Immune Responses to Viral Gene Therapy Vectors. *Mol Ther* 28: 709–722

Sinangil F, Loyter A & Volsky DJ (1988) Quantitative measurement of fusion between human immunodeficiency virus and cultured cells using membrane fluorescence dequenching. *FEBS Lett* 239: 88–92

Sioud M, Fløisand Y, Forfang L & Lund-Johansen F (2006) Signaling through Toll-like Receptor 7/8 Induces the Differentiation of Human Bone Marrow CD34+ Progenitor Cells along the Myeloid Lineage. *J Mol Biol* 364: 945–954

Smith S, Weston S, Kellam P & Marsh M (2014) IFITM proteins—cellular inhibitors of viral entry. *Curr Opin Virol* 4: 71–77

Soldi M, Sergi Sergi L, Unali G, Kerzel T, Cuccovillo I, Capasso P, Annoni A, Biffi M, Rancoita PMV, Cantore A, *et al* (2020) Laboratory-Scale Lentiviral Vector Production and Purification for Enhanced Ex Vivo and In Vivo Genetic Engineering. *Mol Ther - Methods Clin Dev* 19: 411–425

Solis M, Nakhaei P, Jalalirad M, Lacoste J, Douville R, Arguello M, Zhao T, Laughrea M, Wainberg MA & Hiscott J (2011) RIG-I-Mediated Antiviral Signaling Is Inhibited in HIV-1 Infection by a Protease-Mediated Sequestration of RIG-I. *J Virol* 85: 1224–1236

Sprenger H-G, MacVicar T, Bahat A, Fiedler KU, Hermans S, Ehrentraut D, Ried K, Milenkovic D, Bonekamp N, Larsson N-G, *et al* (2021) Cellular pyrimidine imbalance triggers mitochondrial DNA–dependent innate immunity. *Nat Metab* 3: 636–650

St Gelais C & Wu L (2011) SAMHD1: a new insight into HIV-1 restriction in myeloid cells. *Retrovirology* 8: 55

Stavrou S, Aguilera AN, Blouch K & Ross SR (2018) DDX41 Recognizes RNA/DNA Retroviral Reverse Transcripts and Is Critical for *In Vivo* Control of Murine Leukemia Virus Infection. *MBio* 9

Stavrou S, Blouch K, Kotla S, Bass A & Ross SR (2015) Nucleic Acid Recognition Orchestrates the Anti-Viral Response to Retroviruses. *Cell Host Microbe* 17: 478–488

Stavrou S, Nitta T, Kotla S, Ha D, Nagashima K, Rein AR, Fan H & Ross SR (2013) Murine leukemia virus glycosylated Gag blocks apolipoprotein B editing complex 3 and cytosolic sensor access to the reverse transcription complex. *Proc Natl Acad Sci* 110: 9078–9083

Stoye JP & Yap MW (2008) Chance favors a prepared genome. *Proc Natl Acad Sci* 105: 3177–3178

Stremlau M, Owens CM, Perron MJ, Kiessling M, Autissier P & Sodroski J (2004) The cytoplasmic body component TRIM5α restricts HIV-1 infection in Old World monkeys. *Nature* 427: 848–853

Stremlau M, Perron M, Lee M, Li Y, Song B, Javanbakht H, Diaz-Griffero F, Anderson DJ, Sundquist WI & Sodroski J (2006) Specific recognition and accelerated uncoating of retroviral capsids by the TRIM5α restriction factor. *Proc Natl Acad Sci* 103: 5514–5519

Stremlau M, Perron M, Welikala S & Sodroski J (2005) Species-Specific Variation in the B30.2(SPRY) Domain of TRIM5α Determines the Potency of Human Immunodeficiency Virus Restriction. *J Virol* 79: 3139–3145

Styczyński J, Tridello G, Koster L, Iacobelli S, van Biezen A, van der Werf S, Mikulska M, Gil L, Cordonnier C, Ljungman P, *et al* (2020) Death after hematopoietic stem cell transplantation: changes over calendar year time, infections and associated factors. *Bone Marrow Transplant* 55: 126–136

Sudarsanam H, Buhmann R & Henschler R (2022) Influence of Culture Conditions on Ex Vivo Expansion of T Lymphocytes and Their Function for Therapy: Current Insights and Open Questions. *Front Bioeng Biotechnol* 10

Suddala KC, Lee CC, Meraner P, Marin M, Markosyan RM, Desai TM, Cohen FS, Brass AL & Melikyan GB (2019) Interferon-induced transmembrane protein 3 blocks fusion of sensitive but not resistant viruses by partitioning into virus-carrying endosomes. *PLOS Pathog* 15: e1007532

Sunseri N, O'Brien M, Bhardwaj N & Landau NR (2011) Human Immunodeficiency Virus Type 1 Modified To Package Simian Immunodeficiency Virus Vpx Efficiently Infects Macrophages and Dendritic Cells. *J Virol* 85: 6263–6274

Sutton RE, Reitsma MJ, Uchida N & Brown PO (1999) Transduction of Human Progenitor Hematopoietic Stem Cells by Human Immunodeficiency Virus Type 1-Based Vectors Is Cell Cycle Dependent. *J Virol* 73: 3649–3660

Taft J, Markson M, Legarda D, Patel R, Chan M, Malle L, Richardson A, Gruber C, Martín-Fernández M, Mancini GMS, *et al* (2021) Human TBK1 deficiency leads to autoinflammation driven by TNF-induced cell death. *Cell* 184: 4447-4463.e20

Tang D, Kang R, Coyne CB, Zeh HJ & Lotze MT (2012) PAMPs and DAMPs: signal 0s that spur autophagy and immunity. *Immunol Rev* 249: 158–175

Tartour K, Nguyen X-N, Appourchaux R, Assil S, Barateau V, Bloyet L-M, Burlaud Gaillard J, Confort M-P, Escudero-Perez B, Gruffat H, *et al* (2017) Interference with the production of infectious viral particles and bimodal inhibition of replication are broadly conserved antiviral properties of IFITMs. *PLOS Pathog* 13: e1006610

Tatematsu M, Nishikawa F, Seya T & Matsumoto M (2013) Toll-like receptor 3 recognizes incomplete stem structures in single-stranded viral RNA. *Nat Commun* 4: 1833

tenOever BR, Sharma S, Zou W, Sun Q, Grandvaux N, Julkunen I, Hemmi H, Yamamoto M, Akira S, Yeh W-C, *et al* (2004) Activation of TBK1 and IKKε Kinases by Vesicular Stomatitis Virus Infection and the Role of Viral Ribonucleoprotein in the Development of Interferon Antiviral Immunity. *J Virol* 78: 10636–10649

Thompson AA, Walters MC, Kwiatkowski J, Rasko JEJ, Ribeil J-A, Hongeng S, Magrin E, Schiller GJ, Payen E, Semeraro M, *et al* (2018) Gene Therapy in Patients with Transfusion-Dependent β-Thalassemia. *N Engl J Med* 378: 1479–1493

Till JE & McCulloch EA (1961) A Direct Measurement of the Radiation Sensitivity of Normal Mouse Bone Marrow Cells. *Radiat Res* 14: 213

Tucci F, Galimberti S, Naldini L, Valsecchi MG & Aiuti A (2022) A systematic review and meta-analysis of gene therapy with hematopoietic stem and progenitor cells for monogenic disorders. *Nat Commun* 13: 1315

Ulm JW, Perron M, Sodroski J & C. Mulligan R (2007) Complex determinants within the Moloney murine leukemia virus capsid modulate susceptibility of the virus to Fv1 and Ref1-mediated restriction. *Virology* 363: 245–255

Unterholzner L & Dunphy G (2019) cGAS-independent STING activation in response to DNA damage. *Mol Cell Oncol* 6: 1558682

Unterholzner L, Keating SE, Baran M, Horan KA, Jensen SB, Sharma S, Sirois CM, Jin T, Latz E, Xiao TS, *et al* (2010) IFI16 is an innate immune sensor for intracellular DNA. *Nat Immunol* 11: 997–1004

Urnov FD (2020) Prime Time for Genome Editing? *N Engl J Med* 382: 481–484

Velten L, Haas SF, Raffel S, Blaszkiewicz S, Islam S, Hennig BP, Hirche C, Lutz C, Buss EC, Nowak D, *et al* (2017) Human haematopoietic stem cell lineage commitment is a continuous process. *Nat Cell Biol* 19: 271–281

Vigna E & Naldini L (2000) Lentiviral vectors: excellent tools for experimental gene transfer and promising candidates for gene therapy. *J Gene Med* 2: 308–316

Vogt V (1997) Retroviral Virions and Genomes

Volkman HE, Cambier S, Gray EE & Stetson DB (2019) Tight nuclear tethering of cGAS is essential for preventing autoreactivity. *Elife* 8

Wagner JE, Brunstein CG, Boitano AE, DeFor TE, McKenna D, Sumstad D, Blazar BR, Tolar J, Le C, Jones J, *et al* (2016) Phase I/II Trial of StemRegenin-1 Expanded Umbilical Cord Blood Hematopoietic Stem Cells Supports Testing as a Stand-Alone Graft. *Cell Stem Cell* 18: 144–155

Wang CX, Sather BD, Wang X, Adair J, Khan I, Singh S, Lang S, Adams A, Curinga G, Kiem H-P, *et al* (2014) Rapamycin relieves lentiviral vector transduction resistance in human and mouse hematopoietic stem cells. *Blood* 124: 913–923

Watanabe N & McKenna MK (2022) Generation of CAR T-cells using γ-retroviral vector. In pp 171–183.

Watanabe S & Temin HM (1982) Encapsidation sequences for spleen necrosis virus, an avian retrovirus, are between the 5’ long terminal repeat and the start of the gag gene. *Proc Natl Acad Sci* 79: 5986–5990

Weidner JM, Jiang D, Pan X-B, Chang J, Block TM & Guo J-T (2010) Interferon-Induced Cell Membrane Proteins, IFITM3 and Tetherin, Inhibit Vesicular Stomatitis Virus Infection via Distinct Mechanisms. *J Virol* 84: 12646–12657

Weisser M, Demel UM, Stein S, Chen-Wichmann L, Touzot F, Santilli G, Sujer S, Brendel C, Siler U, Cavazzana M, *et al* (2016) Hyperinflammation in patients with chronic granulomatous disease leads to impairment of hematopoietic stem cell functions. *J Allergy Clin Immunol* 138: 219-228.e9

White TE, Brandariz-Nuñez A, Valle-Casuso JC, Amie S, Nguyen L, Kim B, Brojatsch J & Diaz-Griffero F (2013) Contribution of SAM and HD domains to retroviral restriction mediated by human SAMHD1. *Virology* 436: 81–90

Winkler IG, Pettit AR, Raggatt LJ, Jacobsen RN, Forristal CE, Barbier V, Nowlan B, Cisterne A, Bendall LJ, Sims NA, *et al* (2012) Hematopoietic stem cell mobilizing agents G-CSF, cyclophosphamide or AMD3100 have distinct mechanisms of action on bone marrow HSC niches and bone formation. *Leukemia* 26: 1594–1601

Wittmann S, Behrendt R, Eissmann K, Volkmann B, Thomas D, Ebert T, Cribier A, Benkirane M, Hornung V, Bouzas NF, *et al* (2015) Phosphorylation of murine SAMHD1 regulates its antiretroviral activity. *Retrovirology* 12: 103

Wu X, Anderson JL, Campbell EM, Joseph AM & Hope TJ (2006) Proteasome inhibitors uncouple rhesus TRIM5α restriction of HIV-1 reverse transcription and infection. *Proc Natl Acad Sci* 103: 7465–7470

Wu X, Dao Thi VL, Huang Y, Billerbeck E, Saha D, Hoffmann H-H, Wang Y, Silva LAV, Sarbanes

S, Sun T, *et al* (2018) Intrinsic Immunity Shapes Viral Resistance of Stem Cells. *Cell* 172: 423-438.e25

Wu Y, Zeng J, Roscoe BP, Liu P, Yao Q, Lazzarotto CR, Clement K, Cole MA, Luk K, Baricordi C, *et al* (2019) Highly efficient therapeutic gene editing of human hematopoietic stem cells. *Nat Med* 25: 776–783

Wyman C & Kanaar R (2006) DNA Double-Strand Break Repair: All's Well that Ends Well. *Annu Rev Genet* 40: 363–383

Xagorari A & Chlichlia K (2008) Toll-Like Receptors and Viruses: Induction of Innate Antiviral Immune Responses. *Open Microbiol J* 2: 49–59

Xiao TS & Fitzgerald KA (2013) The cGAS-STING Pathway for DNA Sensing. *Mol Cell* 51: 135–139

Xu L, Wang W, Li Y, Zhou X, Yin Y, Wang Y, de Man RA, van der Laan LJW, Huang F, Kamar N, *et al* (2017) RIG-I is a key antiviral interferon-stimulated gene against hepatitis E virus regardless of interferon production. *Hepatology* 65: 1823–1839

Yahata T, Takanashi T, Muguruma Y, Ibrahim AA, Matsuzawa H, Uno T, Sheng Y, Onizuka M, Ito M, Kato S, *et al* (2011) Accumulation of oxidative DNA damage restricts the self-renewal capacity of human hematopoietic stem cells. *Blood* 118: 2941–2950

Yamashita M & Emerman M (2004) Capsid Is a Dominant Determinant of Retrovirus Infectivity in Nondividing Cells. *J Virol* 78: 5670–5678

Yan J, Kaur S, DeLucia M, Hao C, Mehrens J, Wang C, Golczak M, Palczewski K, Gronenborn AM, Ahn J, *et al* (2013) Tetramerization of SAMHD1 Is Required for Biological Activity and Inhibition of HIV Infection. *J Biol Chem* 288: 10406–10417

Yang L, Bryder D, Adolfsson J, Nygren J, Mañsson R, Sigvardsson M & Jacobsen SEW (2005) Identification of Lin−Sca1+kit+CD34+Flt3− short-term hematopoietic stem cells capable of rapidly reconstituting and rescuing myeloablated transplant recipients. *Blood* 105: 2717–2723

Yang L, Yang B & Chen J (2019) One Prime for All Editing. *Cell* 179: 1448–1450

Yap MW, Nisole S, Lynch C & Stoye JP (2004) Trim5α protein restricts both HIV-1 and murine leukemia virus. *Proc Natl Acad Sci* 101: 10786–10791

Yap MW, Nisole S & Stoye JP (2005) A Single Amino Acid Change in the SPRY Domain of Human Trim5α Leads to HIV-1 Restriction. *Curr Biol* 15: 73–78

Yeh W-H, Chiang H, Rees HA, Edge ASB & Liu DR (2018) In vivo base editing of post-mitotic sensory cells. *Nat Commun* 9: 2184

Yu SF, von Rüden T, Kantoff PW, Garber C, Seiberg M, Rüther U, Anderson WF, Wagner EF & Gilboa E (1986) Self-inactivating retroviral vectors designed for transfer of whole genes into mammalian cells. *Proc Natl Acad Sci* 83: 3194–3198

Zeng J, Wu Y, Ren C, Bonanno J, Shen AH, Shea D, Gehrke JM, Clement K, Luk K, Yao Q, *et al* (2020) Therapeutic base editing of human hematopoietic stem cells. *Nat Med* 26: 535–541

Zhang X-H, Tee LY, Wang X-G, Huang Q-S & Yang S-H (2015) Off-target Effects in CRISPR/Cas9-mediated Genome Engineering. *Mol Ther - Nucleic Acids* 4: e264

Zhang Y & Liang C (2016) Innate recognition of microbial-derived signals in immunity and inflammation. *Sci China Life Sci* 59: 1210–1217

Zhao X, Li J, Winkler CA, An P & Guo J-T (2019) IFITM Genes, Variants, and Their Roles in the

Control and Pathogenesis of Viral Infections. *Front Microbiol* 9

Zhao Y, Stepto H & Schneider CK (2017) Development of the First World Health Organization Lentiviral Vector Standard: Toward the Production Control and Standardization of Lentivirus-Based Gene Therapy Products. *Hum Gene Ther Methods* 28: 205–214

Zhong L, Hu M-M, Bian L-J, Liu Y, Chen Q & Shu H-B (2020) Phosphorylation of cGAS by CDK1 impairs self-DNA sensing in mitosis. *Cell Discov* 6: 26

Zhou R, Zhang Q & Xu P (2020) TBK1, a central kinase in innate immune sensing of nucleic acids and beyond. *Acta Biochim Biophys Sin (Shanghai)* 52: 757–767

Zimran E, Papa L & Hoffman R (2021) Ex vivo expansion of hematopoietic stem cells: Finally transitioning from the lab to the clinic. *Blood Rev* 50: 100853

Zonari E, Desantis G, Petrillo C, Boccalatte FE, Lidonnici MR, Kajaste-Rudnitski A, Aiuti A, Ferrari G, Naldini L & Gentner B (2017) Efficient Ex Vivo Engineering and Expansion of Highly Purified Human Hematopoietic Stem and Progenitor Cell Populations for Gene Therapy. *Stem Cell Reports* 8: 977–990

Zufferey R, Nagy D, Mandel RJ, Naldini L & Trono D (1997) Multiply attenuated lentiviral vector achieves efficient gene delivery in vivo. *Nat Biotechnol* 15: 871–875